

MANA Progress Report

Research Digest 2015



World Premier International (WPI) Research Center
**International Center for
Materials Nanoarchitectonics (MANA)**



National Institute for Materials Science (NIMS)

The scientific art pictures used in this report were provided by



Makoto Sakurai (MANA Scientist)



Kohsaku Kawakami (MANA Scientist)



Li Liang (MANA Research Associate)



Chunyi Zhi (former MANA Scientist)

Preface

Masakazu Aono
MANA Director-General
NIMS



The International Center for Materials Nanoarchitectonics (MANA) was founded in 2007 as one of the first five centers under the World Premier International Research Center Initiative (WPI Program) of Japan's Ministry of Education, Culture, Sports, Science and Technology (MEXT). In all the way of this period, MANA has conducted its research on the basis of our own "nanoarchitectonics" concept. All the members of MANA including permanent scientists, postdoctoral researchers, technical and administrative staff and students are happy to see that MANA has become a really world-top-level research center in the field of material science and technology. In fact, until December 2014, MANA has published 2,850 papers and 106 of them are world-top-1% most-cited papers. Also the field weighted citation impact (FWCI), which was devised by Elsevier B.V. to evaluate the quality of papers published from individual institutions fairly, is as large as 2.45 for MANA. This number is comparable to those of world-top universities and research institutions.

The MANA Progress Report consists of two booklets named "Research Digest 2015" and "Facts and Achievements 2015". This booklet "Research Digest 2015" presents MANA research activities and the other booklet "Facts and Achievements 2015" serves as a summary to highlight the progress of the MANA project.



MANA Research Digest 2015

MANA Principal Investigators (19) and Associate Principal Investigators (2)

Nano-Materials Field

Takayoshi SASAKI (Field Coordinator, PI).....	6
Inorganic Nanosheets	
Katsuhiko ARIGA (PI).....	7
Supramolecular Materials	
Yoshio BANDO (MANA Chief Operating Officer, PI).....	8
Inorganic Nanostructured Materials	
Toyohiro CHIKYOW (PI).....	9
Nano Electrics and Related Materials	
Dmitri GOLBERG (PI).....	10
Nano-Opto-Mechano-Electrical Studies in HRTEM	
Zhong Lin WANG (Satellite PI).....	11
Nanogenerators as a New Energy Technology	
Minoru OSADA (API).....	12
Nanosheet Electronics	

Nano-System Field

Masakazu AONO (MANA Director-General, Field Coordinator, PI).....	13
Nano-System Architectonics	
James K. GIMZEWSKI (Satellite PI).....	14
MANA Brain: Neuromorphic Atomic Switch Networks	
Xiao HU (PI).....	15
Novel Quantum Functionality in Topological Systems	
Christian JOACHIM (Satellite PI).....	16
Surface Atomic Scale Logic Gate	
Tomonobu NAKAYAMA (Administrative Director, former PI).....	17
Integration of Nano Functionality for Novel Nanosystems	
Kazuhito TSUKAGOSHI (PI).....	18
Self-Limiting Layer-by-Layer Oxidation of Atomically Thin WSe ₂	

Nano-Power Field

Jinhua YE (Field Coordinator, PI)..... 19
 Nanoarchitectonics of Hybrid Artificial Photosynthetic System

Kazunori TAKADA (PI)..... 20
 Solid-State Batteries

Kohei UOSAKI (PI)..... 21
 Construction of Interphases with Atomic/Molecular Order for Efficient Conversion of Energy and Materials

Omar M. YAGHI (PI)..... 22
 Reticular Materials

David BOWLER (Satellite API)..... 23
 Dye-Sensitized Solar Cells and Core-Shell Nanowires

Nano-Life Field

Guoping CHEN (Field Coordinator, PI)..... 24
 Preparation of Surface Functionalized Nanoparticles for Controlling Stem Cell Functions and Cancer Therapy

Yukio NAGASAKI (Satellite PI)..... 25
 Nanotherapeutics Based on Redox Polymer Nanoarchitectonics

Françoise M. WINNIK (Satellite PI)..... 26
 Nanoarchitectonics-Driven Interfaces and Nanoparticles for Therapeutic Applications

Group Leaders (11)

Naoki FUKATA (Nano-Materials Field)..... 27
 Next-Generation Semiconductor Nanodevices

Nobutaka HANAGATA (Nano-Life Field)..... 28
 Development of Nanomedicines

Masanori KIKUCHI (Nano-Life Field)..... 29
 Bioactive Ceramics Materials

Hisatoshi KOBAYASHI (Nano-Life Field)..... 30
 Materials for Functional Nanomedicine

Takao MORI (Nano-Materials Field)..... 31
 Functionalization of Atomic Network Materials

Tadaaki NAGAO (Nano-System Field)..... 32
 Nano Devices for Infrared Light Applications

Takashi SEKIGUCHI (Nano-Materials Field).....	33
Characterization and Control of Defects in Semiconductors	
Akiyoshi TANIGUCHI (Nano-Life Field).....	34
Development of Sensor Cells for Nanomaterials Safety Evaluation	
Yoshitaka TATEYAMA (Nano-Power Field).....	35
Nano-System Computational Science	
Kazuya TERABE (Nano-System Field).....	36
Modulation of Superconducting Critical Temperature in Niobium Film Achieved by Using a Nano-Ionics Device	
Akiko YAMAMOTO (Nano-Life Field).....	37
Effect of Carbonate Buffer System on the Biodegradation of Mg Alloys	

MANA Independent Scientists (13)

Ryuichi ARAFUNE	38
Laser-Based Inelastic Photoemission Spectroscopy	
Alexei A. BELIK	39
Search for New Ferroelectric, Magnetic, and Multiferroic Materials Using High-Pressure Technique	
Ryoma HAYAKAWA	40
Towards Development of Vertical Quantum Field Effect Transistors with Attractive Molecular Dots	
Joel HENZIE	41
Bifunctional Oxygen Electrocatalysis with Phase-Pure α -Mn ₂ O ₃ Prisms	
Takeo MINARI	42
Ultra-High-Resolution Patterning of Functional Inks for Fully-Printed Electronic Devices	
Satoshi MORIYAMA	43
Quantum Devices in Nanomaterials	
Jun NAKANISHI	44
Development of Photoresponsive Biointerfaces	
Takashi NAKANISHI	45
Photo-energy Converting Alkylated-C ₆₀ /Graphene Hybrid using Alkyl Chains as Glue between Nanocarbons	
Liwen SANG	46
Novel Solar Cell Concept with a Super-wide Response Spectrum Based on III-V Nitride Semiconductors	
Naoto SHIRAHATA	47
Green Nanochemistry: Bandgap Engineering for Group IV Nanostructures	

Satoshi TOMINAKA	48
Proton/electron Transports in Dense Metal Organic Frameworks	
Yusuke YAMAUCHI	49
Tailored Synthesis of Nanoporous Pt with Various Architectures	
Genki YOSHIKAWA	50
Nanomechanical Sensors towards Mobile Olfaction	

ICYS-MANA Researchers (10)

Alexandre FIORI	51
Diamond Power Devices – Defects Control by Multilayer Formation	
Yohei KOTSUCHIBASHI	52
New Polymeric Nano-System for Diagnosis and Therapy	
Huynh Thien NGO	53
Directional Control of Energy and Electron Transfer by Metal Ion Choices in Porphyrinoids	
Thanh Cuong NGUYEN	54
Theoretical Design of Nanocarbon Materials for Device Applications	
Gauthier RYDZEK	55
Nanostructured Polymeric Nanomaterials	
Kota SHIBA	56
Development of Versatile Receptor Layer Materials for Nanomechanical Sensor-based Detection/ Discrimination	
Xi WANG	57
Advanced Binder-free Anodes for the Energy Storage Application and their Storage Mechanisms at Atomic Scale	
Xue-Bin WANG	58
Nanosheets of Boron-Carbon-Nitrogen System for Energy and Composite Applications	
Hamish Hei-Man YEUNG	59
Towards Metal-Organic Framework Nanoarchitectonics: Fundamentals of Synthesis and Design	
Shunsuke YOSHIKAWA	60
Engineering Topological Superconductivity in Surface Materials	

Inorganic Nanosheets

MANA Principal Investigator

(Field Coordinator)

MANA Scientist
MANA Research Associate
Graduate Student

Takayoshi SASAKI

Yasuo Ebina, Renzhi Ma, Nobuyuki Sakai
Jianghua Wu, Pan Xiong, Yang Zhang
Xingke Cai, Yeji Song, Leanddas Nurdwijayanto,
Tatsumasa Hoshide, Kei Kamanaka



1. Outline of Research

We aim at producing two-dimensional (2D) inorganic nanosheets as a unique class of nanoscale materials by delaminating various layered compounds through soft-chemical processes. Particular attention is paid to fine control of their composition and structure via doping and substitution of constituent elements, expecting new or enhanced properties.

We develop a new nanofabrication process for precisely organizing colloidal nanosheets into multilayer or superlattice assemblies through solution-based processes (Fig. 1). Based on this novel approach with the nanosheets (soft-chemical nanoarchitectonics), we establish the tailoring ability and controllability over nanostructures with a precision down to 1 nm, which is comparable to that in lattice engineering utilizing modern vapor-phase deposition techniques.

In the second stage, we take challenges to develop innovative nanostructured materials and nanodevices through nanoscale assembly of nanosheets and a range of foreign modules (organic compounds, metal complexes, clusters...). In particular, we attempt to realize new or sophisticated functions by cooperative interaction between nanosheets themselves or between nanosheets and other functional modules.

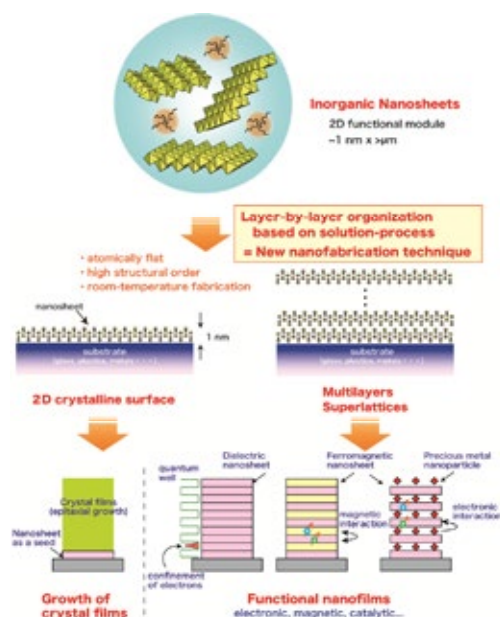


Fig. 1. Conceptual explanation of the research plan.

2. Research Activities

(1) Modification of surface charge of 2D nanosheets.¹⁾

We successfully modified the surface negative charge of 2D nanosheets such as graphene oxide (GO), $\text{Ti}_{0.87}\text{O}_2^{0.52}$ and

$\text{Ca}_2\text{Nb}_3\text{O}_{10}^-$ simply by mixing their suspension with a solution of polycation having a high molecular weight. The nanosheets did not undergo flocculation but remained monodispersed in solution (Fig. 2), likely due to the long polycation chains running off the edges of nanosheets and folding over. This process to tune the surface charge of 2D materials is important because a great majority of them are negatively charged. We showed that superlattice composites of these 2D materials could be readily obtained at bulk-scale by mixing suspensions of pristine negatively charged nanosheets and those with a tuned positive charge.

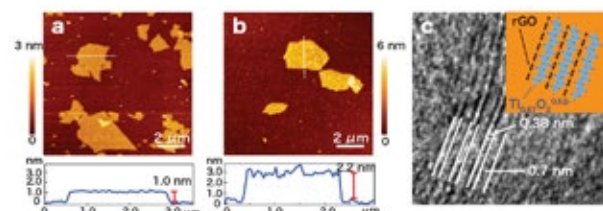


Fig. 2. a, b: AFM images of pristine and modified GO. GO got thicker upon modification. c: TEM image of the superlattice composite of GO/ $\text{Ti}_{0.87}\text{O}_2$.

(2) Electrocatalysts of alternately stacked hydroxide nanosheets and graphene.²⁾

We have successfully synthesized 3d transition metal layered double hydroxides (LDH) with varied Ni/Fe contents. The exfoliated Ni-Fe LDH nanosheets were hetero-assembled with GO as well as reduced graphene oxide (rGO) into superlattice-like hybrids, in which two kinds of oppositely charged nanosheets were stacked face-to-face in alternating sequence. The composites exhibited excellent oxygen evolution reaction (OER) efficiency with a small overpotential. The optimized combination ($\text{Ni}_{2/3}\text{Fe}_{1/3}$ -rGO) has achieved the overpotential as low as 0.21 V (Fig. 3). The composite catalysts were also found to be effective for hydrogen evolution reaction. An electrolyzer cell powered by a single AA battery of 1.5 V was demonstrated by using the newly developed bi-functional catalysts.

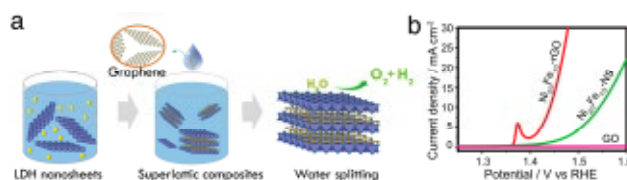


Fig. 3. a: Schematic illustration of hetero-assembling LDH nanosheets and graphene (oxide). b: OER catalytic activity of the superlattice composites.

References

- X. Cai, T. C. Ozawa, A. Funatsu, R. Ma, Y. Ebina, T. Sasaki, *J. Am. Chem. Soc.* **137**, 2844 (2015). Selected as JACS spotlights.
- W. Ma, R. Ma, C. Wang, J. Liang, X. Liu, K. Zhou, T. Sasaki, *ACS Nano* **9**, 1977 (2015).

Supramolecular Materials

MANA Principal Investigator

MANA Scientist

MANA Research Associate

Katsuhiko ARIGA

Jonathan P. Hill, Qingmin Ji, Lok Kumar Shrestha,
Waka Nakanishi

Jia Liu, Shangbin Jin, Partha Bairi



1. Outline of Research

Functional materials have been wisely constructed via bottom-up approaches as seen in preparation of molecular and nano patterns, complexes, and nanomaterials organized nano- and microstructures, and function materials. We are working in exploratory research for innovative materials and sensing systems based on supramolecular concept.¹⁻⁵⁾

2. Research Activities

(1) Control of molecular machine by size-extremely different actions.

We have succeeded in manipulating molecular machines by size- extremely-different modes. As ultimately small size, manipulating the rotational direction of the molecular motors with a nano-level sharpened tip has been realized upon collaboration with Dr. Uchihashi.⁶⁾ A motor made of a supramolecule rotates in one direction when electric current is injected from the tip into the molecule. In addition, reversing the motor rotational direction by rearranging motor parts via application of electric current under certain conditions was also achieved. As approach from visible-size actions, we applied mechanical energy to molecular machines (molecular pliers) that aggregated at the air–water interface (Fig. 1). The level of mechanical energy we applied in this study was much smaller than the levels of optical and thermal energies normally used to run molecular machines,

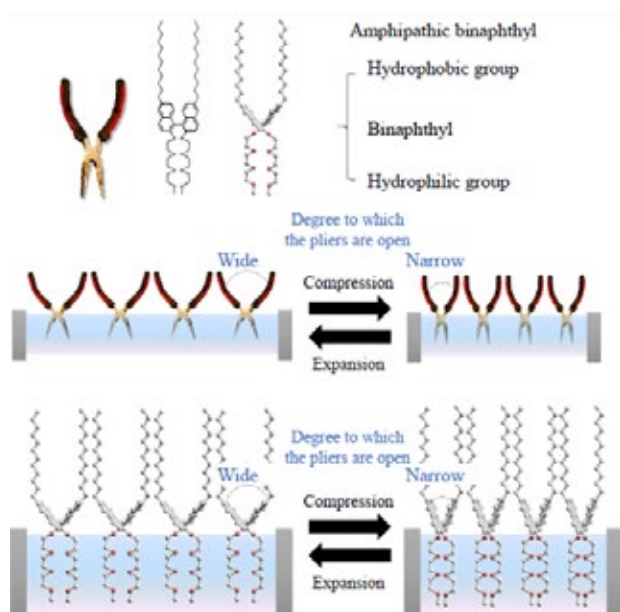


Fig. 1. Mechanical control of molecular pliers.

there are high expectations on this technology for its potential to develop into a simple and energy-saving new nanotechnology.⁷⁾

(2) Control of cell differentiation by supramolecular fullerene assembly.

We have demonstrated that aligned 1D fullerene whisker scaffolds induce myogenic differentiation from myoblast to myotube. Micrometer-scale fullerene whiskers were aligned on substrates by a simple method using the interfacial alignment (Fig. 2). The aligned fullerene whisker substrate showed significant enhancement of myogenic differentiation and regulated the direction of myotube formation. With its potential to induce myogenic differentiation, and to control growth direction, as well as its biocompatibility, our aligned FW scaffolds are promising platforms for a useful alternative to micro patterned cell scaffolds for tissue engineering.⁸⁾

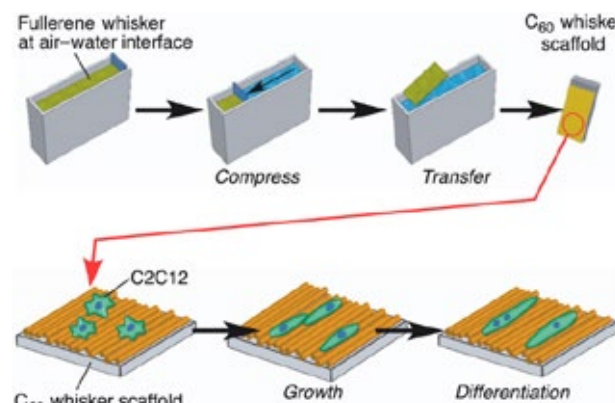


Fig. 2. Alignment of fullerene whiskers and cell differentiation control.

References

- 1) L.K. Shrestha, R.G. Shrestha, Y. Yamauchi, J.P. Hill, T. Nishimura, K. Miyazawa, T. Kawai, S. Okada, K. Wakabayashi, K. Ariga, *Angew. Chem. Int. Ed.* **54**, 951 (2015).
- 2) J. Labuta, J.P. Hill, S. Ishihara, L. Hanykova, K. Ariga, *Acc. Chem. Res.* **48**, 521 (2015).
- 3) R. Kodiyath, G.V. Ramesh, E. Koudelkova, T. Tanabe, M. Ito, M. Manikandan, S. Ueda, T. Fujita, N. Umezawa, H. Noguchi, K. Ariga, H. Abe, *Energy Environ. Sci.* **8**, 1685 (2015).
- 4) N.C. Huang, Q. Ji, K. Ariga, S.H. Hsu, *NPG Asia Mater.* **7**, e184 (2015).
- 5) J. Kim, B. Kim, C. Anand, A. Mano, J.S.M. Zaidi, K. Ariga, J. You, A. Vinu, E. Kim, *Angew. Chem. Int. Ed.* **54**, 8407 (2015).
- 6) P. Mishra, J.P. Hill, S. Vijayaraghavan, W. Van Rossam, S. Yoshizawa, M. Grisolia, J. Echeverria, T. Ohno, K. Ariga, T. Nakayama, C. Joachim, T. Uchihashi, *Nano Lett.* **15**, 4793 (2015).
- 7) D. Ishikawa, T. Mori, Y. Yonamine, W. Nakanishi, D. Cheung, J.P. Hill, K. Ariga, *Angew. Chem. Int. Ed.* **54**, 8988 (2015).
- 8) K. Minami, Y. Kasuya, T. Yamazaki, Q. Ji, W. Nakanishi, J.P. Hill, H. Sakai, K. Ariga, *Adv. Mater.* **27**, 4020 (2015).

Inorganic Nanostructured Materials

MANA Principal Investigator

(MANA Chief Operating Officer)

MANA Scientist

MANA Research Associate

MANA Visiting Scientist

Yoshio Bando

Ryutaro Souda, Yusuke Ide

Xiangfen Jiang, Qunhong Weng, Pengcheng Dai

Cuiling Li

Min Zhou



1. Outline of Research

Hybridization is an important route for material functionalization, which can incorporate the advantages of each component in materials to realize the desired and enhanced properties. We have developed novel binary and ternary h-BN and carbon-based composites, such like BN-Ag, BN-Au-TiO₂ and MoS₂-C. Their performances in the corresponding application fields have been improved compared with the solo components.

2. Research Activities

(1) *Porous Boron Nitride Microfibers Coated with Silver Nanoparticles for Pollutant Concentration and SERS Detection.*¹⁾

We conceived a new route for high-sensitive pollutant SERS detection in aqueous solutions by using the porous BN substrate to concentrate the pollutants (Fig. 1). The decorated Ag nanoparticles provide the SERS activity, which are stabilized by the porous BN substrates as well. The key function of porous BN used in this composite is to capture the organic molecules on the material surface, and thus to increase the SERS detection limit for low-concentration solutions. Our result showed that the detection limits for organic dyes was improved from 10⁻⁶ M to 10⁻⁹ M.

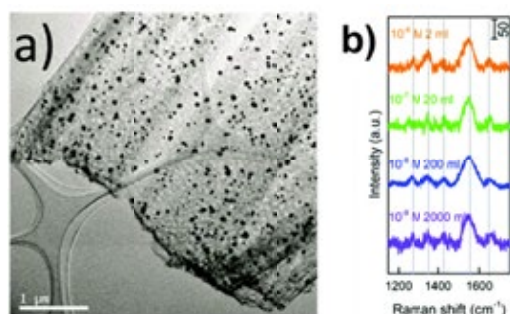


Fig. 1. (a) TEM image of a BN microfiber coated with uniform Ag nanoparticles. (b) Raman spectra of the RhB solutions with the same amount but different concentrations.

(2) *Boron Nitride Nanosheets as Effective Additives for Photocatalysis in BN-Au-TiO₂ Composite.*²⁾

h-BN itself doesn't show photocatalysis properties under normal UV and visible light range due its high band gap. However, we found h-BN nanosheets can effectively enhance the plasmonic photocatalytic effect of Au-TiO₂ for decomposition of formic acid in water by forming the ternary composite (BN-Au-TiO₂, Fig. 2). The used h-BN may assist avoiding the recombination of photo-excited electron-hole pairs and thus improve the photo-catalysis efficiency by 3 times under the visible light range ($\lambda > 420$ nm).

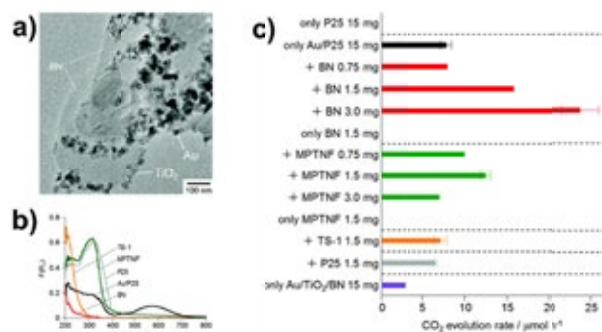


Fig. 2. (a) TEM images of BN-Au-TiO₂ composite. (b) UV-vis spectra of TiO₂ (P25), Au/P25, BN, microporous titanate nanofiber (MPTNF) and titanasilicate zeolite (TS-1). (c) Photocatalytic activities for the oxidation of formic acid in water to CO₂ over different samples under visible light irradiation ($\lambda > 420$ nm).

(3) *Molybdenum Disulfide Nanosheets Wrapped with Microporous Carbon Layer Used for Supercapacitors.*³⁾

We have designed a core-shell structure made of pseudocapacitive 2D MoS₂ nanosheets as the core, and metal-organic framework-derived microporous carbons as the shell for advanced supercapacitive energy storage (Fig. 3). The porous carbon shell can enrich electrolyte ions, and serve as core protection and electron transport network. Thus, the resultant composite showed a high capacitance of 189 F·g⁻¹ at 1 A·g⁻¹, high-rate and long cyclic performances. These performances are better than solo MPC and MoS₂ components.

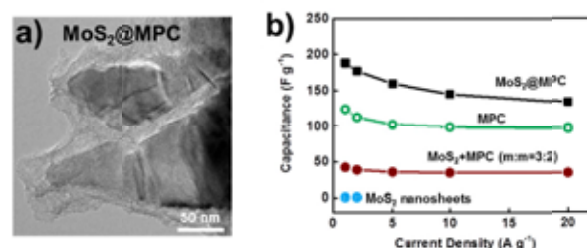


Fig. 3. (a) TEM image of MOF-derived microporous carbon coated MoS₂ nanosheets. (b) Specific capacitance of the MoS₂@MPC sample, MPC, the mixture of MoS₂ and MPC and MoS₂ nanosheets at various current densities.

References

- 1) P. Dai, Y. Xue, X. Wang, Q. Weng, C. Zhang, X. Jiang, D. Tang, X. Wang, N. Kawamoto, Y. Ide, M. Mitome, D. Golberg, Y. Bando, *Nanoscale* **7**, 18992 (2015).
- 2) Y. Ide, K. Nagao, K. Saito, K. Komaguchi, R. Fuji, A. Kogure, Y. Sugahara, Y. Bando, D. Golberg, *Phys. Chem. Chem. Phys.* **18**, 79 (2016).
- 3) Q. Weng, X. Wang, X. Wang, C. Zhang, X. Jiang, Y. Bando, D. Golberg, *J. Mater. Chem. A* **3**, 3097 (2015).

Nano Electrics and Related Materials

MANA Principal Investigator
MANA Scientist

Toyohiro CHIKYOW

Toshihide Nabatame, Masahiro Goto, Yutaka Wakayama, Jin Kawakita, Takahiro Nagata, Takayuki Nakane, Shinjiro Yagyu, Michiko Yoshitake, Yoshiyuki Yamashita



1. Outline of Research

The memristor, which is a non-volatile memory device that meets the scalability and switching speed requirements for low power consumption, has been investigated.¹⁾ Memristors based on metal-insulator-metal (MIM) structures enable the fabrication of three-dimensional and crossbar array structures required for the memory manufacturing process. The ability to have multilevel states and the prospect of using these states in both artificial biological systems and reconfigurable nano electronics is of particular interest. The memristor was first proposed theoretically in 1971.^{2,3)} An atomic switch and related phenomena were reported.^{4,5)} Also this memoristor is focused for neuron type function to emulate brain. The most popular approaches to understanding the resistance switching mechanism. The major model is based on changes in the oxygen vacancy (VO) concentrations in the filaments. Recently, a resistive switching random access memory (ReRAM) with a TiO₂-Al₂O₃ bilayer structure has been investigated with the aim of reducing the device operating currents.⁶⁾ To clarify the mutual influence of the two layers and the device switching behavior, Al₂O₃/TiO₂ bilayer were investigated in this research.

2. Research Activities

MIM capacitors with Pt electrodes were prepared with either Al₂O₃/TiO₂ bilayer structure on a 100-nm-thick SiO₂ layer formed on a p type Si (100) substrate. A 10-nm-thick titanium adhesion layer was then deposited on the SiO₂ layer, followed by deposition of the 100-nm-thick platinum bottom electrode by the DC sputtering method. Then, the Al₂O₃/TiO₂ (5 nm / 60 nm) bilayer structure was deposited by the atomic layer deposition (ALD) method at 200 °C. Post-deposition annealing (PDA) was carried out at 200 °C for 30 s under an oxygen ambient. Finally, the Pt top

electrode was formed. The current-voltage (I-V) characteristics of the structures was measured to evaluate the device function.

In the initial state, the Pt electrode scavenges oxygen from the TiO₂ layer, which results in uniformly distributed VO formation. Fig. 1 shows the I-V characteristics of the device. The I-V characteristics demonstrate bipolar resistive switching behavior between two stable nonvolatile states, i.e., the high resistance state (HRS) and the low resistance state (LRS). Stable bipolar resistive switching with an on-resistance/off-resistance (R_{on}/R_{off}) ratio of ~100 controlled by a small voltage of ±0.8 V was observed after completion of the forming processes. The forming process was performed in two steps. The first step was the irreversible breakdown of the Al₂O₃ layer, which occurred under application of a positive voltage on the Pt with a current limit of 10 mA. When the applied voltage was increased to +5 V, the current increased dramatically as the resistance decreased by two orders of magnitude. The system then changed from the initial state to an “intermediate” state. The second step was the creation of a TiO_{2-x} layer that included oxygen vacancies near the Pt electrode and the TiO₂ layer but without VO near the Pt-BE; this occurs on application of -2.2 V to the Pt-TE, and the system then changed from the “intermediate” state to the HRS. Using this type of structure, we can generate reproducible and stable switching between the two states, and electron transport occurs as a result of the movement of the VO. The structure becomes less conductive as the applied voltage becomes more negative.

We observed the resistive switching characteristics of Pt/Al₂O₃/TiO₂/Pt capacitors. The Pt/Al₂O₃/TiO₂/Pt capacitor exhibits bipolar resistive switching with two stable nonvolatile states of low and high resistance. The forming process occurs in two steps. The switching voltage is a small value of approximately ±0.8 V. The switching mechanism of the set and reset processes occurs because the VO transfer into the TiO₂ layer when voltage applied positive and negative directions.

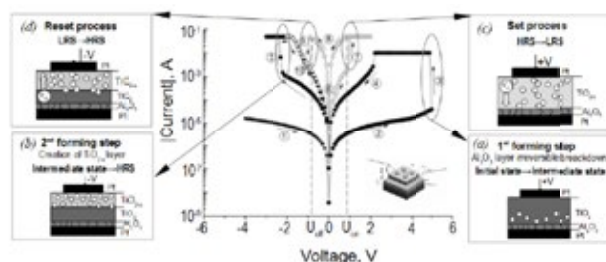


Fig. 1. I-V characteristics of Pt/Al₂O₃/TiO₂/Pt MIM capacitors, and schematic illustrations of (a) first and (b) second steps of forming process; (c) set and (d) reset switching processes.

References

- 1) L.O. Chua, *Appl. Phys. A* **102**, 765783 (2011).
- 2) L.O. Chua, *IEEE Trans.* **18**, 507 (1971).
- 3) L.O. Chua, S.M. Kang, *Proc. IEEE* **64**, 209 (1976).
- 4) R. Waser, M. Aono, *Nature Mater.* **6**, 833 (2007).
- 5) T. Nagata, Y. Yamashita, H. Yoshikawa, M. Imura, S. Oh, K. Kobashi, T. Chikyow, *Jpn. J. Appl. Phys.* **54**, 06FG01 (2015).
- 6) M.J. Kim, I.G. Baek, Y.H. Ha, S.J. Baik, J.H. Kim, D.J. Seong, S.J. Kim, Y.H. Kwon, C.R. Lim, H.K. Park, D. Gilmer, P. Kirsch, R. Jammy, Y.G. Shin, S. Choi, C. Chung, *IEEE IEDM*, p. 444 (2010).

Nano-Opto-Mechano-Electrical Studies in HRTEM

MANA Principal Investigator

MANA Scientist
MANA Research Associate
NIMS Post-Doctoral Researcher
Graduate Student

Dmitri GOLBERG

Masanori Mitome, Naoyuki Kawamoto
Ovidiu Cretu, Katherine Moore, Zhi Xu
Yanming Xue
Chao Zhang



1. Outline of Research

The fundamental and technological issues of flexible nanoscale electronics, optoelectronics and photovoltaics are coming to the forefront of the modern Materials Science. While trying to shed an additional light on these important problems, for the first time, we performed new challenging opto-mechano-electrical experiments inside a high-resolution transmission electron microscope (HRTEM) on individual nanostructures, Fig. 1, aimed at clear understanding of nanomaterial electromechanical and photo-responses to the external deformation stimuli.

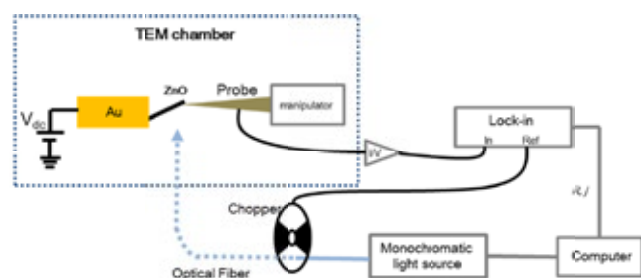


Fig. 1. Scheme of experimental configuration inside and outside of a 300 kV JEM-3100FEF (Omega Filter) HRTEM.

2. Research Activities

(1) Photocurrent spectroscopy on bent ZnO nanowires.

Photocurrent spectroscopy under bending of individual free-standing ZnO nanowires (NWs) inside HRTEM was firstly analyzed.¹⁾ By using an assembled optical *in situ* TEM system capable of scanning tunneling microscopy (STM) probing paired with light illumination, opto-mechano-electrical tripling phenomena in ZnO NWs were discovered. Splitting of photocurrent spectra at around 3.3 eV under *in situ* HRTEM NW bending directly corresponded to NW deformation. Theoretical simulation of a bent ZnO NW using Density Functional Tight Binding (DFTB) approach had an excellent agreement with the experimental data (Fig. 2). Splitting was nicely explained by a change in the valence band structure of ZnO NW due to a lattice strain, namely, the observed red and blue shifts of NW photocurrent peaks were confirmed to be directly related to the splitting of levels in the valence band at Γ point. The detected strain-induced splitting provides important clues for future flexible piezo-phototronics.

(2) Lateral piezopotential-gated transistor on individual ZnO nanowire.

We demonstrated a new design of a strain-gated single ZnO NW transistor made and tested inside HRTEM.²⁾ Our measurements showed that the NW conductivity decreases up to two orders of magnitude when a 2.63% bending strain is applied to it. The analysis revealed that the regarded

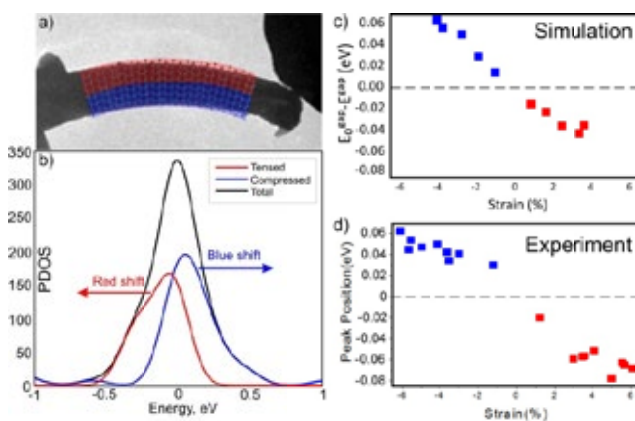


Fig. 2. (a) Simulated geometry of a bent ZnO nanowire in comparison with the experimental picture. (b) PDOS of extended (red) and compressed (blue) sides of the ZnO nanowire. Black curve denotes the total DOS for the bent wire. Bending strain is about 4%. (c) Dependence of the ZnO wire band gap on the bending deformation in the frame of the DFTB approach utilized; (d) Dependence of the photocurrent peak position on the bending strain obtained experimentally. Red and blue colours correspond to the extended and compressed regions of ZnO nanowires, respectively.

change in conductivity was not due to a Schottky barrier at the contact interface but originated from the carrier depletion caused by the lateral piezoelectric NW potential. Based on this finding, a new device performing as an ultimate strain gauge/sensor was designed (Fig. 3). The sensor possesses the key advantages: (i) Bending deformation is much easier to be actualized than compression/stretching; (ii) Not like the previously reported contact-modulated piezoelectric potential-gated transistors, Schottky contact is not necessary in our device. While working in the saturation region, both Ohmic and Schottky contacts are applicable; (iii) The setup conductivity is extremely sensitive to a bending strain. The new mechanism-driven piezo-transistor timely enriches the piezotronics device family. It particularly shows the unlimited possibilities when piezoelectricity is coupled to semiconductivity.

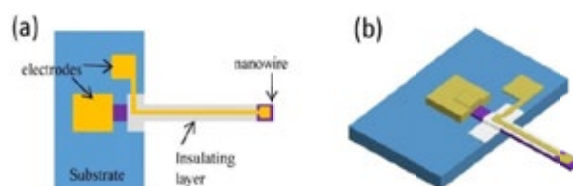


Fig. 3. Schematic drawing of a designed prototype ZnO nanowire strain sensor placed on the substrate. (a) Top view. (b) 3-D view.

References

- 1) C. Zhang, Z. Xu, D.G. Kvashnin, D.M. Tang, Y.M. Xue, Y. Bando, P.B. Sorokin, D. Golberg, *Appl. Phys. Lett.* **107**, 091103 (2015).
- 2) Z. Xu, C. Zhang, W.L. Wang, Y. Bando, X.D. Bai, D. Golberg, *Nano Energy* **13**, 233 (2015).

Nanogenerators as a New Energy Technology

MANA Principal Investigator **Zhong Lin WANG**
 (Satellite at Georgia Tech, USA)
 Graduate Student

Simiao Niu, Ruomeng Yu



1. Outline of Research

Triboelectric nanogenerator (TENG) technology has emerged as a new mechanical energy harvesting technology with numerous advantages.^{1,2)} We systematically analyzed the theoretical system of TENGs, which can be utilized as a guideline for TENG designers to continue improving TENG output performance.^{3,4)}

2. Research Activities

The characteristics of utilizing a TENG to charge a capacitor were discussed in depth. First, the easiest unidirectional charging was analyzed to show the importance of impedance match in the design of such systems. Then, a much more complicated multicycle charging process was analyzed to show the unique TENG charging characteristics. An optimum load capacitance was observed for the maximized energy storage. To obtain the optimized design strategy for such system, the analytical solution of the optimum load capacitance was detected and its dependence on the charging cycle numbers and TENG structural parameters was shown. Finally, corresponding experiments were performed to further validate the above theoretical prediction and show its application in guiding experiments.

The structure of this TENG is shown in Fig. 1(a) and its working principle is very similar to the single-electrode TENG. We can obtain the numerical results of this nonlinear time-variant system shown in Fig. 1(b) from the TENG-simulator demonstrated in our previous work. The simulation results are shown in Fig. 2. A saturation charging curve is observed for all the load capacitors, which is very similar to a typical resistor-capacitor (RC) charging curve in shape. At $t = 0$, the load capacitor is charging at a maximum speed. Then, the charging speed gradually slows down and finally the same saturation voltage ~ 104.8 V is reached for all the different load capacitors. It takes less time to charge a

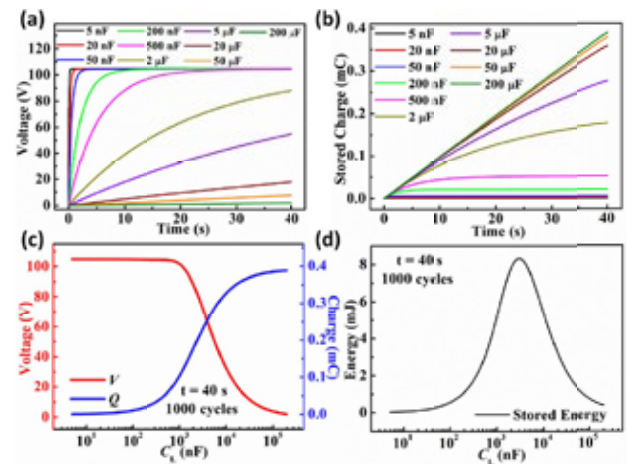


Fig. 2. TENG charging characteristics under periodic mechanical motion. (a) Voltage-time relationship at different load capacitances. (b) Stored charge time relationship at different load capacitances. (c) Influence of the load capacitance on the final voltage and charge stored in the load capacitor. (d) Final stored energy profile with load capacitance.

smaller C_L to reach its saturation voltage. However, a different trend is observed for the stored charges. At beginning, the curves for all load capacitors converge to one linear curve, with the charging rate of $2Q_{SC, max}$ per cycle. However, when time increases, the curves from small C_L shift downward first and finally get saturated. At this moment, very few charges can be pumped into the capacitor. The voltage and the stored charge of the load capacitor after 1000 charging cycles are shown in Fig. 2(c), which have the similar trend as the unidirectional charging case. When C_L is small enough, the voltage on the load capacitor is approximately its saturation voltage while the stored charges are close to zero and proportional to C_L . When C_L is large enough, the stored charges are approximately $2kQ_{SC, max}$ while the voltage is close to zero and inversely proportional to C_L . Similar to the previous unidirectional charging, an optimum capacitance for maximum stored energy is also observed in the transition region of C_L .

Experiments were performed to further validate our theoretical anticipation. Our work clearly shows the unique TENG charging characteristics, which can serve as an important guidance to design an integrated TENG energy harvesting system for practical application.

References

- 1) S.M. Niu, Y. Liu, Y.S. Zhou, S.H. Wang, L. Lin, Z.L. Wang, *IEEE Trans. Electron Devices* **62**, 641 (2015).
- 2) R.M. Yu, X.F. Wang, W.Z. Wu, C.F. Pan, Y. Bando, N. Fukata, Y.F. Hu, W.B. Peng, Y. Ding, Z.L. Wang, *Adv. Funct. Mater.* **25**, 5277 (2015).
- 3) S.M. Niu, Y. Liu, X.Y. Chen, S.H. Wang, Y.S. Zhou, L. Lin, Y.N. Xie, Z.L. Wang, *Nano Energy* **12**, 760 (2015).
- 4) S.M. Niu, Z.L. Wang, *Nano Energy* **14**, 161 (2015).

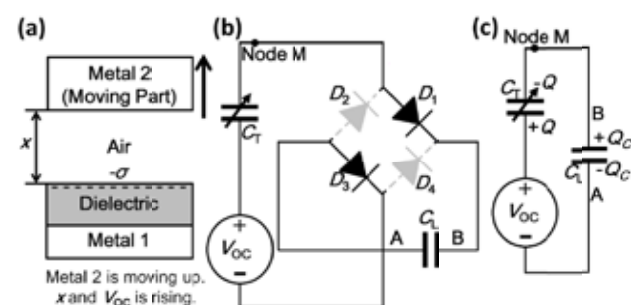


Fig. 1. Equivalent circuit diagram for TENG charging performance calculation under periodic mechanical motion. (a) Structure of the contact mode attached-electrode TENG used in the calculation. (b) Circuit diagram showing the conduction condition of full-bridge rectifier in the first half cycle. (c) Simplified circuit diagram under ideal diode approximation in the first half cycle.

Nanosheet Electronics

Associate Principal Investigator

MANA Scientist
Post-doc
Graduate Student (Waseda University)

Minoru OSADA

Takaaki Taniguchi
Junzheng Wang, Hyung-Jun Kim
Yoon-Hyun Kim, Lei Dong, Muhammad Shuaib Khan



1. Outline of Research

Two-dimensional (2D) materials with atomic scale thickness are emerging as a new frontier of materials science. The discovery of graphene can be considered as a defining point in the research and development of truly 2D material systems. This breakthrough has opened up the possibility of exploring the fascinating properties of non-graphene 2D nanosheets. In particular, 2D inorganic nanosheets will offer new properties and novel applications beyond graphene. We are working on the creation of 2D oxide nanosheets and the exploration of their novel functionalities in electronic applications.

2. Research Activities

(1) Monolayer Devices Based on 2D Nanosheets.¹⁾

We fabricated monolayer devices based on 2D oxide nanosheets, and explored novel electronic properties of genuine 2D systems. For this purpose, we demonstrated the possibility in quantifying the thicknesses in 2D oxide nanosheets, and proposed a universal optical method for rapid identification of single- to quindécuple-layers in oxide nanosheets ($\text{Ti}_{0.87}\text{O}_2$, $\text{CaNb}_3\text{O}_{10}$, $\text{Ca}_2\text{NaNb}_4\text{O}_{13}$, RuO_2 , MnO_2) and their architectures (Fig. 1). Combining this optical method, we newly developed nanosheet-transfer system to fabricate monolayer devices. We are now performing on the characterization for 2D phenomena in individual nanosheets (including high electron mobility in 2D semiconductors, superconducting properties in NbS_2 , Bi_2Te_3 , ferroelectricity/ piezoelectricity in perovskites).

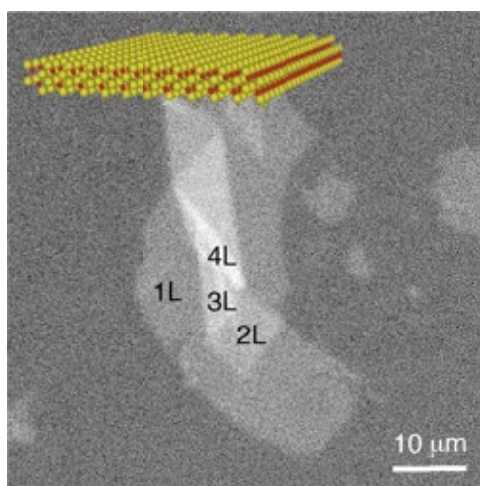


Fig. 1. Thickness identification of $\text{Ti}_{0.87}\text{O}_2$ nanosheet by optical microscopy.

(2) High-*k* Nanosheets and Their Applications.²⁻⁵⁾

We performed characterization and reliability test of

nanosheet-based high-*k* capacitors. Through various *in situ* characterizations, we found a robust thermal stability of titania and perovskite nanosheets. We extended our research to energy-storage devices. We found that perovskite nanosheets exhibited outstanding energy storage capabilities, even comparable to that of Li-ion battery. Nanosheet capacitors also showed thermal stability even at 300 °C.^{2,3)} The simultaneous improvement of energy density and thermal stability in dielectric capacitors is of critical importance, and perovskite nanosheet has great potential for a rational design and construction of new energy storage devices.

We also utilized high-*k* nanosheets as building blocks in the nanoarchitectonics, and successfully developed new artificial materials including Pb-free ferroelectrics (Fig. 2),⁴⁾ multiferroics, magneto plasmonic metamaterials, actuator crystals,⁵⁾ etc.

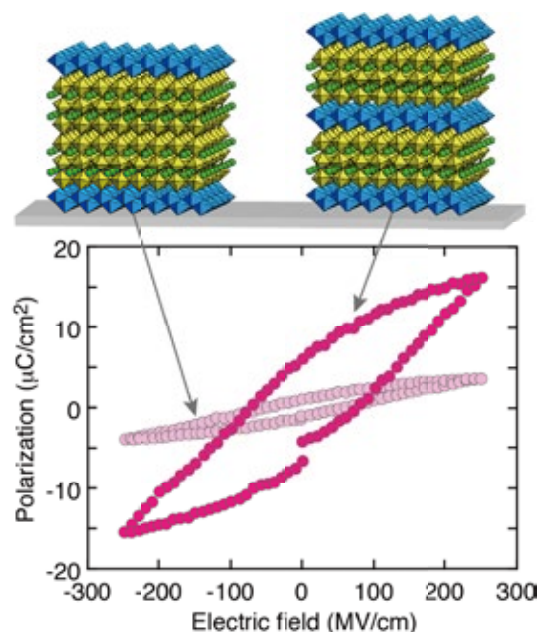


Fig. 2. New ferroelectrics ($\text{Ti}_{0.87}\text{O}_2/\text{Ca}_2\text{Nb}_3\text{O}_{10}$) using nanosheet architectonics.

References

- 1) H.J. Kim, M. Osada, Y. Ebina, W. Sugimoto, K. Tsukagoshi, T. Sasaki, *Sci. Rep.* **5**, 19402 (2015).
- 2) B.W. Li, M. Osada, Y. Ebina, K. Akatsuka, K. Fukuda, T. Sasaki, *ACS Nano* **8**, 5449 (2014).
- 3) Y.H. Kim, H.J. Kim, M. Osada, B.W. Li, Y. Ebina, T. Sasaki, *ACS Appl. Mater. Interface* **6**, 19510 (2014).
- 4) Y.H. Kim, L. Dong, M. Osada, B.W. Li, Y. Ebina, T. Sasaki, *Nanotechnology*, **26**, 244001 (2015).
- 5) Y.S. Kim, M. Liu, Y. Ishida, Y. Ebina, M. Osada, T. Sasaki, T. Hikima, M. Takata, T. Aida, *Nature Mater.* **14**, 1002 (2015).

Nano-System Architectonics

MANA Principal Investigator Masakazu AONO

(MANA Director-General, Field Coordinator)

MANA Scientist

MANA Research Associate

Yuji Okawa, Makoto Sakurai, Hideo Arakawa,
Masanori Kohno
Koley Pradyot, Elisseos Verveniots



1. Outline of Research

The goal of our Nano-System Organization Group is to create new nano-systems having novel functionality by the use of various key technologies and theories based on “nanoarchitectonics” and put the created nano-systems to practical use for contributing to our society in such forms as next-generation information processing and communication and environmental and energy sustainability.

2. Research Activities

Aiming at the realization of single-molecule electronics, we have developed a novel method to wire two conductive polydiacetylene (PDA) chains to a single organic molecule (phthalocyanine (Pc)), which we named “chemical soldering”. As the next step, we are trying to measure the electric properties of the PDA-Pc-PDA diode system using a sophisticated graphene substrate. Fig. 1a shows a schematic illustration of the measurement system. In the ‘insulated region’ in the figure, the conduction properties of graphene are locally tuned by embedding low-density defects in the lattice of graphene, by using an accelerated helium ion beam. Namely, graphene locally becomes insulator by Anderson localization. By fabricating the PDA-Pc-PDA system on it, the electric current will flow through the pristine graphene-PDA interface and thus we can measure the electric properties of the system. In order to realize this measurement, the selection of the substrate under the graphene is very important: this should be atomically flat and insulating. We explored several substrates and found that hexagonal boron nitride and sapphire are promising substrates for this purpose. Fig. 1b is a scanning electron microscopy (SEM) image of a fabricated test system. Here, graphene and metal electrodes are deposited on an ultrapolished sapphire substrate, followed by irradiating a thin line with accelerated helium ion beam. We are now evaluating the measurement system.

We have studied a long-standing and central issue in solid-state physics regarding the nature of the Mott

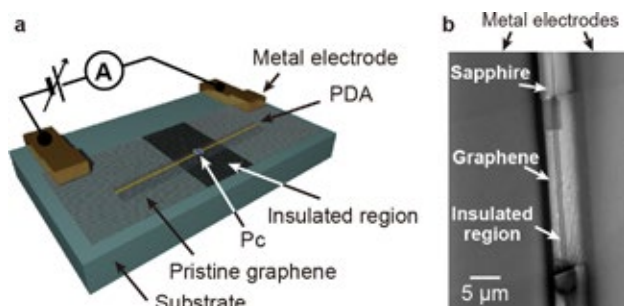


Fig. 1. (a) Schematic illustration of the measurement system. PDA-Pc-PDA system is fabricated on the locally insulated graphene substrate. (b) SEM image of a locally insulated graphene on a sapphire substrate.

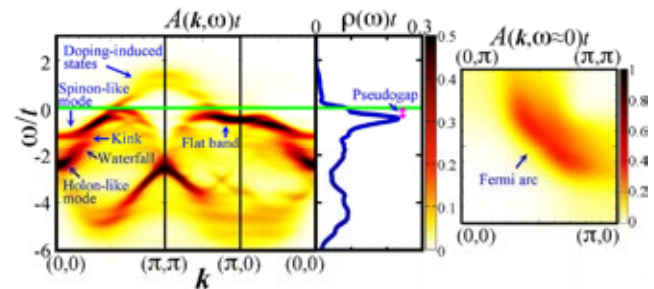


Fig. 2. Numerical results for the spectral function $A(k, \omega)$ and the single-particle density of states $\rho(\omega)$ of the 2D t - J model near the Mott transition, taken from Ref. 2. The features indicated on the panels correspond to those observed in cuprate high- T_c superconductors.

transition: how electrons behaving single particles in a metal change into those exhibiting spin-charge separation in a Mott insulator. We have theoretically shown that the magnetically excited states of a Mott insulator generally emerge in the single-particle spectrum with the dispersion relation shifted by the Fermi momentum following the doping of the Mott insulator.¹⁾ This implies that the low-energy electrons behaving single particles lose their spectral weights in the electron-addition spectrum while their dispersion relation transforms into the momentum-shifted magnetic dispersion relation of the Mott insulator as the Mott transition is approached from the metallic side. This suggests that the Mott transition is characterized by freezing of the charge degrees of freedom with the spin degrees of freedom active.

In addition, we have collectively explained various anomalous features observed in cuprate high-temperature (high- T_c) superconductors by using the two-dimensional (2D) t - J model (a minimal model of high- T_c cuprates, Fig. 2).²⁾ The results suggest that the anomalous features can be interpreted in terms of characteristics near the Mott transition, such as the reduction in spectral weights and the emergence of multiple modes having different energy scales, which are difficult to interpret from conventional single-particle viewpoints. Also we have studied unique hierarchical microstructures of biomaterials^{3,4)} to achieve platforms of next-generation devices. Defects-manipulation by stress and voltage in SnO_2 microrod devices produced novel photodetectors, which gave a solution to the persistent photoconductivity (PPC) problem in wide-band gap semiconductors.⁵⁾

Related Publications

- 1) M. Kohno, *Phys. Rev. B* **92**, 085129 (2015).
- 2) M. Kohno, *Phys. Rev. B* **92**, 085128 (2015).
- 3) P. Koley, M. Sakurai, M. Aono, *J. Mater. Sci.* **50**, 3139 (2015).
- 4) P. Koley, M. Sakurai, M. Aono, *ACS Appl. Mater. Interfaces* **8**, 2380 (2016).
- 5) K.W. Liu, M. Sakurai, M. Aono, D. Shen, *Adv. Funct. Mater.* **25**, 3157 (2015).

MANA Brain: Neuromorphic Atomic Switch Networks

MANA Principal Investigator

(Satellite at UCLA, USA)
MANA Satellite Vice Director
Student Researchers

James K. GIMZEWSKI

Adam Z. Stieg
Renato Aguilera, Eleanor Demis, Kelsey Scharnhorst



1. Outline of Research

Development of cognitive computing technology and hardware is hampered by the current limits of complementary metal oxide semiconductor (CMOS) operating principles and difficulties in utilizing high density interconnections meaningfully. Atomic Switch Networks (ASNs) are a unique platform specifically developed to overcome the current barriers to realizing cognitive and neuromorphic technology through a merger of top-down and bottom-up methods. ASNs are composed of a massively interconnected network of atomic-scale switches and are structurally reminiscent of the brain. ASNs possess memory capacity, multi-state switching, power-law dynamics and non-linear transformations of input signals. Such memory and complexity are characteristic of biological neurons, enabling the ASN as a potential hardware implementation for next-generation computational paradigms that fall into the field of natural computing, such as reservoir computing (RC).

2. Research Activities

ASN devices consist of a vast number of interacting nonlinear elements in (1) scalable self-organized systems which exhibit (2) emergent complex behaviors which (3) can be applied towards the field of natural computing.

(1) Next-generation devices.¹⁾

Previously reported ASN devices have been scaled from 16 I/O electrodes to 128 in order to more effectively characterize spatiotemporal network dynamics as shown in Fig. 1. The centrally-located network has quadrupled in size and measurement channels (64) compared to previous generation devices. Despite this increase in size, the same emergent complex behaviors have been observed.

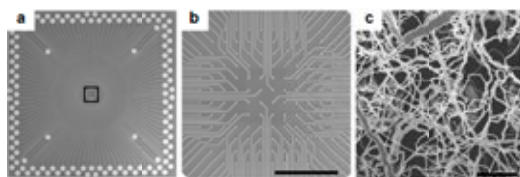


Fig. 1. A 128 electrode device (left) with an inner electrode array (center) and a Ag/Ag₂S/Ag ASN network (right). A custom electrical set up is capable of recording 64 channels of data.

(2) Nonlinear dynamics.²⁾

Interactions amongst atomic switches, facilitated by the recurrently connected network of silver nanowires, produce emergent, system-wide behaviors in the measured output including: 1/f noise, temporal metastability, and persistent fluctuations correlated in space and time indicating a critical regime. Due to the volatility of individual atomic switches, the ASN holds constantly reconfiguring potential pathways and results in robust electrical activity distributed through the network. These nonlinearly transformed signals, shown in Fig. 2, vary across the network and support the ASNs potential application to natural computing problems.

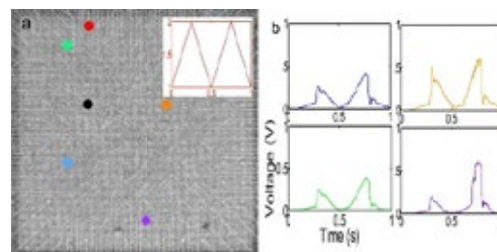


Fig. 2. A unipolar 2V triangle wave (inset) is input into the ASN at the red point and grounded at the black point. a) Distributed network activity causes voltage signals that are input to the device to be transformed into higher-dimensional output representations. All 64 channels show the great diversity of behavior, and several color-coded (b) channels are plotted to show the variation in output.

(3) Natural computing.³⁾

RC has become an accepted method for utilizing dynamical systems to perform computation due to its versatility in applications such as speech recognition, pattern classification and time series prediction. The ASN is a unique physical platforms capable of performing RC. All necessary criteria such as short-term memory, increased fault tolerance, and an arbitrarily scalable number of higher-dimensional outputs are fulfilled by the ASN. Within the context of the RC, each atomic switch is a functional node in the reservoir and the connective weights between each node are mediated by the silver nanowires. Waveform regression is an important prerequisite for RC and experimental performance of various waveform tasks using ASN devices are presented in Fig. 3.

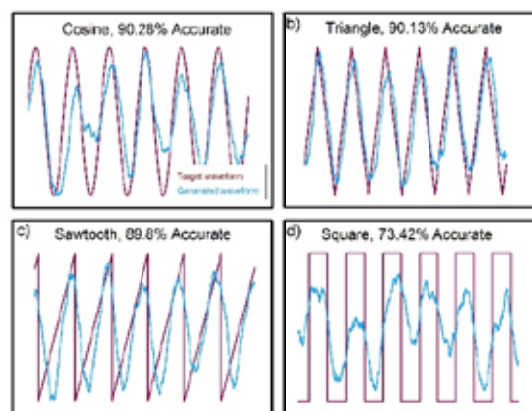


Fig. 3. Using the ASN to transform a sinusoidal input signal into various output waveforms (sawtooth, square, triangle, and cosine). The desired signal (red) and the computed signal (blue) are shown. Accuracy w.r.t. the desired signal is reported.

Selected Publications with MANA recognition

- 1) E. Demis, R.C Aguilera, H.O. Sillin, K. Scharnhorst, E.J. Sandouk, M. Aono, A.Z. Stieg, J.K Gimzewski, *Nanotechnology* **26**, 204003 (2015).
- 2) E.J. Sandouk, J.K. Gimzewski, A.Z. Stieg, *Sci. Technol. Adv. Mater.* **16**, 054004 (2015).
- 3) R.C. Aguilera, E. Demis, K. Scharnhorst, A.Z. Stieg, M. Aono, J.K. Gimzewski, *IEEE International Interconnect Technology Conference*, p. 165 (2015). DOI: 10.1109/IITC-MAM.2015.7325611.

Novel Quantum Functionality in Topological Systems

MANA Principal Investigator
 MANA Research Associate
 NIMS Postdoctoral Scientist
 Graduate Student

Xiao HU
 Takuto Kawakami, Rui Yu, Hai Li
 Bin Xi
 Feng Liu, Zhao Huang, Long-Hua Wu



1. Outline of Research

The discovery of quantum Hall effect (QHE) by von Klitzing opened a new chapter in condensed matter physics. It was revealed that the integer coefficient in Hall conductance is given by the Chern number which is the integration of Berry curvature associated with the Bloch electronic wave functions in momentum space. Since then to explore possible topological states in terms of spin-orbit coupling and magnetic properties inherent in materials, instead of a strong external magnetic field required by the QHE, has been one of the main driving forces in study of condensed matter physics. Similar to the QHE, an insulator of quantum anomalous Hall effect (QAHE) supports dissipationless edge current.¹⁾

The concept of topology fostered for electrons has been extended to a wealth of systems such as superconductors and electromagnetic (EM) waves. It is revealed theoretically that in a topological superconductor, unique quasiparticle excitations known as Majorana bound states (MBSs) obey non Abelian statistics and can be used for implementing decoherence-free quantum computation. In topological photonic crystals, unidirectional propagation of light and/or microwave can be achieved at the sample edge. To explore novel functionality derived from nontrivial topology is one of the new frontiers of materials science.

2. Research Activities

(1) Spin texture of the Majorana bound state.²⁾

In terms of Bogoliubov-de Gennes approach, we investigate MBS in vortex of topological superconductor as shown schematically in Fig. 1. Mapping out the local density of states (LDOS) of quasiparticle excitations as a function of energy and distance from vortex center, it is found that the spectral distribution evolves from V-shape to Y-shape with emergence of MBS upon variation of chemical potential, consistent with the STM/STS measurement in a very recent experiment. Moreover, we demonstrate that as shown in Fig. 1 there is a checkerboard-type pattern in the relative LDOS between the spin-up and -down channels,

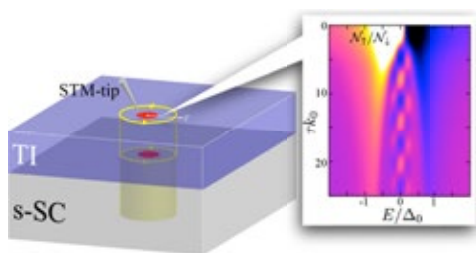


Fig. 1. Schematics for the hetero structure of 3D topological insulator and s-wave superconductor where two MBSs appear as denoted by the red dots. The relative spin-resolved LDOS as a function of energy and distance from the vortex center exhibits a checkerboard-type pattern.

where the quantum mechanical wave function of MBS manifests itself clearly as a single quantum state. Therefore, spin-resolved STM/STS technique is expected to be able to provide phase sensitive evidence for MBS in topological superconductor.

We also investigate one-dimensional (1D) MBSs realized in terms of the helical edge states of a 2D quantum spin Hall insulator (QSHI) in a hetero structure with a superconducting substrate and two ferromagnetic insulators (FIs). We demonstrate that there is a helical spin texture in the MBS wave function with a pitch proportional to the Fermi momentum. We reveal that the interference between the spin textures of two MBSs gives rise a unique fractional Josephson relation.

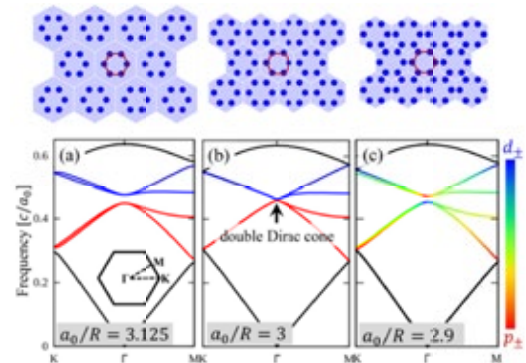


Fig. 2. Structure and photonic band for photonic crystals (PCs) of dielectric cylinders forming triangular lattice of hexagons (i.e. six neighboring cylinders). Center: Dirac semi-metallic PC with lattice constant corresponding to honeycomb lattice; Left/Right: trivial/ topological insulating PC with larger/smaller lattice constant.

(2) Topological photonics by plain dielectric material.³⁾

We propose to derive topological photonic states purely based on conventional dielectric materials by deforming a honeycomb lattice of cylinders into a triangular lattice of cylinder hexagons as shown in Fig. 2. The photonic topology is associated with a pseudo time-reversal (TR) symmetry constituted by the TR symmetry respected in general by Maxwell equations and the C_6 crystal symmetry upon design, which renders the Kramers doubling in the present photonic system. It is shown explicitly that the role of pseudo spin is played by the angular momentum of wave functions of electromagnetic fields. We solve Maxwell equations and demonstrate the new photonic topology by revealing pseudo-spin-resolved Berry curvatures of photonic bands and helical edge states characterized by Poynting vectors.

References

- 1) H.M. Weng, R. Yu, X. Hu, X. Dai, Z. Fang, *Adv. Phys.* **64**, 227 (2015).
- 2) Y.T. Kawakami, X. Hu, *Phys. Rev. Lett.* **115**, 177001 (2015).
- 3) L.H. Wu, X. Hu, *Phys. Rev. Lett.* **114**, 223901 (2015).

Surface Atomic Scale Logic Gate

MANA Principal Investigator
(Satellite at CNRS Toulouse, France)
Toulouse Scientist
MANA Research Associate

Christian JOACHIM

Mohamed Hliwa
Jorges Echeverria, Maricarmen Grisolia, Ghassen Dridi
Delphine Sordes, Jianshu Jiang



1. Outline of Research

The Pico-Lab CEMES-CNRS Toulouse MANA satellite is working on the experimental and theory of QHC logic gates design, their current intensity drive, their mechanical inputs and on the exploration of the atomic scale logic gate complexity roadmap to master the emergence of a maximum quantum computing power inside a single molecule or at the surface of a passivated semi-conductor.

2. Research Activities

(1) Running the LT-UHV – 4 STM/NC-AFM & UHV SEM.

The Toulouse MANA satellite is now running its LT-UHV 4 STM/NC-AFM & UHV SEM equipment. Two probes floating dI/dV experiments were performed on the Au(111) surface with an inter tip distance below 1 μm (Fig. 1).¹⁾ The first scanning, I-Z and I-V measurements were performed on an UHV debonded Si(100)H surface on purpose supported by a non-doped Si 1.5 cm x 1.5 cm sample diced from a 200 mm wafer in preparation of atomic scale logic gate construction and interconnects.¹⁾

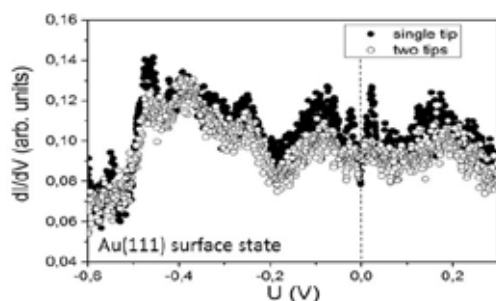


Fig. 1. 1 tip and 2 tips (floating ground) dI/dV recording on the Au(111) surface with an atomic scale positioning precision of the 2 tips and a 800 nm apex to apex inter tip distance on the surface.

(2) Design of complex QHC logic gates.

The mathematics behind the Quantum Hamiltonian Computing (QHC) theory of designing Boolean logic gates with a quantum system have been now fully described and related to the quantum eigenvalue repulsion effect. QHC 2 inputs-1 output AND, NAND, OR, NOR, XOR, NXOR Boolean matrices were constructed using their corresponding quantum graph followed by the construct of a QHC 1/2 adder requiring only 6 states to fulfil a 1/2 adder Boolean logical truth table for 2 inputs (Fig. 2). This was extended for the design of a complete 2 x 2 digital adder requiring only 16 quantum states to be compared with the 32 transistors required in nano-electronics.²⁾

(3) Construction of a DB QHC logic gate.

Starting from the above quantum graph theory, we have reported the design and LT-UHV-STM construction of the first ever QHC atomic scale Boolean logic gate constructed atom by atom on Si(001)H. The NOR/OR gate truth table was confirmed by dI/dV local STM measurements to follow how the surface states of the QHC quantum circuit are

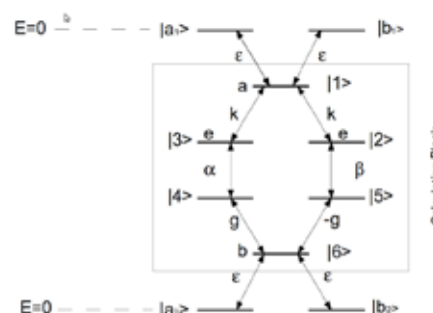


Fig. 2. The 10 states quantum graph of a QHC $\frac{1}{2}$ adder with 6 states for the calculating block and 2 per reading heads. (α , β) are the electronic couplings for the classical logical inputs shared by the bottom and down part of this diagram. The coupling k , g and energies a , b , e are the structural parameters defining the $\frac{1}{2}$ adder Boolean truth table (output at $E = 0$ eV).²⁾

shifted in energy according to the input logical status.³⁾

(4) Mechanics.

We continued to explore the driving power of an inelastic tunneling current able to switch a molecule-latch or to drive a molecule-motor. With MANA Tsukuba, it was demonstrated and interpreted⁴⁾ how a single molecule motor rotate step by step a nearby single molecule-rotor (Fig. 3). In parallel, it was demonstrated how a 4 wings molecule rotates step by step one or two Au atoms.⁵⁾ This is a proof that a single Au logical input acting on a molecule QHC logic gate can be triggered not only by the tip apex of an STM but also by another nearby molecule in the prospect to match the scale difference between the actual smallest 30 nm in diameter solid state nano-gears and the atomic scale.

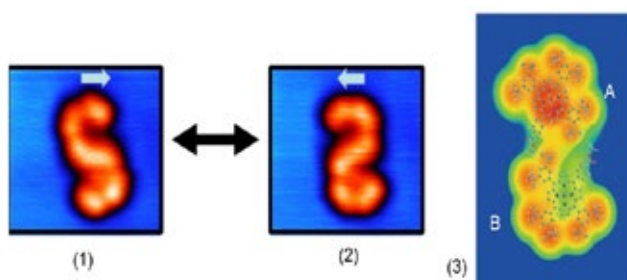


Fig. 3. Extraction (3) from ESQC constant current STM calculations of the atomic coordinates of a motor-rotor single molecule complex rotating clockwise (1) and anti-clockwise (2) depending on the position of the molecule-motor B relative to the molecule rotor A.³⁾

References

- 1) J. Yang, D. Sordes, M. Kolmer, D. Martrou, C. Joachim, *Eur. J. Phys.*, in press (2016).
- 2) G. Dridi, R. Julien, M. Hliwa, C. Joachim, *Nanotechnology* **26**, 344003 (2015).
- 3) M. Kolmer, R. Zuzak, G. Dridi, S. Godlewski, C. Joachim, M. Szymanski, *Nanoscale* **7**, 12325 (2015).
- 4) P. Mishra, J.P. Hill, S. Vijayaraghavan, W. Van Rossom, S. Yoshizawa, M. Grisolia, J. Echeverria, T. Ono, K. Ariga, T. Nakayama, C. Joachim, T. Uchihashi, *Nano Lett.* **15**, 4793 (2015).
- 5) R. Ohmann, J. Meyer, A. Nickel, J. Echeverria, M. Grisolia, C. Joachim, F. Moresco, G. Cuniberti, *ACS Nano* **9**, 8394 (2015).

Integration of Nano Functionality for Novel Nanosystems

MANA Principal Investigator **Tomonobu NAKAYAMA**

(MANA Administrative Director from May 2015)
MANA Scientist

MANA Research Associate
Visiting Scientist
Senior Visiting Scientist
Graduate Student

Takashi Uchihashi, Yoshitaka Shingaya,
Katsumi Nagaoka
Rintaro Higuchi, Shrestharkha Goswami, Ming Li
Osamu Kubo, Sho Tonegawa
Makoto Sawamura, Masami Suganuma
Miao Difei, Li Qiao



1. Outline of Research

We develop novel techniques and methodologies toward the realization of novel nanosystems for future information technology. Development and application of multiple-probe scanning probe microscopes (MP-SPMs) and fundamental researches on molecular manipulations, low-dimensional nanostructures and neuromorphic networks, are explored. These research activities contribute to functionalizing nanosystems to transmit and transduce electrical, optical, mechanical, ionic and magnetic signals.

2. Research Activities

(1) Multiple-probe Scanning Probe Microscopes.^{1,2)}

MP-SPM has simultaneously and independently controlled 2 to 4 scanning probes¹⁾ which are brought into electrical contact to a single nanostructure and reveals its electrical property.²⁾ Implementation of Kelvin-probe force microscopy (KPFM) mode in our MP-SPM realized non-contact observation of potential distribution over a nanosystem under a current bias. As an alternative non-contact MP-SPM operation, eddy-current damping microscopy (ECDM) mode was successfully introduced by detecting eddy-current induced damping of an oscillating magnetic probe, which is useful to obtain a conductance distribution over the nanosystem.

(2) Fabrication of functional nanostructures and nanomaterials.^{3,4)}

Creating functional nanostructures and nanomaterials, followed by measurements of their physical properties, is an important part of our research towards a realization of functional nanosystems. We are currently working on surface superconductivity for quantum computing, neuromorphic networks for massively parallel analog computing (brain-type computing), and other related functionalities of nanoscale structures and materials.

For neuromorphic networks, we have developed several

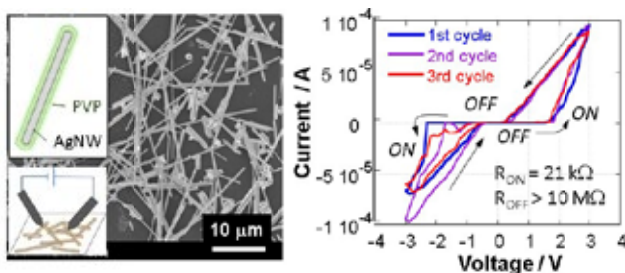


Fig. 1. Chemically prepared Ag nanowires (AgNW) covered with insulating PVP layer was used to form neuromorphic network. Using MP-SPM, interesting “network switching” was found as shown in the right panel. ON/OFF ratio of more than 500 was observed.

conductive nanowires and fibers³⁾ and assembled into the form of entangled complex network. In the case Ag nanowires (AgNWs), we found interesting switching properties as shown in Fig. 1. It is interesting to point out that the observed switching behavior seem to be cooperative property of massive number of junctions involved in the AgNW network. Further investigation on the AgNW network showed the ON and OFF states respectively exhibit different fluctuation nature in the noise of transmitting electrical current, indicating a possibility of a new devices utilizing dynamic noise control.

We also started working on surface-supported molecular motors,⁴⁾ which are nanomechanical devices of particular interest in terms of future nanoscale applications. Platinum-porphyrin-based supramolecularly-assembled dimers are formed on an Au(111) surface and we demonstrated that they can be rotated with high directionality using the tunneling current of a scanning tunneling microscope (STM). Rotational direction is dependent on the surface chirality of the dimer and the chirality can be inverted *in-situ* by STM-induced intra-dimer rearrangement (Fig. 2). This result opens the way for the construction of complex molecular machines on a surface to mimic at a smaller scale versatile biological supramolecular motors. This work was done in collaboration with Dr. J. Hill, Dr. K. Ariga, and Dr. C. Joachim of MANA and Prof. T. Ono of Kyoto University.

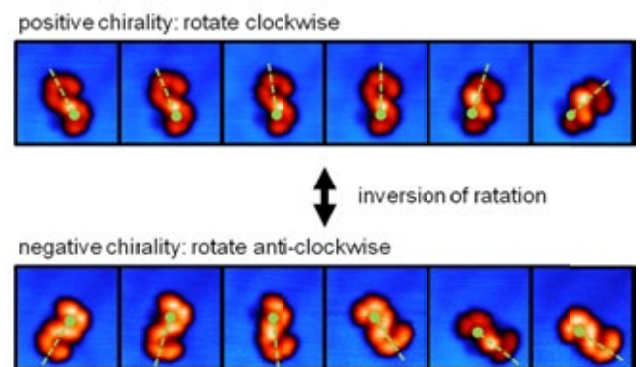


Fig.2. Rotation and directional switching of a Pt-porphyrin-based supramolecularly-assembled dimer on a Au(111) surface imaged with a scanning tunneling microscope.

References

- 1) T. Nakayama, O. Kubo, Y. Shingaya, S. Higuchi, T. Hasegawa, C.S. Jiang, T. Okuda, Y. Kuwahara, K. Takami, M. Aono, *Adv. Mater.* **24**, 1675 (2012).
- 2) O. Kubo, Y. Shingaya, M. Nakaya, M. Aono, T. Nakayama, *Appl. Phys. Lett.* **88**, 254101 (2006).
- 3) R. Creasey, Y. Shingaya, T. Nakayama, *Mater. Chem. Phys.* **158**, 52 (2015).
- 4) P. Mishra, J.P. Hill, S. Vijayaraghavan, W. Van. Rossom, S. Yoshizawa, M. Grisolia, J. Echeverria, T. Ono, K. Ariga, T. Nakayama, C. Joachim, T. Uchihashi, *Nano Lett.* **15**, 4793 (2015).

Self-Limiting Layer-by-Layer Oxidation of Atomically Thin WSe₂

MANA Principal Investigator
MANA Scientist
MANA Research Associate

Kazuhiro TSUKAGOSHI
Shu Nakaharai
Mahito Yamamoto



1. Outline of Research

Growing a high-quality oxide film with a tunable thickness on atomically thin transition metal dichalcogenides is of great importance for the electronic and optoelectronic applications. Here we report that ozone exposure of atomically thin WSe₂ leads to homogenous oxidation of the surface with a self-limiting thickness from single- to trilayers, depending on temperatures.¹⁾

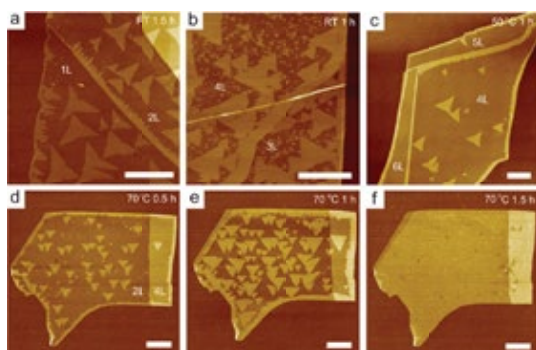


Fig. 1. AFM images of thin WSe₂ flakes on SiO₂ after O₃ exposure (a) at RT for 1.5 h, (b) at RT for 1 h, (c) at 50 °C for 1 h, and at 70 °C for (d) 0.5, (e) 1, and (f) 1.5 h. The number of layers (NL with N = 1 to 6) of each flake is indicated. The scale bars are 2 μm.

2. Research Activities

Here, we demonstrate that ozone (O₃) exposure leads to homogeneous surface oxidation of atomically thin WSe₂ with a self-limiting thickness from single- to trilayers, depending on temperature. Below 100 °C, the O₃ treatment of WSe₂ results in the formation of tungsten oxide with a thickness of about 2 nm, nucleated from edges and defects on the surface. With further exposure to O₃, the oxides grow laterally along selenium zigzag edge ($\bar{1}010$) orientations,

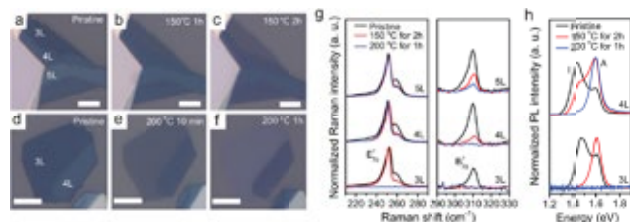


Fig. 2. Optical images of trilayer (3L), four-layer (4L), and five-layer (5L) WSe₂ (a,d) before and after the O₃ treatment (b) at 150 °C for 1 h, (c) at 150 °C for 2 h, (e) at 200 °C for 10 min, and (f) at 200 °C for 1 h. The scale bars are 5 μm. (g) Raman spectra of 3L to 5L WSe₂ before (black lines) and after the O₃ treatment at 150 °C for 2 h (red lines) and at 200 °C for 1 h (blue lines). The Raman intensities are normalized with the E1 2g peak intensity of pristine 3L WSe₂. (h) PL spectra of 3L and 4L WSe₂ before (black lines) and after the O₃ treatment at 150 °C for 2 h (red lines) and at 200 °C for 1 h (blue lines). The PL peak intensities are normalized with the I peak intensity of pristine 3L WSe₂.

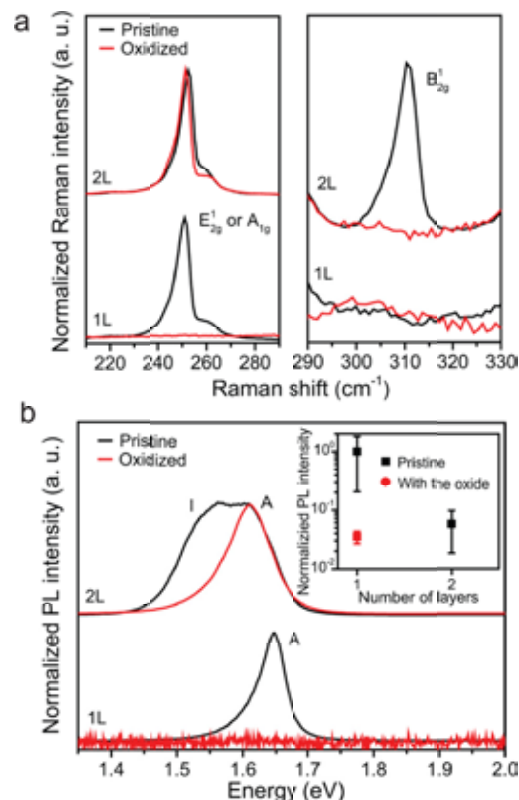


Fig. 3. (a) Raman spectra of single-layer (1L) and bilayer (2L) WSe₂ before (black lines) and after (red lines) the O₃ treatment at 100 °C for 1 h. The Raman peak intensities of pristine and oxidized 2L WSe₂ are normalized with the E12g peak intensity of pristine 1L WSe₂. (b) PL spectra of 1L and 2L WSe₂ before (black lines) and after (red lines) the O₃ treatment at 100 °C for 1 h. The PL intensities of pristine and oxidized 2L WSe₂ are normalized with the A peak intensity of pristine 1L WSe₂. The inset shows normalized PL intensities of the A peaks of 1L and 2L WSe₂ without (black squares) and with (red circle) the top oxide.

until the top layer is fully oxidized (Fig. 1). However, no underlying layers are oxidized at those temperatures. With increasing temperature, oxidation progresses layer-by-layer up to trilayers (Fig. 2). The oxide films formed on WSe₂ are nearly atomically flat. Single-layer WSe₂ produced by surface oxidation of a few-layer counterpart shows well-defined Raman and photoluminescence peaks consistent with single layer thickness but with shifts in peak positions due to hole doping (Fig. 3). Our findings are a first step toward controllable growth of oxides on layered transition metal dichalcogenides for applications ranging from tunnel barriers to gate dielectrics.

Reference

- 1) M. Yamamoto, S. Dutta, S. Aikawa, S. Nakaharai, K. Wakabayashi, M.S. Fuhrer, K. Ueno, K. Tsukagoshi, *Nano Lett.* **15**, 2067 (2015).

Nanoarchitectonics of Hybrid Artificial Photosynthetic System

MANA Principal Investigator

Jinhua YE

(Field Coordinator)
MANA Research Associate
Graduate Student

Huimin Liu, Huabin Zhang, Kun Chang
Guigao Liu, Mu Li, Qing Yu, Li Shi



1. Outline of Research

Fundamental research and development of artificial photosynthesis technology comprising of nano-structured metal/inorganic/organic semiconductor hybrid system will be conducted. Special attention will be paid to the design of new nano semiconductor materials harvesting major part of solar light, understanding of interactions between photon, carrier, molecules, and manipulation of these interactions for realization of higher photon efficiency by nanoarchitectonics. A breakthrough in the efficiency of solar-chemical energy conversion is expected.

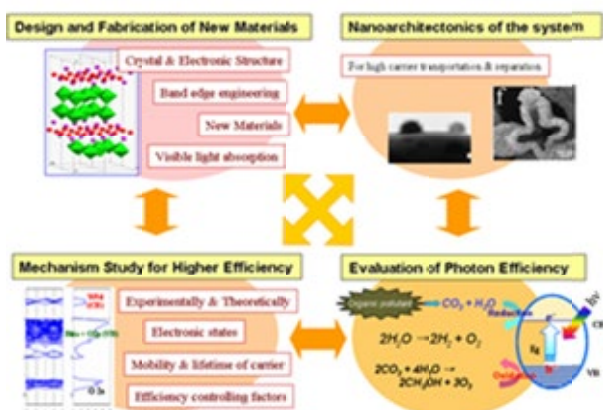


Fig. 1. Four sub-themes and their organic coordination for conducting effective materials exploration research.

In order to accomplish this purpose, we set following four sub-themes and are conducting the materials exploration research effectively by organically coordinating these sub-themes (Fig. 1):

1) Design and fabrication of new semiconductors which can utilize solar energy sufficiently by energy band structure engineering, with the help of theoretical calculation basing on the first principle theory. Engineering of band gap as well as CB, VB potentials will be carried out simultaneously to meet the potential requirement of photosynthetic reaction.

2) Nanoarchitectonics of the photosynthesis system will be conducted, by not only fabrication of nano particles using various soft chemical method, but also assembling of nano-metal/nano-oxide hybridized system to achieve efficient transportation and separation of electron-hole charge carriers.

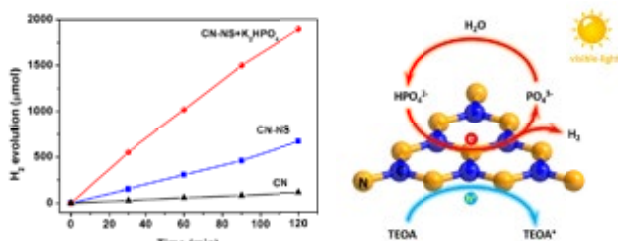


Fig. 2. Left: H_2 production over $g-C_3N_4$ nanosheets with K_2HPO_4 . Right: Schematic illustration of photocatalytic H_2 evolution under the proton-reduction mechanism involving HPO_4^{2-} .¹⁾

3) Evaluation of photon efficiency in various reactions will be performed using a solar-simulator and various gas chromatography.

4) Photosynthetic mechanism will be investigated experimentally and theoretically, to establish guidelines for development of higher efficient system.

2. Research Activities

(1) *Highly efficient photocatalytic H_2 production via natural photosynthesis mimicking.*¹⁾

Inspired by the vital roles of phosphates in natural photosynthesis, we succeeded in exploring an environmental “phosphorylation” strategy (precisely, the presence of HPO_4^{2-} ions) for achieving highly efficient photocatalytic H_2 production over graphitic carbon nitride ($g-C_3N_4$) nanosheets (Fig. 2), which is nearly three times higher than the present record. Such significant improvement in H_2 production relies on the multi-functions of phosphates resembling those in natural photosynthesis: as a proton pump facilitating the proton transfer in reaction solutions, and as a mediator directly participating in proton reduction, thus leading to a Calvin-cycle-like H_2 -evolution pathway. This strategy could also be applied to other photocatalysis system and provide a promising and facile approach to highly efficient photocatalysis for solar-energy conversion.

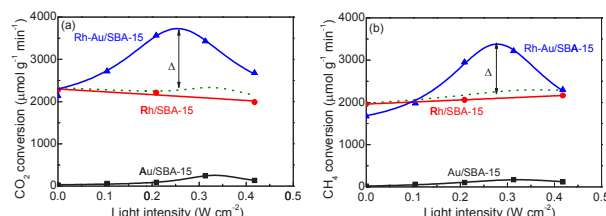


Fig. 3. (a) CH_4 conversion and (b) CO_2 conversion in DRM over the catalysts at different light intensities.²⁾

(2) *Exploiting CO_2 reforming of methane as a novel CO_2 photoreduction method.*²⁾

Visible light assisted thermal-driven CO_2 reforming of methane (DRM) was firstly developed as a novel method for CO_2 photoreduction. Rh-Au/SBA-15 was synthesized and employed as catalyst in this reaction with Rh and Au playing the roles as thermal-driven active site and plasmonic promoter, respectively (Fig. 3). The activity of Rh-Au/SBA-15 was 1.7 times enhanced with visible light irradiation. Mechanism study revealed that the hot electrons excited via plasmonic Au facilitated the activation of CO_2 and CH_4 under thermal assistance. This work provides a new route for CO_2 photoreduction and offers a distinctive method to photo-catalytically activate nonpolar molecules.

References

- G. Liu, T. Wang, H. Zhang, X. Meng, D. Hao, K. Chang, P. Li, T. Kako, J. Ye, *Angew. Chem. Int. Ed.* **54**, 13561 (2015).
- H. Liu, X. Meng, T.D. Dao, H. Zhang, P. Li, K. Chang, T. Wang, M. Li, T. Nagao, J. Ye, *Angew. Chem. Int. Ed.* **54**, 11545 (2015).

Solid-State Batteries

MANA Principal Investigator

MANA Scientist
MANA Research Associate

Kazunori TAKADA

Tsuyoshi Ohnishi
Koichi Okada



1. Outline of Research

Lithium-ion batteries have been powering portable electronics including cellular phones and note PC's for more than 20 years. In addition, they are expected to play new roles for realizing a low-carbon society as power sources in electric vehicles and energy storage devices in smart grids. However, there are still some issues to be solved. Because part of the issues arise from the organic electrolytes used in the batteries, they are expected to be solved in solid-state batteries.

2. Research Activities

(1) $\text{Li}_x\text{La}_{2/3-x}\text{TiO}_3$ epitaxial films.¹⁾

Battery performance is governed not only by bulk properties of the battery components but also by their interfaces; however, studies on the interfacial ionic conduction are still in their infant stage. Deep insights into ionic conduction at such a hetero-interface will be gained from an ideal interface model, which is formed between single-crystal ionic conductors with simple geometry, e.g. between epitaxially-grown thin-films of battery materials with atomically-flat surface. We have succeeded in epitaxial growth of high-quality LiCoO_2 films as an electrode material on SrTiO_3 substrates with perovskite structure and thus aim at epitaxial growth of perovskite-type $\text{Li}_x\text{La}_{2/3-x}\text{TiO}_3$ (LLTO) as its counterpart solid electrolyte in this study.

The LLTO films are grown by pulsed laser deposition. A preliminary study has revealed that high oxygen pressure (P_{O_2}) above 10 Pa is necessary to obtain crystallized films, while it tends to scatter light Li selectively and make the films Li-deficient. On the other hand, the LLTO also contains heavy La, which makes composition control very difficult. After optimizing every deposition condition, e.g. target composition, substrate temperature, and P_{O_2} , conductivity of the film has reached almost $10^{-3} \text{ S}\cdot\text{cm}^{-1}$. Although the obtained films are single-phase and comparable in the conductivity to bulk samples, intrinsic defects exist.

La atoms are ordered in the LLTO to form alternate La-rich and poor layers and thus make the *c*-axis length doubled,

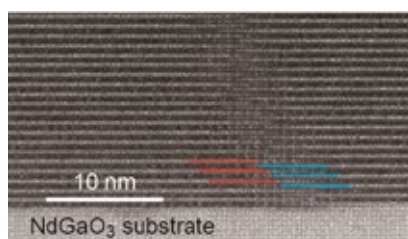


Fig. 1. A cross-sectional HAADF-STEM image of a $\text{Li}_x\text{La}_{2/3-x}\text{TiO}_3$ epitaxial film. La-rich layers indicated by red and blue lines are shifted by one perovskite unit to form an antiphase boundary.

while step height of the substrate surface is one perovskite unit. Therefore, when the LLTO is grown across the steps, the alternate La-rich and poor layers are shifted by one perovskite unit to form so-called “antiphase boundaries” starting from the steps, as observed in Fig. 1, which may affect ionic conduction in the films. Comparison between the ionic conductivities parallel and perpendicular to the steps will show the influence. The conductivities measured for the films grown on off-cut substrates to align the boundaries do not show significant differences, and thus it can be concluded that the antiphase boundaries do not interfere the ionic conduction.

(2) Silicon anodes in solid-state system.²⁾

Lithium–silicon alloys are regarded as anode materials with the greatest potential because of the high theoretical capacity more than ten times higher than that of graphite, low electrode potential, and high abundance. However, the alloy electrodes have never expressed their excellent potential in liquid electrolytes due to the decomposition products heavily formed on the electrode surface. Because continuous decompositions hardly take place in solid electrolytes, Li–Si alloys exhibit high performance in solid-state batteries, as demonstrated in Fig. 2.

An amorphous Si (*a*-Si) film prepared by r.f. sputtering delivers ca. $2400 \text{ mAh}\cdot\text{g}^{-1}$ even at a high discharge current density of $10 \text{ mA}\cdot\text{cm}^{-2}$. The increasing current density increases the overvoltage; however, the electrochemical impedance spectroscopy has revealed that the overvoltage mainly originates from the resistance of the electrolyte layer in the electrochemical cell. That is, polarization of the *a*-Si anode itself is negligible even at the high rate discharge.

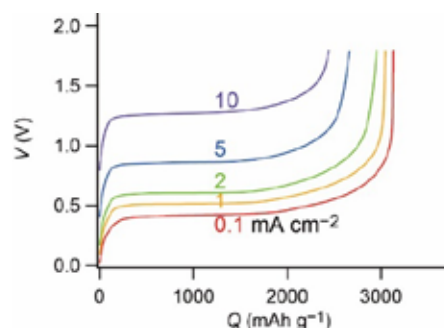


Fig. 2. Discharge curves of an *a*-Si film in a solid electrolyte under various current densities.

References

- 1) T. Ohnishi, K. Mitsuishi, K. Nishio, K. Takada, *Chem. Mater.* **27**, 1233 (2015).
- 2) R. Miyazaki, N. Ohta, T. Ohnishi, I. Sakaguchi, K. Takada, *J. Power Sources* **272**, 541 (2014).

Construction of Interphases with Atomic/Molecular Order for Efficient Conversion of Energy and Materials

MANA Principal Investigator

MANA Scientist
MANA Research Associate

Graduate Student

Kohei UOSAKI

Hidenori Noguchi, Ken Sakaushi
Yuki Morita, Kazuhisa Wada, Hung Cuong Dinh,
Xinlei Yan
Cepi Kurniawan, Shuo Yang, Huiwen Lin



1. Outline of Research

One of the most challenging tasks for chemists/ material scientists is the construction of efficient conversion systems of energy and materials. We are trying to establish techniques to construct interfacial phases for highly efficient conversion of energy and materials, mainly at solid/liquid interfaces, by arranging metal, semiconductor, organic molecules, and nanomaterials with atomic/ molecular resolution. Furthermore, development of novel methods to characterize the structure and functions of the interfaces *in situ* and theoretical study are carried out so that structure-function relations should be established and rational design and construction of the desired interfacial phases become possible.

2. Research Activities

(1) Construction of catalytic interfaces by ordered modification of metal surfaces.

Development of highly efficient electrocatalysts is the key to achieve sustainable society because of their central role in interfacial energy conversion such as fuel cell. Oxygen reduction reaction (ORR) is one of the most important processes in fuel cells and Li-air battery. Although Pt based materials are currently the most efficient electrocatalyst for ORR in fuel cells, they have several problems such as high cost, less abundance, poor stability, and still sluggish kinetics and there are many efforts to find alternative catalysts. We are developing various types of electrocatalysts for ORR without Pt group metals. Recently, we theoretically predicted that hexagonal boron nitride (h-BN) placed on various metal substrates act as an effective electrocatalyst for ORR¹⁻⁴⁾ and experimentally proved^{4,5)} that Au electrodes modified with various types of h-BN indeed act as effective ORR electrocatalysts. Since the activity of this system is still much lower than that of Pt, more efforts are required. We have found that the ORR activity of BNNS is much improved by increasing the gold-BN interactions as not only the overpotential is reduced but also the fraction for 4 electron reduction to water is increased. We also developed a new method to obtain nanoporous C, N architectures with high activities for both ORR and hydrogen evolution reaction.⁶⁾

(2) Investigations of Structure and Electron Transfer Processes at Solid/liquid Interfaces.

In order to understand mechanism and improved the efficiency of interfacial energy conversion processes, it is essential to have information of geometric, electronic, and molecular structures of the interfaces *in situ* in real time.^{7,8)} Surface x-ray scattering technique was used to monitor the potential induced structure changes such as surface

reconstruction lifting, adsorption of oxygen species, formation of surface oxide bilayer, reduction of surface oxide, and surface reconstruction of Au(111) and Au(100) in H₂SO₄ solution by surface x-ray scattering (SXS) *in situ* in real time.⁸⁾ The techniques to obtain electronic structure of solid/liquid interfaces where many important energy conversion processes take place are very limited because spectroscopy using electron as a probe, which is the power tool obtaining information on the electronic structure in vacuum, cannot be used in solution. Potential dependent IR/visible double resonance sum frequency generation (DR-SFG) spectroscopy was developed. Effectiveness of this method to probe the electronic structure at electrochemical interfaces was demonstrated at the pre-adsorbed CO/Pt(111) interface (Fig. 1). SFG intensity increased anomalously prior to the oxidation and the potential of SFG peak shifted with the visible light energy by 1 V/eV, showing that the origin of the anomalous increase of SFG intensity is not due to the potential dependent geometric structure change of the adsorbed CO but due to a resonance of visible and/or SF light with electronic transition from the Fermi level of Pt(111) to the 5σ_a anti-bonding state of the adsorbed CO.⁹⁾

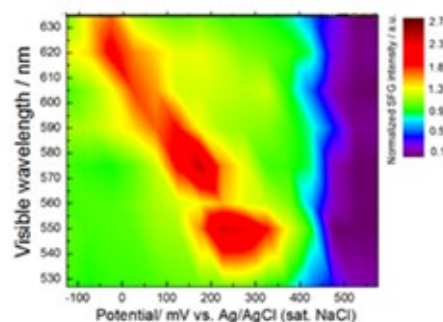


Fig. 1. Contour map of the SFG amplitude as functions of the potential and wavelength of visible light obtained by using 8 different visible light energy (527 nm ~ 635 nm).

References

- 1) A. Lyalin, A. Nakayama, K. Uosaki, T. Taketsugu, *PCCP* **15**, 2809 (2013).
- 2) A. Lyalin, A. Nakayama, K. Uosaki, T. Taketsugu, *J. Phys. Chem. C* **117**, 21359 (2013).
- 3) A. Lyalin, A. Nakayama, K. Uosaki, T. Taketsugu, *Topics.Catal.* **57**, 1032 (2014).
- 4) K. Uosaki, G. Elumalai, H. Noguchi, T. Masuda, A. Lyalin, A. Nakayama, T. Taketsugu, *J. Am. Chem. Soc.* **136**, 6542 (2014).
- 5) G. Elumalai, H. Noguchi, K. Uosaki, *PCCP* **16**, 13755 (2014).
- 6) K. Sakaushi, K. Uosaki, *ChemNanoMat*, in press.
doi: 10.1002/cnma.201500189
- 7) K. Uosaki, *Jpn. J. Appl. Phys.* **54**, 030102 (2015).
- 8) T. Kondo, J. Zegenhagen, S. Takakusagi, K. Uosaki, *Surf. Sci.* **631**, 96 (2015).
- 9) S. Yang, H. Noguchi, K. Uosaki, *J. Phys. Chem. C* **119**, 26056 (2015).

Reticular Materials

MANA Principal Investigator

 MANA Scientist
 MANA Research Associate

Omar M. YAGHI

 Kentaro Tashiro
 Pradip Sukul, Purnandhu Bose


1. Outline of Research

The synthesis of mononuclear metal complexes by design is a well-established process. In sharp contrast, however, a protocol for the synthesis of complexes containing multiple homo- or hetero-metals, in a designed fashion, remains largely absent so far, where it is inevitable to get a mixture of products with respect to the number, nuclearity, or sequence of metal centers.¹⁻⁵⁾

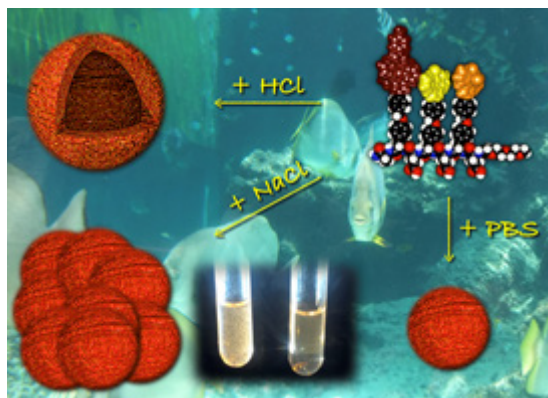


Fig. 1. Schematic representation of the self-assembling behaviors of **1**.

2. Research Activities

 (1) Unconventional Anion Dependency in the Self-Assembly of Water-Soluble MOCAs in Aqueous Media.⁶⁾

Water-Soluble MOCA containing three different metal centers (Figs. 1, 2) was molecularly dispersed in aqueous media containing 10% CH₃CN, while upon lowering the pH value into acidic conditions (Table 1, condition 2) it self-assembled to give hollow spherical objects, as visualized by microscopic observations. When an aqueous solution of **1** (10% CH₃CN) was salted with NaCl (10 mM; Table 1, condition 3), the resultant solution again turned into non-transparent in 2 days at 37 °C to afford a suspension. In contrast to the case of acidification, however, NaCl-induced

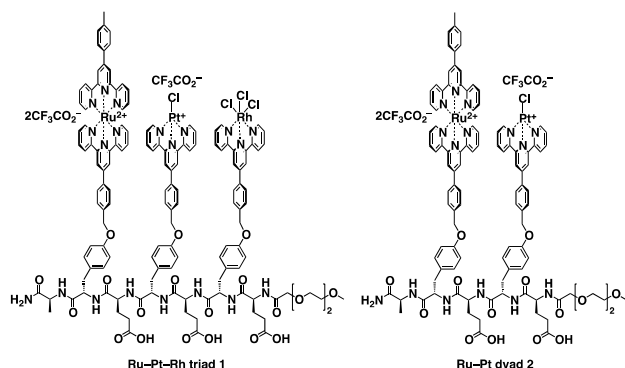


Fig. 2. Molecular structures of water-soluble metal-organic complex array **1** and its reference **2**.

No.	Additives	pH	Morphology of the assembly
1	No	4.52	Not Detected
2	HCl (10 mM)	1.98	Spheres
3	NaCl (10 mM)	5.42	Amorphous aggregates
4	NaCl (100 mM)	5.34	Amorphous aggregates
5	NaOCOCF ₃ (100 mM)	5.41	Not Detected
6	NaCl/NaOCOCF ₃ (100/100 mM)	5.44	Not Detected
7	NaCl/KCl/Na ₂ HPO ₄ /KH ₂ PO ₄ (120/2.4/9/1.6 mM)	7.54	Spheres
8	NaCl/NaOH (100/0.0024 mM)	7.61	Amorphous aggregates

Table 1. Self-assembling behaviours of **1** (50 μM) in aqueous media (10% CH₃CN) in response to additives.

assembly of **1** gave only amorphous aggregates larger than 500 nm, as observed by DLS and TEM. Increase of NaCl concentration to one order of magnitude larger (100 mM; Table 1, condition 4) just slightly enlarged the size of aggregates. We also tested NaOCOCF₃ (100 mM; Table 1, condition 5) as a reference of NaCl, where no aggregate was detected by DLS. NaOCOCF₃ even repelled the effect of NaCl, as NaCl-induced aggregates of **1** apparently disappear in a few minutes by the post addition of NaOCOCF₃ (Table 1, condition 6) where a homogeneous solution without any DLS signals resulted after 3 h. Although PBS contains more than 100 mM of NaCl, DLS profile of a PBS solution (10% CH₃CN) of **1** displayed no light scatterings in μm-scale region but those only at below 100 nm. Suppression of the NaCl-induced aggregation of **1** in PBS is not due to the increase of pH value of the media up to 7.54, as the salting-out effect of NaCl on **1** was preserved at pH of 7.61 (Table 1, condition 8). TEM as well as cryogenic TEM observations on the PBS solution of **1** visualized spheres whose sizes are less than 100 nm. The observed small salting-out effect of PBS on **1**, less significant than that of NaCl under the same pH condition (condition 8), is unique for self-assembly of peptide amphiphiles as generally kosmotropic anions such as HPO₄²⁻ and H₂PO₄⁻ in the Hofmeister series promote assemblies of peptides and proteins more efficiently than Cl⁻. Presence of the water-insoluble, charge neutral Rh-complex moiety in the molecular structure of **1** is also responsible for its spherical assembly formation in PBS, as reference dyad **2** (Fig. 2) did not form any assemblies detectable by DLS under the same condition although **2** as well as **1** aggregated heavily under condition 8.

References

- 1) P. Vairaprakash, H. Ueki, K. Tashiro, O.M. Yaghi, *J. Am. Chem. Soc.* **133**, 759 (2011).
- 2) M. Jacoby, *C&EN* **89**, 8 (2011).
- 3) K. Tashiro, *Gendaikagaku* **484**, 48 (2011).
- 4) A.M. Fracaroli, K. Tashiro, O.M. Yaghi, *Inorg. Chem.* **51**, 6437 (2012).
- 5) K.V. Sajna, A.M. Fracaroli, O.M. Yaghi, K. Tashiro, *Inorg. Chem.* **54**, 1197 (2015).
- 6) P.K. Sukul, P. Bose, T. Takei, O.M. Yaghi, Y. He, M. Lee, K. Tashiro, *Chem. Commun.* **52**, 1579 (2016).

Dye-Sensitized Solar Cells and Core-Shell Nanowires

Associate Principal Investigator David BOWLER
(Satellite at University College London, UK)



1. Outline of Research

Our ultimate aim is to understand advanced nanostructured materials for applications in photovoltaic devices, as well as future electronic devices. Our research combines close collaboration with experiment and theoretical modeling to give a detailed insight into the properties of the materials. In our first satellite project, we investigated how to combine biological inspiration with electronics to give high efficiency materials and solar cells with applications to energy and sustainability. In our new project, we are studying the growth and properties of silicon-germanium nanostructures, both nanowires and clusters formed on surfaces, to optimize their characteristics, particularly concentrating on the mobility and location of dopants.

We are leading the development of *ab initio* methods that can be applied to large systems. Much of our research involves development of the CONQUEST linear scaling DFT code, which has been developed through a long-term collaboration between UCL and NIMS.

We have established a network of collaboration between MANA in NIMS, the Computational Materials Science Center (CMSC) in NIMS and the London Centre for Nanotechnology in University College London. In this year, we have arranged collaborative research visits to MANA for the API and the MANA UCL student, as well as visits to UCL from researchers in NIMS.

2. Research Activities

(1) Growth and structure of nano-islands on Si(001).

We have been studying the three dimensional islands of Ge that self-assemble on Si(001) during epitaxial growth for some time. These systems are extremely challenging, as they require quantum mechanical simulations to find the correct structure, but contain several tens of thousands of atoms (at least).

After establishing the reconstruction of the faces of the islands,¹⁾ we have considered how the islands grow.²⁾ We have studied the energies of new pairs of Ge atoms on the faces, and show that the faces grow from the apex of the island. This matches what is observed in experiment, and we are now studying the origins of this behavior.

(2) Properties of Semiconductor Nanowires.

We have continued our work on the growth and properties of silicon nanowires and germanium-silicon core-shell nanowires, in collaboration with Dr. N. Fukata in MANA, who grows the nanowires. We have started by investigating the strain distribution in the nanowires induced by the differing lattice constants in silicon and germanium. In Fig. 1 we have plotted the strain in bonds along different directions in nanowires with a silicon core and a germanium

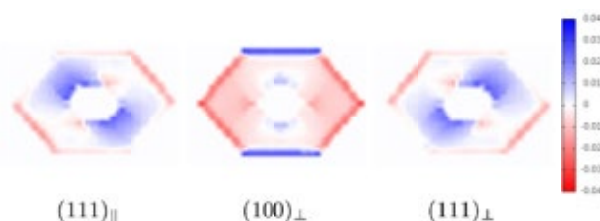


Fig. 1. Maps of average bond strain in Ge shell of a SiGe core-shell nanowire along different directions. Extension is shown in blue and compression in red.

shell, showing only the data for the Ge shell. The strain varies with thickness of shell and size of core, and changes when the order of core and shell is reversed (i.e. germanium core and silicon shell). We are now investigating the effect of the confinement on electronic states in the nanowires.

As part of this study, we have been awarded a Leadership Project on the UK high-performance computing facility, ARCHER, and will use this to study the dynamics and properties of dopants in the nanowires.

(3) Development of novel methods.

We have continued the development of the CONQUEST large scale DFT code. We have improved our approach to exact large-scale calculations³⁾ allowing us to apply the code to 10,000+ atoms without any approximations. We have also implemented time-dependent DFT,⁴⁾ which enables greater accuracy, as well as exploration of the dynamics of electronic structure. This implementation scales linearly with system size, as shown in Fig. 2.

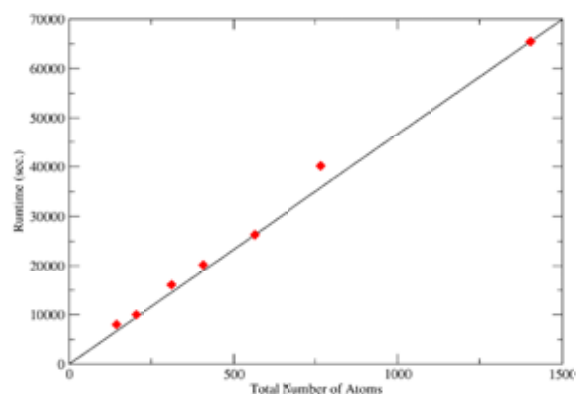


Fig. 2. Time taken to perform TDDFT calculation (vertical axis) for alkane chains of increasing length (horizontal axis), demonstrating linear scaling performance of CONQUEST.

References

- 1) T. Miyazaki, D.R. Bowler, M.J. Gillan, T. Ohno, *J. Phys. Soc. Jpn.* **77**, 123706 (2008).
- 2) M. Arita, S. Arapan, D.R. Bowler, T. Miyazaki, *J. Adv. Simul. Sci. Eng.* **1**, 87 (2014).
- 3) A. Nakata, D.R. Bowler, T. Miyazaki, *Phys. Chem. Chem. Phys.* **17**, 31427 (2015).
- 4) C. O'Rourke, D.R. Bowler, *J. Chem. Phys.* **143**, 102801 (2015).

Preparation of Surface Functionalized Nanoparticles for Controlling Stem Cell Functions and Cancer Therapy

MANA Principal Investigator **Guoping CHEN**

(Field Coordinator)
MANA Scientist
MANA Research Associate
NIMS Junior Researcher

Naoki Kawazoe
Jia'En Jasmine Li
Hongli Mao, Jingchao Li



1. Outline of Research

Nanomaterials have attracted broad attention in tissue engineering, stem cell research and cancer therapy because of their similarity to the nanostructured nature of cellular microenvironments and versatility in surface functionalization. Presenting functional chemical moieties on the surface of nanomaterials is anticipated to more closely mimic the microenvironments and to be appropriate to investigate the effect of the physiochemical cues on cell functions. In this study, gold nanoparticles and iron-iron oxide core-shell magnetic nanoparticles were prepared and used for cell culture to investigate their effects on cell functions. At first, gold nanospheres (AuNSPs) were prepared and modified with different functional groups to investigate their effects on the functions of stem cells.¹⁾ Subsequently, gold nanostars were prepared and modified with bovine serum albumin-folic acid conjugate for targeted photo thermal ablation of cancer cells.²⁾ Finally, AFM was used to identify the subtle change in cells induced by nanomaterials.³⁾

2. Research Activities

AuNSPs were synthesized and functionalized with amine (-NH₂), carboxyl (-COOH) and hydroxyl (-OH) terminated alkanethiols.¹⁾ The size measured in the TEM images showed AuNSPs with a diameter size below 26 nm. Human bone marrow-derived mesenchymal stem cells (hMSCs) were cultured with the surface functionalized AuNSPs and assessed for cell viability and osteogenic differentiation ability. The hMSCs cultured with the surface modified AuNSPs showed no adverse cell viability and were well tolerated for up to 21 days. The surface modified AuNSPs were taken up by hMSCs but positive charged surfaces promoted higher uptake in hMSCs. Surface modification did not inhibit osteogenic differentiation of hMSCs, however AuNSPs-COOH treatment reduced ALP activity and matrix mineralization in hMSCs compared to the controls (Fig. 1). The results will contribute to our growing knowledge of nanoparticles in biomimetic cues on hMSC differentiation and shed light on the possible roadmap on the control of these cues for tissue engineering.

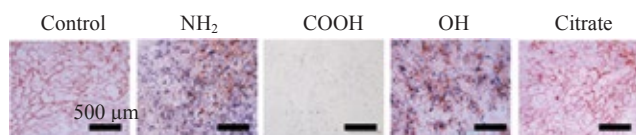


Fig. 1. Matrix mineralization of hMSCs after culture with AuNSPs in osteogenic induction medium for 21 days. Red web-like staining indicated calcium deposits while the blue/purple spots indicated aggregation of AuNSPs.

To prepare functional gold nanoparticles for targeted photothermal ablation of cancer cells, gold nanostars (AuNSTs) were prepared and modified with bovine serum albumin-folic acid conjugate (BSA-FA).²⁾ AuNSTs were used as a photothermal conversion agent due to their tunable

plasmon band and high photothermal conversion efficiency. Naturally derived polymer, bovine serum albumin (BSA), was used to improve the physiological stability and biocompatibility of AuNSTs. Folic acid (FA) was used as a targeting ligand for cancer cells. BSA-FA conjugate was first synthesized via an amidation reaction, which was further used as a stabilizer to coat the AuNSTs for surface modification (Fig. 2). The BSA-FA-AuNSTs showed good dispersibility and colloidal stability in different media. The BSA-FA-AuNSTs were used for culture of HeLa cells (cancer cells). The BSA-FA-AuNSTs not only had a very low cytotoxicity in the studied concentrations, but also showed targeting specificity to FA receptors-overexpressed cancer cells, which was confirmed by studying the cellular uptake. In addition, the BSA-FA-AuNSTs displayed a much better therapeutic efficiency to HeLa cells under the near-infrared laser irradiation when compared with BSA-AuNSTs without FA modification. The BSA-FA-AuNSTs should have a great potential as a photothermal conversion agent for the receptor-mediated treatment of cancer cells.

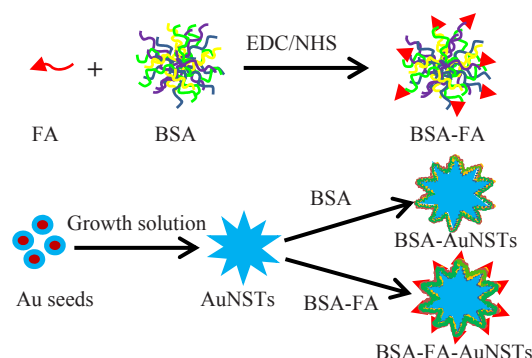


Fig. 2. Preparation of BSA-FA-AuNSTs.

Furthermore, the interaction between cells and iron-iron oxide core-shell magnetic nanoparticles was investigated by AFM.³⁾ After being exposed to the nanoparticles even at a high concentration (50 μg/mL), no obvious difference was observed by using conventional methods including the WST-1 assay and live/dead staining. However a significant difference of Young's modulus of the cells was detected by AFM even when the concentration of nanoparticles applied in the cell culture medium was low (10 μg/mL). The difference of cellular Young's modulus increased with the increase of nanoparticle concentration. The results suggested that AFM should be a useful technique to identify the subtle change of cells when they were exposed to nanomaterials even at a low concentration.

References

- 1) J. Li, N. Kawazoe, G. Chen, *Biomaterials* **52**, 199 (2015).
- 2) J. Li, R. Cai, N. Kawazoe, G. Chen, *J. Mater. Chem. B* **3**, 5806 (2015).
- 3) H. Mao, J. Li, I. Dulińska-Molak, N. Kawazoe, Y. Takeda, H. Mamiya, G. Chen, *Biomater Sci.* **3**, 1284 (2015).

Nanotherapeutics Based on Redox Polymer Nanoarchitectonics

MANA Principal Investigator **Yukio NAGASAKI**
(Satellite at Univ. Tsukuba, Japan)
Lecturer
Post-doc

Yutaka Ikeda
Long Binh Vong, Babita Shashni



1. Outline of Research

The objective of our research is to create new bioactive materials for high performance therapeutic system. In order to use materials in vivo, interactions between materials surface and bio-components such as blood and tissue must be controlled. Non-biofouling surface is one of the most important characters for high performance biomaterials design. Using our surface constructing technique thus developed, we have developed novel bionanoparticles, which scavenge excessively generated reactive oxygen species (ROS). Nitric oxide generation from newly designed nanoparticle could be also achieved.

2. Research Activities

(1) Preparation of redox injectable gels (RIG) and application for periodontitis.¹⁾

Local inflammation often spread entire body and causes severe intractable disorders. In order to eliminate local inflammation, we newly designed redox injectable gels (RIG), which possess nitroxide radicals as a reactive oxygen species (ROS) scavenger (Fig. 1). We applied this RIG for treatment of periodontitis. When newly applied the RIG to periodontal pocket in rat, it converted to gel and retained for 1 week. We evaluated inhibitory effects of RIG on *Porphyromonas gingivalis* (Pg)-induced bone loss in rat experimental periodontitis model, which has been reported to be related to ROS. In this study, alveolar bone loss was imaged by Micro-computerized tomography (Micro-CT), the gingival blood flow was not suppressed for RIG treatments compared with control. From the micro-CT analysis, it was clearly observed the inhibitory effects of RIG on Pg-induced bone loss (Fig. 2).

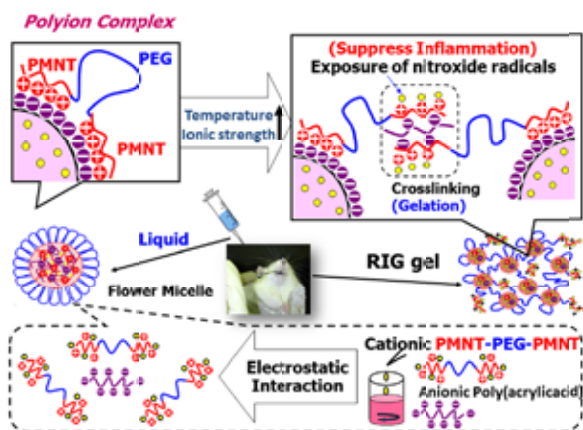


Fig. 1. Redox Injectable Gel.

(2) Preparation of macrophage-triggered nitric oxide (NO)-releasing nanoparticle.²⁾

Nitric oxide (NO) is a free radical endogenously

synthesized in the body and plays multiple physiological roles, including vasodilation, angiogenesis, neurotransmission, and immune response. Depending on its concentration and localization, NO changes its roles. We have hypothesized that site-specific accumulation of NO molecules controls tumor progression. Due to the poor bioavailability of NO, however, great efforts have been made to develop a methodology for the controlled delivery of exogenous NO in living systems. Most of trials were based on slow release of NO molecules from particle formulations. Due to the rapid diffusion, however, it is not easy to control releasing of NO from the particles. In this study, we have designed a new approach of macrophage-triggered cancer NO-immunotherapy. Inducible NO synthase (iNOS) in activated macrophages produces NO using arginine as a substrate. Since huge number of activated macrophage is infiltrated in tumor microenvironment, NO generation can be anticipated if L-arginine is delivered to tumor site. In this study, PEG-block-poly(L-arginine) was originally designed by new synthetic methodology. Our idea was to cooperate our PIC nanoparticle composed of PEG-b-PArg coupled with polyanion, and macrophage in tumor site to generate effective amount of NO molecules. After internalization of this nanoparticle into macrophages, significant increase in NO level was observed in vitro experiment. This nanoparticle can be delivered into tumor tissue via systemic administration (EPR eff.) and confirmed to increase the anti-tumor activity. We believe that the PIC nanoparticle composed of poly(L-arginine) opens new strategy for cancer immunotherapy.

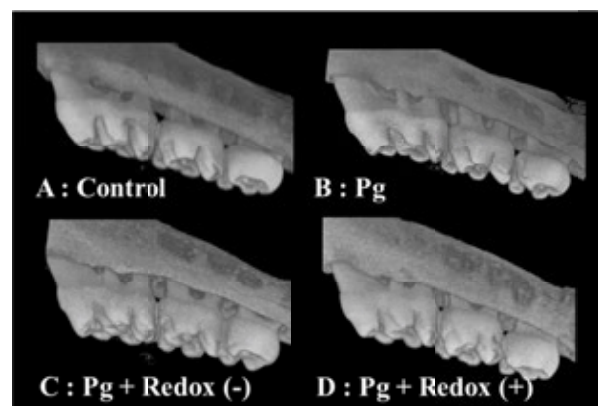


Fig. 2. Micro-CT images of the maxillary molars of rats. Group A, non-infected control; group B, infected with Pg; group C, administered RIG (nitroxide radicals -) and infected with Pg; group D, administered RIG (nitroxide radicals +) and infected with Pg.

References

- 1) M. Saita, J. Kaneko, T. Sato, S. Takahashi, S. Wada-Takahashi, R. Kawamata, T. Sakurai, M.C. Lee, N. Hamada, K. Kimoto, Y. Nagasaki, *Biomaterials* **76**, 292 (2016).
- 2) S. Kudo, Y. Nagasaki, *J. Control. Release* **217**, 256 (2015).

Nanoarchitectonics-Driven Interfaces and Nanoparticles for Therapeutic Applications

MANA Principal Investigator
(Satellite at Univ. Montreal, Canada)
MANA Scientist
Post-doc

Françoise M. WINNIK

P. Kujawa
J. Niskanen, X. Zhang (Univ. Montreal);
U. Nagarajan, S. Chandra, G. Beaune (MANA)



1. Outline of Research

Our research aims to use Materials Nanoarchitectonics to address current challenges in nanomedicine, placing emphasis on therapeutic agents and diagnostic tools.

2. Research Activities

(1) *Formation and spreading of cell-particle hybrid aggregates and their use to model/prevent tumor metastasis.*

Cell aggregates are used to investigate physiological processes, such as cancer metastasis, and to assess the efficacy of cancer drugs. This work,¹⁾ done in collaboration with Prof. F. Brochard-Wyart (Theoretician, Curie Institute, Paris, France), aims at understanding how nanoparticles (NPs) affect the mechanical properties of aggregated cells, in terms of adhesion, proliferation, and motility. Importantly, we observed that NPs can induce the aggregation of cells which lack adhesion proteins on their surface and do not adhere to each other in the absence of NPs. Experimental results were evaluated within the framework of soft-matter physics using a three-states dynamical model where the NPs are free, adsorbed on the cell membrane, or internalized by the cells (Fig. 1 top). Next, we demonstrated that the escape of cells from preformed aggregates is reduced by addition of NPs above a threshold concentration which depends on the NPs size and surface charge (Fig. 1 middle). Controlling the propagation of primary tumors is critical to prevent the epithelial to mesenchymal transition process leading to dissemination and seeding of tumoral cells throughout the body. The recognition that NPs can enhance the cohesion of

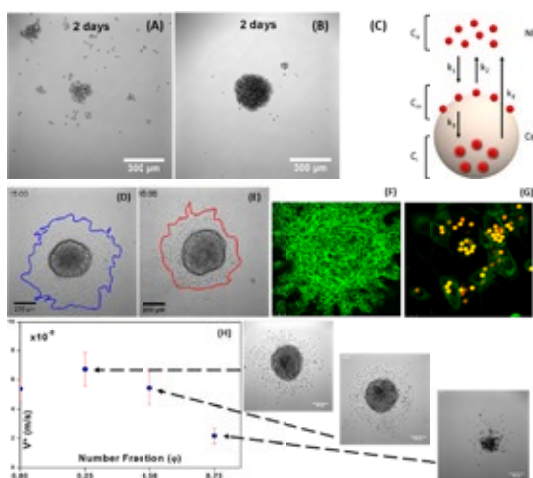


Fig. 1. (Top) Cell aggregates formation (A) without and (B) with NPs and (C) kinetic model of the NPs/cells interactions (Middle) Spreading of cell aggregates (D) without and (E) with NPs (15 h.) Confocal imaging of cells spreading (F) without microparticles (MPs) and (G) with $\phi = 0.75$ of MPs. Scale bars: 25 μm . (Bottom) Spreading velocity (V^*) of cell aggregates as a function of ϕ of MPs.

tissues and tumors may have important applications in cellular therapy and cancer treatment. We are currently studying the impact of microparticles on the formation and spreading of cellular aggregates and particularly how we can induce the liquid – solid transition of the hybrid systems (Fig. 1 bottom).

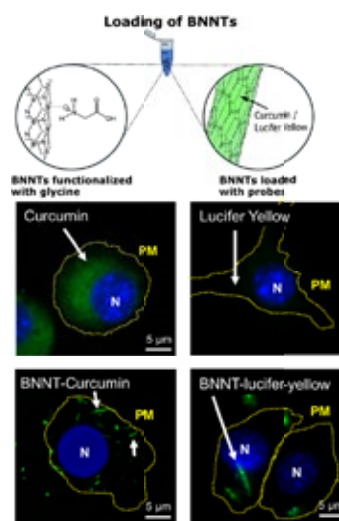


Fig. 2. Drug- and dye-loaded BNNTs: structure and imaging.

(2) *Boron nitride nanotubes (BNNT) as vehicles for intracellular delivery of fluorescent drugs and probes.*

Driven by the current consensus that elongated objects are internalized in cells more readily than spheres, we assessed the use of BNNTs as a mean to transport dyes and drugs inside cells. The inner channel of short ($< 2 \mu\text{m}$) BNNTs coated with glycine was filled with a model drug, curcumin, or fluorescent probes, such as rhodamine-6G, and lucifer yellow (Fig. 2 top). Observations by confocal fluorescence microscopy indicated that the fluorophore-loaded BNNTs were readily internalized by microglia cells. Localized release of their cargo was detected in the vicinity of the internalized tube ends (Fig. 2, bottom). BNNT-loaded curcumin retained its biological activity and reduced the release of inflammatory markers (NO, IL-6, and TNF- α) from microglia cells stimulated with lipopolysaccharides. Moreover, the cell impermeant dye, Lucifer yellow, was transported successfully through the cell membrane when loaded in BNNTs (Fig. 2 bottom).²⁾ These results open a promising path for BNNTs to be used as *in vitro* nanosensors, utilizing BNNTs functionalized with functional receptors or triggers (work in collaboration with Prof. D. Maysinger, McGill University and Dr. D. Golberg, MANA, NIMS).

References

- 1) G. Beaune, F.M. Winnik, F. Brochard-Wyart, *Langmuir* **31**, 12984 (2015).
- 2) J. Niskanen, I.Zhang, Y. Xue, D. Golberg, D. Maysinger, F.M. Winnik *Nanomedicine*, in press. doi: 10.2217/nnm.15.214

Next-Generation Semiconductor Nanodevices

Group Leader
(Nano-Materials Field)

Naoki FUKATA



1. Outline of Research

Considerable efforts have been directed for developing nanoscale silicon devices. Functionalization of semiconducting silicon nanowires (SiNWs) by impurity doping is one of the important processes for their application as next-generation field effect transistors. In order to control the dopant concentration, distribution, and electrical activation, it is necessary to characterize the bonding states, electronic states, and electrical activities of dopant atoms.¹⁻⁴⁾ However, the problem of retardation of carrier mobility caused by impurity scattering must be solved if impurity atoms are doped into the channel region. Core-shell NWs using Si and Ge appear to have major potential for suppression of impurity scattering.

2. Research Activities

(1) Formation of Ge/Si core-shell NWs.

i-Ge/p-Si core-shell NWs were grown by two step growth using chemical vapor deposition. catalytic laser ablation. Here, i-Ge/p-Si means intrinsic-Ge/p-type Si. It means that Si core nanowire regions were doped with boron (B). Representative TEM and EDX images are displayed in Fig. 1. The TEM data showed clear lattice fringes in the core and shell regions. The red represents Si and blue represents Ge in the EDX image. The results clearly show the formation of Ge/Si coreshell NWs.

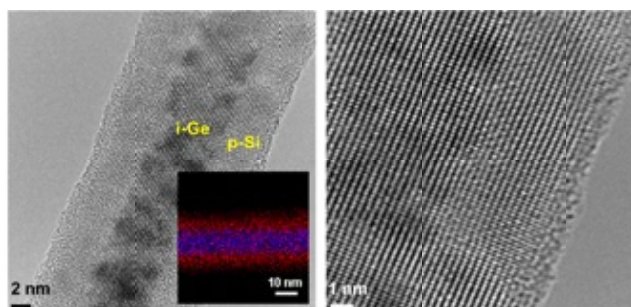


Fig. 1. High-resolution TEM images of i-Ge/p-Si core-shell NWs. An EDX image of i-Ge/p-Si core-shell NW is also shown.

(2) Demonstration of hole gas accumulation in Ge shell.⁴⁾

To demonstrate the hole accumulation into the i-Ge core in i-Ge/p-Si core-shell NWs, we summarized the Raman data as a function of the B₂H₆ gas flux in Fig. 2. The downshift and asymmetric broadening of the Si optical phonon peak, which is due to the Fano effect, becomes more pronounced with increased B₂H₆ gas flux, showing the increase in the B doping concentration in the Si shell layers (Fig. 2b, 2e). The Ge optical phonon peak also clearly shows the downshift and asymmetric broadening with increased the B₂H₆ gas flux for the formation of the p-Si shell layers

(Fig. 2a, 2c, 2d). This downshift and asymmetric broadening can be explained as below. Fig. 2c shows a comparison of the Ge optical phonon peaks observed for i-Ge/p-Si (1.0 sccm) core-shell NWs, i-Ge/i-Si (0 sccm) core-shell NWs, i-GeNWs, and bulk Ge. The Ge optical phonon peak for i-GeNWs shows a slight downshift and asymmetric broadening compared to bulk Ge. This is due to the phonon confinement effect, since the diameter of GeNWs is about 10 nm. The Ge optical phonon peak shows an upshift and asymmetric broadening due to the formation of i-Si shell layers (light blue spectrum). This upshift can be explained by the compressive stress applied by the i-Si shell layers, whereas the asymmetric broadening cannot be explained by compressive stress alone: it suggests the effect of hole accumulation. The Ge optical phonon peak showed a downshift and further asymmetric broadening with increasing B concentration in the Si shell layers, as shown in the red spectrum of the i-Ge/p-Si (1.0 sccm) core-shell NWs. This can be explained in major part by the Fano effect, showing the introduction of a high concentration of holes in the i-Ge core region. The result clearly demonstrates hole accumulation from the p-Si (i-Si) shell to the i-Ge core region that results from the formation of core-shell NW structures.⁴⁾ Fig. 2f shows an abrupt band discontinuity between Si and Ge, which is called the band offset and the hole accumulation in i-Ge region.

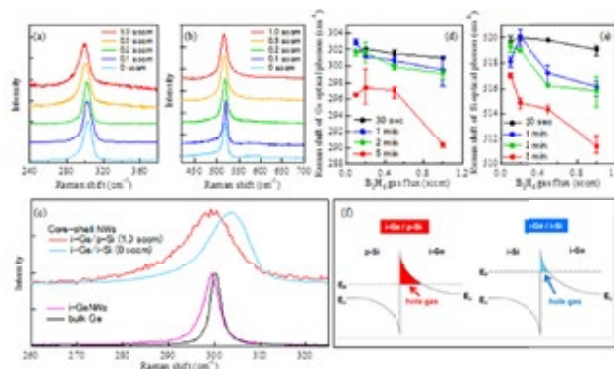


Fig. 2. (a) Ge and (b) Si optical phonon peak observed for i-Ge/p-Si core-shell NWs. (c) Comparison of the Ge optical phonon peaks observed for i-Ge/p-Si (1.0 sccm) core-shell NWs, i-Ge/i-Si (0 sccm) core-shell NWs, i-GeNWs, and bulk Ge. Raman shift of (d) the Ge and (e) the Si optical phonon peaks as a function of the B₂H₆ gas flux. (f) Band diagram around a Si-Ge heterojunction in Ge/Si core-shell NWs.

References

- 1) N. Fukata, *Adv. Mater.* **21**, 2829 (2009).
- 2) N. Fukata, K. Sato, M. Mitome, Y. Bando, T. Sekiguchi, M. Kirkham, J.I. Hong, Z.L. Wang, R.L. Snyder, *ACS Nano* **4**, 3807 (2010).
- 3) N. Fukata, S. Ishida, S. Yokono, R. Takiguchi, J. Chen, T. Sekiguchi, K. Murakami, *Nano Lett.* **11**, 651 (2011).
- 4) N. Fukata, M. Yu, W. Jevasuwan, T. Takei, Y. Bando, W. Wu, Z.L. Wang, *ACS Nano* **9**, 12182 (2015).

Development of Nanomedicines

Group Leader
(Nano-Life Field)

Nobutaka HANAGATA



1. Outline of Research

My challenge is to apply beneficial technologies to society by integrating original biological discoveries with original materials technologies and nanotechnology. The integration of life sciences and nanotechnology/materials science has two approaches. The first approach is to link critical knowledge in the life sciences to technological innovations through the use of nanotechnology and materials science. The other approach is to use nanotechnology and materials science to lead to important discoveries in the life sciences. I addressed the study on elucidation of molecular mechanism of rare bone disease and development of the therapeutic approach using nanomedicines in the first approach. I also addressed the study on DNA nanomedicines for the prevention and treatment of infectious diseases and allergy in the second approach.

2. Research Activities

(1) Regulation of immunostimulatory DNA medicine by using nanomaterials.^{1,2)}

Toll-like receptor 9 recognizes CpG oligodeoxynucleotides (ODNs) and induces immune-mediator cytokines. Natural phosphodiester class B CpG ODNs induce interleukin-6 (IL-6), but not interferon- α (IFN- α). I prepared silicon nanoparticles (Si NPs) with different positive surface charge density and bound negatively charged class B CpG ODN molecules electrostatically. No significant differences in the amount of class B CpG ODN molecules or negative surface charge after binding of the molecules onto naked NPs was observed. However, the profile of cytokine induction from peripheral blood mononuclear cells was correlated with a positive surface charge density of naked NPs prior to binding of CpG ODN molecules. The level of IL-6 induction slightly decreased as the positive surface charge density was increased, while the IFN- α induction significantly increased as the positive surface charge density was increased. This observation demonstrates that the bifurcated cytokine induction can be regulated by the surface charge of naked NPs.

I also proposed to modify mesoporous silica nanoparticles (MSNs) with 3-aminopropyltriethoxysilane (NH₂-TES), aminoethylaminopropyltriethoxysilane (2NH₂-TES) and 3-[2-(2-aminoethylamino)ethylamino] propyl-trimethoxysilane (3NH₂-TES) for binding of cytosine-

phosphate-guanosine oligodeoxynucleotides (CpG ODN), and investigated the effect of different amino groups of MSNs on the CpG ODN delivery. Serum stability, in vitro cytotoxicity, and cytokine interleukin-6 (IL-6) induction by MSN-NH₂/CpG, MSN-2NH₂/CpG and MSN-3NH₂/CpG complexes were investigated in detail. The results showed that three kinds of aminated-MSN-based CpG ODN delivery systems had no cytotoxicity to RAW264.7 cells, and binding of CpG ODN to MSN-NH₂, MSN-2NH₂ and MSN-3NH₂ nanoparticles enhanced the serum stability of CpG ODN due to protection by the nanoparticles. However, three aminated MSN-based CpG ODN delivery systems exhibited different CpG ODN delivery efficiency, and MSN-NH₂/CpG complexes had the highest ability to induce IL-6 secretion.

(2) Immunosuppressive DNA nanomedicine against autoimmune disorders.³⁾

Interferon-induced transmembrane protein 5 (IFITM5) is an osteoblast-specific membrane protein that has been shown to be a positive regulatory factor for mineralization in vitro. However, *Ifitm5* knockout mice do not exhibit serious bone abnormalities, and thus the function of IFITM5 in vivo remains unclear. Recently, a single point mutation (c.-14C>T) in the 5' untranslated region of IFITM5 was identified in patients with osteogenesis imperfecta type V (OI-V). Furthermore, a single point mutation (c.119C>T) in the coding region of IFITM5 was identified in OI patients with more severe symptoms than patients with OI-V. Although IFITM5 is not directly involved in the formation of bone in vivo, the reason why IFITM5 mutations cause OI remains a major mystery. I addressed the identification of molecules that interact with IFITM5 mutants, but the molecules were not identified yet. I also try to construct the model mouse that possesses IFITM5 mutant using genome editing tool CRISPR-Cas9 to develop medicines for this bone disease.

References

- 1) S. Chinnathambi, X.D. Pi, M.S. Xu, N. Hanagata, *J. Drug Deliv. Sci. Technol.* **29**, 251 (2015).
- 2) Y. Xu, P. Claiden, Y.F. Zhu, H. Morita, N. Hanagata, *Sci. Tech. Adv. Mater.* **16**, 045006 (2015).
- 3) N. Hanagata, *J. Bone Miner. Metab.*, in press (DOI: 10.1007/s00774-015-0667-1).

Bioactive Ceramics Materials

Group Leader
(Nano-Life Field)

Masanori KIKUCHI



1. Outline of Research

Bioactive ceramics is divided into two types. One is conventional one that can directly bond with bone but not influences cell functions so much. Another type can activate target cell functions. We have been investigating both type of bioactive ceramics and ceramic/polymer composites for tissue regeneration. In recent years, we have been investigating the NIMS original material of hydroxyapatite/collagen bone-like nanocomposite (HAp/Col) with high performance in activation of cellular functions and incorporation into bone remodeling process (Fig. 1). Another one is to exploit marine waste for functional materials.

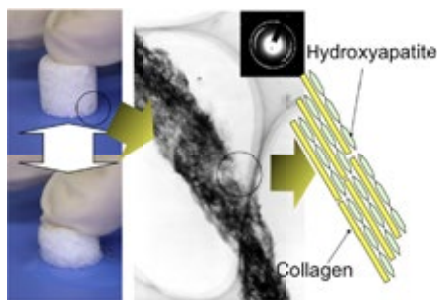


Fig. 1. Hydroxyapatite/collagen self-organized nanocomposite has nanostructure in which apatite and collagen are regularly aligned, and can be formed to sponge-like porous body.

2. Research Activities

(1) Injectable HAp/Col materials.

Injectable artificial bone with bioresorbability is strongly desired in practical medicine to realize good minimum invasive surgery to reduce potential risk of bone fractures as well as inhibition of new bone formation due to remaining of cements in body. Injectable HAp/Col could be good candidate because of its nature to reduce these risks. We utilize (3-glycidoxypropyl)trimethoxy-silane (GPTMS) for gelation agent for injectable HAp/Col. The HAp/Col mixed with GPTMS solution showed excellent anti-decay property (Fig. 2) and viscoelastic mechanical properties. Even the paste hardened had low compressive strength than bone, viscoelastic and hydrogel-like nature of the paste could endure the load when injected it into a bone defect surrounded by cortical bone, which is a general application part for injectable bone paste.

(2) Marine waste to bone.

Interconnected porous structures of marine organisms

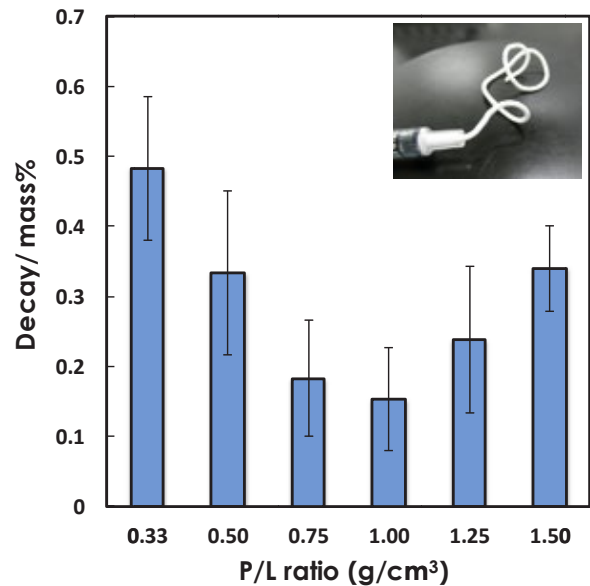


Fig. 2. Anti-decay rates for HAp/Col self-setting paste. The inlet showed injectability of the paste.

attracted researchers on functional materials; in fact, coral is practically used for bone substitutes after hydrothermal conversion from original calcite to hydroxyapatite (HAp). However, coral collection is highly restricted because it plays a very important role on marine eco-system as well as main reservoir for carbonate gas to reduce greenhouse effect. Contrarily, sea urchins are consumed as food or eliminated to prevent sea desertification and their tests are discarded as a waste. To utilize sea urchin tests as bone filler, skeleton of sea urchin tests were collected by remove organic substances followed by hydrothermal treatment in phosphate salt solution. As shown in Fig. 3, Mg-containing calcite in sea urchin skeleton was successfully converted to Mg-containing β -tricalcium phosphate, well-known as a bioresorbable bone filler material.

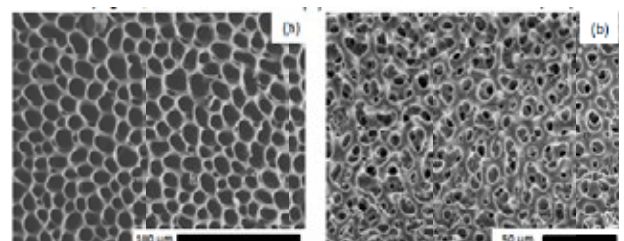


Fig. 3. Sea urchin skeleton (a) before and (b) after hydrothermal treatment for 5 days

Materials for Functional Nanomedicine

Group Leader
(Nano-Life Field)

Hisatoshi KOBAYASHI



1. Outline of Research

In general, organism selected quite limited molecules such as amino acids, lipids, sugar moieties, and limited metals and inorganics, and combined the limited molecules and finally constructed such highly functionalized complex systems. From the structure point of view, the organism is constructed by various nano-fibers and nano-particles under the highly dimensionally controlled condition.

2. Research Activities

(1) Body-fluid Permeable Nanofibrous Materials for Corneal Stromal Regeneration.

To maintain the transparency and to keep the eyeball shape, corneal stroma has unique nano-scale anatomical features such as lattice collagen structure. Lattice collagen structure is made by one-direction aligned collagen fiber sheet stacking, so called “layer-by-layer structure.” Therefore, to develop the regenerative scaffold for corneal stroma, we focused on aligned nanofiber non-woven mat. Nanofiber mat can easily fabricate from polymer solution via electrospinning technologies. Now we focus on silk material because of its well-known biocompatibility.¹⁻³⁾ In this study we evaluated the cellular responses against the silk fibroin materials and its in vivo biocompatibility using rabbit corneal stroma implant model.

Materials and Method. Aqueous silk fibroin solution (9-12 wt%) was kindly donated from National Institute of Agrobiological Sciences. For preparation of electrospinning solution, 8 wt% fibroin aqueous solution was gently mixed with a 5 wt% poly (ethylene oxide) aqueous solution in the volume ratio 4 to 1.⁴⁾ An electrospinning system equipped with a rotation drum collector was used to fabricate aligned mats as following setting; applied voltage was 12 kV, a feeding rate was 0.3 ml/h, a spinning distance was 185 mm, a stainless needle was 25G, a diameter of the drum collector was 100 mm, rotation speed was 3000rpm. HCE-T (human corneal epithelial cell) cells were obtained from RIKEN. DMEM/F12 with 5% FBS, 2% P/S, 0.5% DMSO, 5 µg/ml insulin, and 10 ng/ml hEGF was used as culture medium. 30,000cells/well of HCE-T were seeded. After 3days culture, numbers of proliferated cell were counted. After one week culture on the samples in same condition, the cells were air lifted and continuously cultured another one week to check the differentiation to create multilayered structure. Human keratocyte were also seeded on the samples. After one month culture, the samples were fixed and immunohistostaining were carried out. For the animal study, all

animal experiment was approved by ethical committee in National Institute for Materials Science. Four male Japanese white rabbits (body weight 2.5 - 3.5 kg) were anesthetized by intravenous injection of sodium pentobarbital (0.6 ml per 1 kg body weight). After anesthesia, corneal stromal pocket was created using surgical knife and ophthalmic spatula (Fig. 1). Sterilized fiber mat was put into the corneal stromal pocket. Gross observation of implanted eye was done using surgical microscope at every week after surgery till sacrifice.

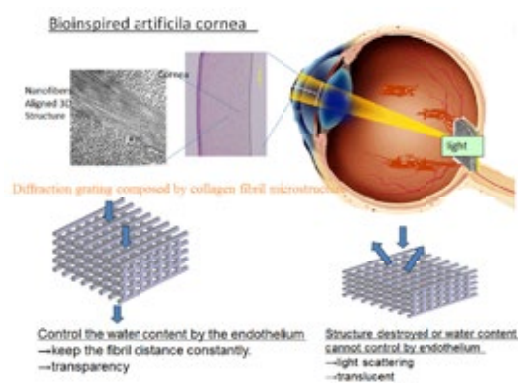


Fig. 1. Schematic illustration of our corneal scaffold.

Results and Discussion. From the in vitro corneal cell seeding tests, human corneal stromal cell well adhered and proliferated not only the fiber mat surface but also migrated into the inside of fiber mat with keeping its phenotype. Moreover, adhered human corneal stromal cell produced regenerate-related proteins such as collagen and crystalline. In rabbit corneal stroma, quite low inflammatory and no-immune reactions were observed till one year after surgery. And corneal epithelium was almost intact on the host cornea and the biodegradation were confirmed by histological evaluation on the samples after 6 month implantation. All the implanted cornea is very clear and almost not light scattering caused by scar is observed. These results have strongly suggested the validity of our approach.

References

- 1) D. Terada, C. Yoshikawa, S. Hattori, H. Teramoto, T. Kameda, Y. Tamada, H. Kobayashi, *Bioinspired, Biomimetic and Nanobiomaterials* **1**, 57 (2012)..
- 2) S. Hattori, D. Terada, A.B. Bintang, T. Honda, C. Yoshikawa, H. Teramoto, T. Kameda, T. Yasushi, H. Kobayashi, *Bioinspired, Biomimetic and Nanobiomaterials* **1**, 195 (2012).
- 3) S. Hattori, D. Terada, T. Honda, H. Teramoto, T. Kameda, Y. Tamada, H. Kobayashi, *J. Silk Sci. Tech. Jpn.* **22**, 117 (2014).
- 4) H.J. Jin, S.V. Fridrikh, G.C. Rutledge, D.L. Kaplan, *Biomacromolecules* **3**, 1233 (2002).

Functionalization of Atomic Network Materials

Group Leader
(Nano-Materials Field)

Takao MORI



1. Outline of Research

Approximately two thirds of primary energy (fossil fuels, etc.) being consumed in the world, sadly turns out to be unutilized, with much of the waste being heat. The direct conversion of waste heat to electricity is a large incentive to find viable thermoelectric (TE) materials.¹⁾ Traditionally, high performance TE materials have tended to not be element friendly; being composed of Bi, Te, Pb, etc. One need exists to develop effective TE materials composed of abundant and safe elements. Another need exists for materials to have good thermal stability when considering mid to high temperature applications. To this end, we aim to functionalize covalent materials composed of elements like XIII–XV group elements (C, B, Si, Al, Sn, etc.) by utilizing their atomic network structure, i.e. clusters, 2D atomic nets, cage-like structures in which the structural order plays a large role in physical properties.²⁻⁴⁾

2. Research Activities

(1) Novel concepts for TE enhancement.

A. Magnetic interactions. We recently clarified the importance of the interaction of the charge carrier and magnons.⁵⁾ This analysis was carried out on the magnetic semiconductor chalcopyrite, and as a striking result we discovered that thermoelectric electricity is indicated to be generated in underwater volcanoes in the deep sea.⁵⁾ We are now attempting to use this principle for the design of materials with even higher performance.

B. Hybrid effect. A hybrid effect was also discovered in which formation of nanocomposites yielded a simultaneous enhancement of electrical conductivity by ~10,000% and Seebeck coefficient by up to 220%, significantly overcoming the tradeoff, a long-time obstacle for TE. We analyze this and give a recipe for application to prospective systems.⁶⁾ The interfaces in nanocomposites may be having an effect also, and this needs to be investigated further.⁶⁾

C. Other novel possibilities. We investigated near the phase boundaries of a chalcogenide with complex phases of CDW and superconductivity in search of new concepts of high TE. No high TE was found, but as a striking by-product of the research, the origin of the phases was elucidated.⁷⁾

(2) Nanostructuring to enhance TE.

Cage compounds skutterudites are one of the most studied TE materials in the world, hoped to be used in vehicles, etc. We developed novel skutterudites which exhibited high TE performance despite being rare earth-free (not dependent on the “rattling” mechanism) and with good resistance to oxidation with $ZT \sim 1.6$ (Fig. 1).⁸⁾ Excellent properties were also realized in magnesium tin silicide in collaboration with Univ. London.⁹⁾

(3) Layered materials and MBE.

MBE of TE materials in order to utilize and definitively prove the “confinement” effect is being carried out, and high quality nitride materials were fabricated. For material design,

calculations show that AMN₂ layered complex metal nitrides with both 2D and 3D electronic structures may be superior to the well-known oxides like SrTiO₃, and anomalous anisotropic properties were newly revealed.^{10,11)}

(4) Development of high temperature TE materials for topping cycles in thermal power plants.

As a high impact application, high temperature TE materials have been proposed to enhance the efficiency of thermal power plants. Advancements have been made in the thermoelectric borides which are promising candidates.

A. Renaissance in RB₆₆ compounds. A couple of discoveries of striking enhancement of figure of merit ZT 30 to 40 times were made for the RB₆₆ system, which happens to be the first actual PGEC (phonon glass electron crystal). An extremely metal-rich YB₄₈ was discovered to exist, with enhancement possibly from delocalization.¹²⁾ Furthermore, SmB₆₂ had a large enhancement possibly related to multivalency.¹³⁾

B. Anisotropy in borosilicides. An interesting anisotropy in the crystal structure with metal layers, and TE properties were observed.¹⁴⁾

(5) Guidelines for the future of thermoelectrics.

A Scripta Viewpoint Set laying out principles and applicative aspects for TE was coedited.¹⁵⁾

(6) Development of thermal insulation materials.

Thermal insulation materials with thermal conductivity smaller than air are being developed with a method compatible with industry, utilizing hollow spheres.¹⁶⁾

References

- 1) “*Thermoelectric Nanomaterials*”, ed. K. Koumoto, T. Mori, Springer Series in Materials Science (Springer, Heidelberg, 2013) pp.1-373.
- 2) T. Mori, in *Handbook on the Physics and Chemistry of Rare Earths*, Vol. 38, (North-Holland, Amsterdam, 2008) p. 105-173.
- 3) T. Mori, in: *Modules, Systems, and Applications in Thermoelectrics*, ed. D.M. Rowe, (CRC Press, Taylor & Francis, London, 2012) 14.
- 4) T. Mori, in: *The Rare Earth Elements: Fundamentals and Application*, ed. D. Atwood (John Wiley & Sons Ltd., Chichester, 2012) p.263-279.
- 5) R. Ang et al., *Angew. Chem. Int. Ed.* **54**, 12909 (2015).
- 6) T. Mori, T. Hara, *Scripta Mater.* **111**, 44 (2016).
- 7) R. Ang et al., *Nature Commun.* **6**, 6091 (2015).
- 8) T. Mori, A.U. Khan, Patent appl. (2014).
- 9) H. Ning et al., *J. Mat. Chem. A* **3**, 17426 (2015).
- 10) I. Ohkubo et al., *Chem. Mat.* **27**, 7265 (2015).
- 11) I. Ohkubo et al., *Eur. J. Inorg. Chem.* **22**, 3715 (2015).
- 12) M.A. Hossain et al., *J. Phys. Chem. Solids* **87**, 221 (2015).
- 13) A. Sussardi et al., *J. Materiomics* **1**, 196 (2015).
- 14) M.A. Hossain et al., *J. Solid State Chem.* **233**, 1 (2016).
- 15) T. Mori, G. Nolas, *Scripta Mater.* **111**, 1 (2016).
- 16) R. Wu et al., JST New Technology Meeting, Sept. 3, 2015.

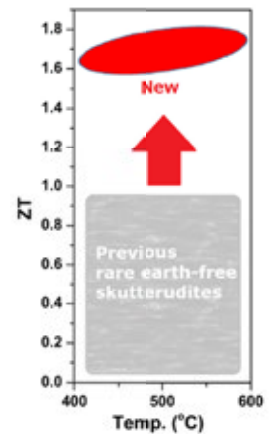


Fig. 1. Enhancement in RE-free skutterudites.

Nano Devices for Infrared Light Applications

Group Leader
(Nano-System Field)

Tadaaki NAGAO



1. Outline of Research

The technology for amplifying, confining, and scattering the light in nanoscale is strongly desired as a key technology in communication, optical sensing, and energy harvesting. Plasmonics and metamaterials are now accepted as useful paradigms for materials science which enable us to control flexibly the light in nanospace. Through this approach we have been developing some materials with extraordinary signal enhancement of molecules, enhanced photocatalytic reaction, and smart solar power harvesting. Our laboratory investigated the functions of thin nanomaterials that are dramatically smaller than the wavelength of light, focused wherein a large number of atoms and electrons oscillate dynamically in a collective manner.

2. Research Activities

Because infrared (IR) radiation is a type of electromagnetic wave that oscillates at approximately the same frequency as the molecular vibration of organic molecules and phonons in crystals, IR radiation is deeply related to material's thermophysical and energy transfer phenomena, and belongs to an extremely important frequency region which is also utilized in medicine and environmental monitoring, the chemical and food industries, and numerous other fields. However, because the wavelength of IR-light is on the μm scale, and IR rays themselves are invisible, it has been difficult to do IR imaging in submicron scale and further improving its spatial resolution. For this reason, there is still little activity in nanoscience research using IR light in comparison with research with visible light. Our laboratory investigated the functions of thin nanomaterials that are dramatically smaller than the wavelength of IR light, focused on basic research on

phonons and the plasmon wherein a large number of atoms and electrons oscillate dynamically in a collective manner.

Infrared perfect absorbers, which can absorb 100% of infrared radiation, have great potential for use in various applications such as sensing of organic molecules in liquids and gases, generation of electricity using thermal radiation as an energy source, etc. We developed a simple lithography method in which microspheres are used as a mask material to pattern metamaterial structures in an inexpensive manner, and developed a technique for fabricating IR perfect absorbers with high accuracy utilizing this method. Using this fabrication method, we realized sharp wavelength-selective IR absorption and high sensitivity molecular sensing (Fig. 1).¹⁾

Other uses of perfect absorbers are the thermal emitter and infrared detectors with wavelength selectivity.^{2,3)} We have realized narrowband IR light emitters using metamaterials based on metal-oxide-metal (MIM) structures made of Al and refractory metal such as Mo and TiN. We are also developing wavelength-selective IR detectors for multiband IR light detection for potential applications in various fields, such as for temperature sensing in houses and in offices, night vision applications for auto mobiles, as well as for the applications in homeland security (Fig. 2).

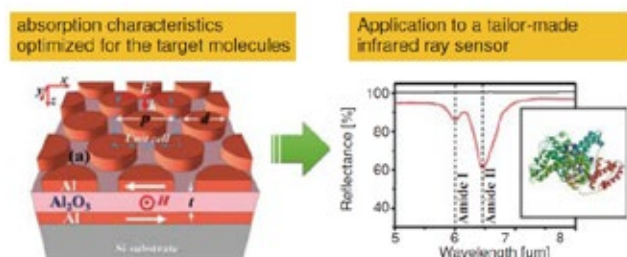


Fig. 1. (left) Schematic diagram of infrared perfect absorber using aluminum. (right) Example of plasmon-enhanced infrared spectroscopy of biomolecules. In observation of the signal from bovine serum albumin on the order of a single molecular layer, a dramatically amplified signal (absorption rate: approx. 30%) could be observed (red line) with the developed IR perfect absorber in comparison with the IR absorption (black line) of a flat aluminum surface.

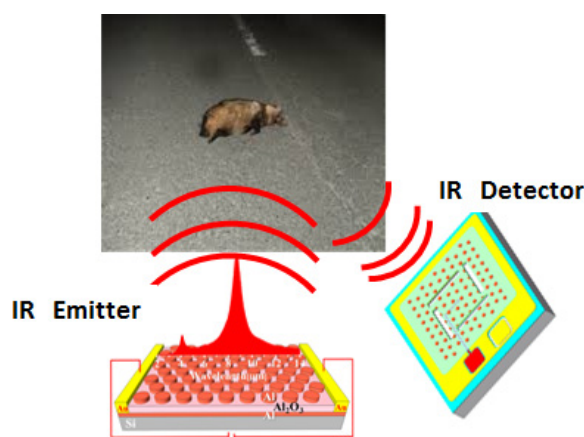


Fig. 2. An example of using wavelength-selective perfect absorbers for an IR light emitter and an IR detector. IR light emitters can be used for inexpensive and intense IR light sources and IR detectors can be used for detecting the IR light at a certain wavelength. The example shows potential use for the sensors for automobiles to detect objects in dark.

References

- 1) K. Chen, T. Dao, S. Ishii, M. Aono, T. Nagao, *Adv. Funct. Mater.* **42**, 6637 (2015).
- 2) NIMS patent application 2014-176247.
- 3) T. Dao, K. Chen, S. Ishii, A. Ohi, T. Nabatame, M. Kitajima, T. Nagao, *ACS Photonics* **2**, 964 (2015).

Characterization and Control of Defects in Semiconductors

Group Leader
(Nano-Materials Field)

Takashi SEKIGUCHI



1. Outline of Research

We have been pursuing 4 projects for semiconductors named “Square Si,” “Multi-dimensional EBIC,” “Anything CL,” and “100V EM”. “Defect Control” is the key issue for these projects. We are characterizing various properties of defects in nanoscale. For this purpose, we have developed special electron beam characterization techniques, such as electron-beam -induced current (EBIC) and cathodoluminescence (CL) as well as the secondary electron (SE) imaging. In 2015, we have completed the project, “mono Si ingot growth for low-cost and high-performance Si solar cells”. We also developed fountain secondary electron detector for advanced scanning electron microscopy.

2. Research Activities

(1) Mono Si growth using seed cast method (Square-Si).

We have succeeded in developing seed cast Si growth technique and grown 50 cm square monocrystalline (mono) Si ingots for photovoltaics application. According to the effort of defects/light element impurities reduction, the performance of solar cells made of our mono Si is significantly improved.¹⁾ Fig. 1 shows the photograph of mono Si ingot (a) and efficiency variation as well as that of CZ Si (b). The efficiency of No. 4 wafer of mono-Si ingot is 18.7 %, which is comparable with CZ Si. Some of these developments have been transferred to the industries.

(2) Fountain Secondary Electron Detector (100V EM).

Scanning electron microscopy (SEM) is now indispensable for nanotechnology and nanoscience. The inlens system and low energy excitation have brought about significant development of SEM technology for both spatial resolution and nanocharacterization. Although inlens system significantly contributes the improvement of resolution, it sacrifices the detailed information of secondary electrons, namely their energy and direction. We have proposed an

outlens secondary electron detector for energy and angle filtered SE images.²⁾ The schematic of this detector is shown in Fig. 2. The low energy secondary electrons emitted from the specimen are reflected by the bias grid and collected by the SE detector beneath the specimen. According the parabolic motion of electrons, we named this “Fountain Detector (FD)”. This setting can select SEs with certain energies and angles.

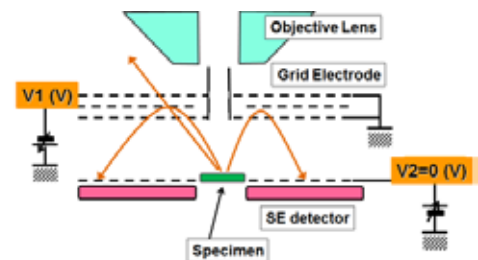


Fig. 2. Schematic of Fountain Detector.

Using this FD, we have started to characterize various materials by low energy SE imaging. Fig. 3 shows an example of GaN islands on Si substrate. (a) shows the SE image taken by conventional ET detector. The components are illustrated in (b). The FD images are shown in (c) and (d), corresponding to [0-10 eV] and [1-6- eV], respectively. The low energy SE image of (c) shows significant difference from conventional one. This indicates that the new information of surface potential and/or material contrast is available from this FD images. This research is now going on.

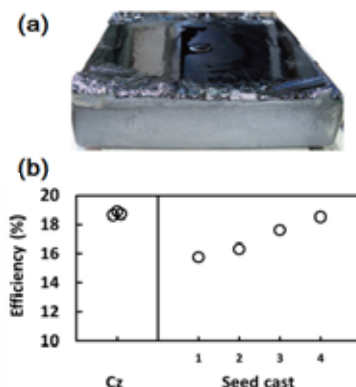


Fig. 1. (a) Photograph of mono Si ingot and its (b) efficiency variation of solar cells made of this ingot.

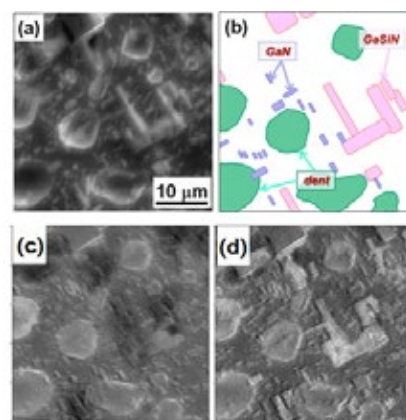


Fig. 3. GaN islands on Si. (a) ET image, (b) schematic of specimen, (c) FD image [0 - 10 eV], (d) FD image [0-60 eV].

References

- 1) Y. Miyamura, H. Harada, K. Jiptner, S. Nakano, B. Gao, K. Kakimoto, K. Nakamura, Y. Ohshita, A. Ogura, S. Sugawara, T. Sekiguchi, *Appl. Phys. Exp.* **8**, 062301 (2015).
- 2) T. Sekiguchi, H. Iwai, *Jpn. J. Appl. Phys.* **54**, 088001 (2015).

Development of Sensor Cells for Nanomaterials Safety Evaluation

Group Leader
(Nano-Life Field)

Akiyoshi TANIGUCHI



1. Outline of Research

Live cell-based sensors are well accepted and used for investigating various signaling cascades caused by cytotoxic effects of reagents, because of their high specificity and sensitivity to their targets' specific gene expression.¹⁾ In our laboratory, next-generation sensor cells are fabricated by molecular biology techniques that can detect changes in gene expression in response to toxic substances or other external stimuli (Fig. 1). We attempted to investigate the interaction between nanoparticles (NPs) and cells through our sensor cells, which can detect stimulation caused by TiO₂ NPs through monitoring induce innate immune responses and other innate cellular stress responses, which we designate as the "First Host Defense System" (FHDS).

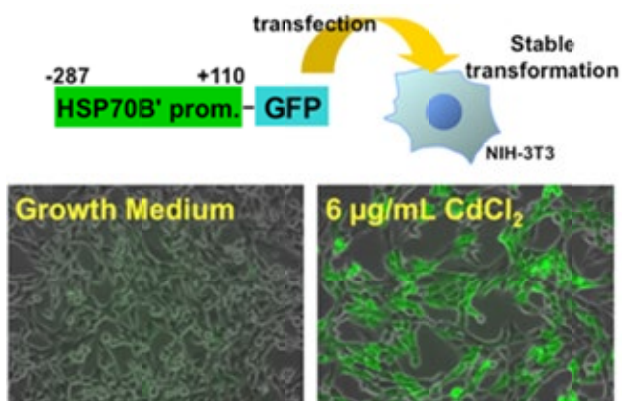


Fig. 1. Construction of sensor cells. Sensor cells were constructed by transfecting plasmids that contain promoter and reporter genes such as HSP70B' and GFP genes in to animal cells.

2. Research Activities

NPs have been manufactured for varied applications. Although they posed a safety risk to our health and environment, recent data have shown the worries concerning their potential toxicity. As we want to develop an effect detection method, how do the nanomaterials affect the cells is important to know. Considering nanomaterials have to be widely synthesized and used for only recent decades, our hypothesis is that there is not enough time for cells to build up specific receptors or signalings for nanomaterials, so the innate cellular defense responses which are against toxins, bacteria, fungi, viruses, and et al., would be used to against the nanomaterials exposure, which we called FHDS (Fig. 2). And this FHDS mainly includes inflammatory response, stress response, and genotoxic response. In nature, different reasons could cause genotoxic response to DNA damage, such as ionizing radiation, ultraviolet light, and oxidizing agents. B-cell translocation gene 2 (BTG2) is implicated in cell cycle regulation, DNA repair, apoptosis and senescence. TiO₂ NPs were used to detect their induced potential

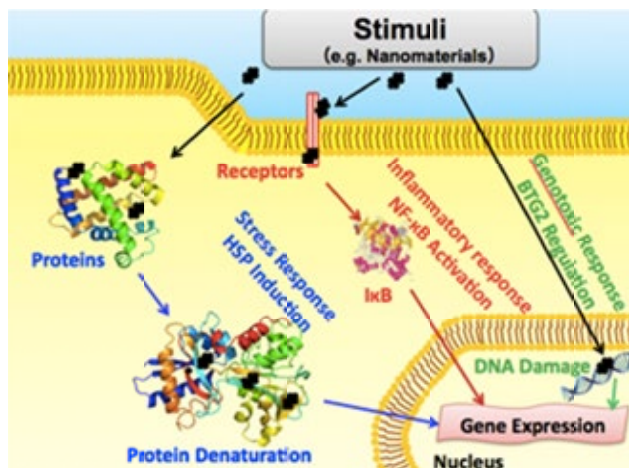


Fig. 2. "First Host Defense System" mainly includes inflammatory response, stress response, and genotoxic response. So that, three effective sensor cells have been developed, recognized by those receptors, and also a "First Host Defense System" response could be induced by the receptors combined with nanomaterials.

genotoxic response using BTG2 sensor cells. The BTG2 sensor cell showed that NPs could induce high genotoxic response. HepG2 cells were exposed to the indicated concentrations of anatase and rutile form, and non-modified mixed crystalline forms of TiO₂ NPs (non-modified TiO₂) and crystalline forms of PEG modified TiO₂ NPs. Anatase forms of TiO₂ NPs showed a significant increase in ROS formation and oxidative stress responses, when compared to rutile forms exposure, and the localization of both anatase and rutile into cells was almost the same (Fig. 3).²⁾ The results suggests that anatase TiO₂ particles exhibit faster migration of electrons and holes from the interior to its surface, and hence greater ROS generation, compared to rutile.

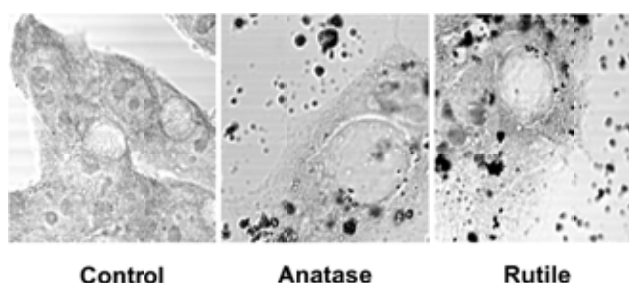


Fig. 3. The localization of TiO₂ NPs anatase and rutile crystalline forms in HepG2 cells that showed almost the same incorporation. (A) Control cells; (B) Cells exposed to 10µg/ml TiO₂ NPs anatase crystalline form for 48 h., (C) Cells exposed to 10µg/ml TiO₂ NPs rutile crystalline form for 48 h.

References

- 1) A. Taniguchi, *Biomater.* **31**, 5911 (2010).
- 2) S.K. El-Said, E. Mostafa, K. Kanehira, K.A. Taniguchi, *J. Nanobiotech.*, in press.

Nano-System Computational Science

Group Leader
(Nano-Power Field)

Yoshitaka TATEYAMA



1. Outline of Research

We are challenging to make novel theoretical frameworks for physicochemical phenomena such as electron transfer, proton transfer & photoexcitation (Fig. 1), since their quantitative calculations are still less established than the conventional techniques for ground state properties.

Our main projects are as follows; (1) development and/or establishment of theories and computational methods for problems in physical chemistry based on the “density functional theory (DFT) and ab-initio calculation techniques,” and (2) understanding microscopic mechanisms of elementary reactions in physical chemistry problems by applying these computational techniques. Of particular interest are surface/interface electrochemistry in photocatalysis, dye-sensitized solar cell, and Li-ion battery.

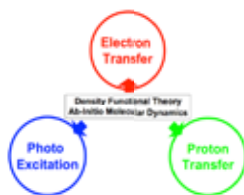


Fig. 1. Research targets in the Nano-System Computational Science group in MANA.

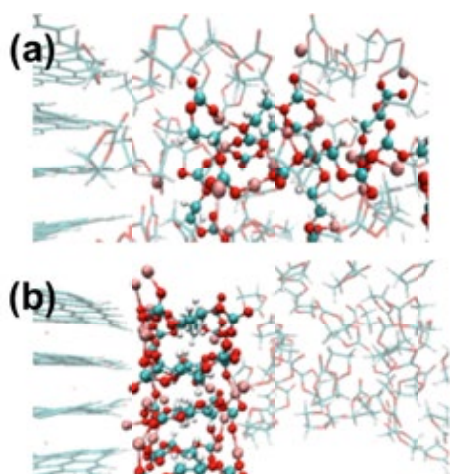


Fig. 2. A proposed formation mechanism “near-shore aggregation mechanism” of organic SEI layer. (a) Organic SEI components aggregate at near-shore. (b) Then, the grown aggregate coalescence with the negative electrode.

2. Research Activities

Recent results are illustrated in Figs. 2-4 for a project on electrolyte–electrode interface in Lithium ion battery (Fig. 2),¹⁾ a project on degradation of perovskite solar cells (Fig. 3),²⁾ and CeO₂ catalysis project (Fig. 4).³⁾

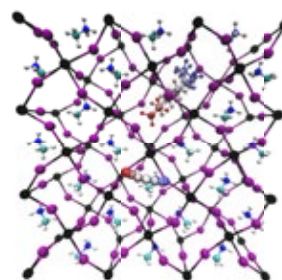


Fig. 3. In addition to halide anion, we have demonstrated molecular cations can move with a low barrier. This may induce significant structural change, which can be a probable origin of degradation of perovskite materials in perovskite solar cells (PSCs).

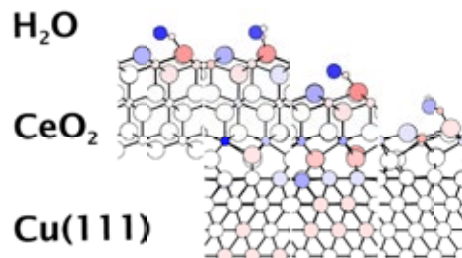


Fig. 4. A schematic picture of electron transfer at hydrated CeO₂ surfaces supported by Cu(111). (Blue atoms: negative change. Red atoms: positive change.)

We have also demonstrated new types of calculations: redox potential calculations in non-aqueous solutions,⁴⁾ and excited states dynamics simulations through real-time propagation time-dependent DFT (TDDFT).⁵⁾

References

- 1) K. Ushirogata, K. Sodeyama, A. Futera, Y. Tateyama, Y. Okuno, *J. Electrochem. Soc.* **162**, A2670 (2015).
- 2) J. Haruyama, K. Sodeyama, L.H. Han, Y. Tateyama, *J. Am. Chem. Soc.* **137**, 10048 (2015). Press release by NIMS and JST.
- 3) L. Szabova, Y. Tateyama, V. Matolin, S. Fabris, *J. Phys. Chem. C* **119**, 2537 (2015).
- 4) R. Jono, Y. Tateyama, K. Yamashita, *Phys. Chem. Chem. Phys.* **17**, 27103 (2015).
- 5) Y. Miyamoto, Y. Tateyama, N. Oyama, T. Ohno, *Sci. Rep.* **5**, 18220 (2015).

Modulation of Superconducting Critical Temperature in Niobium Film Achieved by Using a Nano-Ionics Device

Group Leader

(Nano-System Field)
MANA Research Associate

Kazuya TERABE

Takashi Tsuchiya



1. Outline of Research

Not only fabrication scale for the conventional semiconductor devices, but also the physical operating is being reached limit in near future. One possible way to overcome these technological and physical limits of the existing conventional semiconductor device is to achieve breakthroughs in device materials and novel device-operation principle using nanotechnology. A promising type of such nano-devices is the nano-ionics device,¹⁾ which is operated by controlling the local ion migration and electrochemical reaction instead of electron and hole migration. Our group has been focusing to develop novel nano-ionics device with unique functions such as superconducting.

Application of high-temperature superconducting is one of promising approach to solve serious energy and environmental problems in present-day world. Thus, there have been many researches to try to discover superconductors with high critical temperature (T_c) that is based on a synthesis of novel bulk materials and a chemical doping. The highest T_c achieved so far is 164 K for a Hg-1223 cuprate superconductor under high pressure, but it has not been bettered for more than a decade although new classes of superconductor have been discovered. As a result, research attention has shifted to exploring exotic conditions under which potential superconducting materials become superconductors or to greatly increasing the T_c of conventional superconductors. The promising approach is based on the expectation that T_c will increase with the carrier density, which is based on a relationship given in standard BCS theory

$$T_c = 1.14 \frac{\hbar \omega_D}{k_B} \exp\left(-\frac{1}{D(0)V}\right)$$

The $D(0)$ and V are the density of states (DOS) near the Fermi level and the electron-phonon interaction, respectively. Recent superconductivity research has used an electric double layer (EDL) transistor composed of liquid electrolytes to achieve high carrier density.²⁾ The achievement of 10^{14} cm^{-2} order carrier density enabled interface superconductivity in insulators and semiconductors, which are not normally superconductors due to their intrinsic low carrier density. This approach is particularly advantageous due to the freedom from the structural disorder inherent in chemical doping. However, practical application is difficult due to the low compatibility with other electronic devices caused by the use of liquids and gels. It is considered that EDL transistor should be composed of solid electrolytes to create practical

superconductivity devices.

In our study, we have succeeded to demonstrate the electric modulation of T_c by using an EDL at a superconductor/solid electrolyte interface in the solid nanoionics device.³⁾

2. Research Activities

An all-solid-state EDL transistor composed of Nb film epitaxially grown on $\alpha\text{-Al}_2\text{O}_3$ (0001) and Li_4SiO_4 solid electrolyte was fabricated (Fig. 1a). The $T_{c,\text{onset}}$ of the Nb film was modulated from 8.33 to 8.39 K while gate bias (V_g) was reduced from 2.5 to 2.5 V (Fig. 1b). The specific difference in $T_{c,\text{onset}}$ for the applied V_g was calculated to be 12 mK/V, which is larger than the value reported for an EDLT composed of ionic liquid. In addition to the T_c modulation by EDL charging, T_c was enhanced by 300 mK at the $\text{Li}_4\text{SiO}_4/\text{Nb}$ film interface. This is attributed to an increase in DOS near the Fermi level due to lattice constant modulation. This solid electrolyte gating method should enable development of practical superconducting devices highly compatible with other electronic devices. It should also create extremely exotic conditions resulting in high carrier density and a solid/solid interface effect, both of which are promising for achieving high T_c superconductivity. This method can be used for discovering new functions in a wide spectrum of electronic materials as well as for increasing the T_c for superconducting.

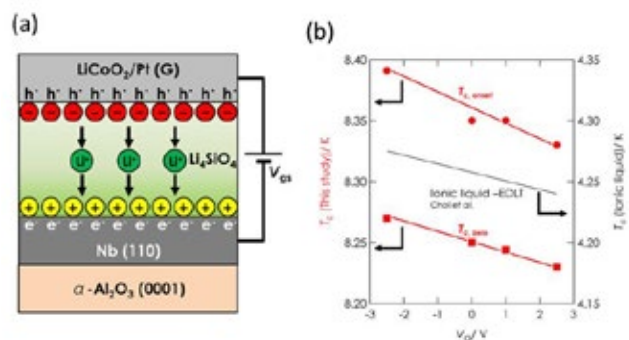


Fig. 1. (a) Schematic illustration of Nb-based EDL transistor composed of Li_4SiO_4 , Li^+ ion conductor and LiCoO_2/Pt gate electrode. Yellow and red circles represent positive and negative charges accumulated at interfaces due to Li^+ ion migration. (b) Variation of $T_{c,\text{onset}}$ and $T_{c,0}$ zero plotted with respect to gate bias (V_g).³⁾

References

- 1) K. Terabe, T. Hasegawa, C. Liang, M. Aono, *Sci. Tech. Adv. Mater.* **8**, 536 (2007).
- 2) K. Ueno, S. Nakamura, H. Shimotani, A. Ohtomo, N. Kimura, T. Nojima, H. Aoki, Y. Iwasa, M. Kawasaki, *Nat. Mater.* **7**, 855 (2008).
- 3) T. Tsuchiya, K. Terabe, M. Aono, *Appl. Phys. Lett.* **107**, 013104 (2015).

Effect of Carbonate Buffer System on the Biodegradation of Mg Alloys

Group Leader
(Nano-Life Field)

Akiko YAMAMOTO



1. Outline of Research

Magnesium and its alloys are expected to be used as biodegradable implant devices since they are easily corroded by reacting with water in the body fluid. For the success of their biomedical application, it is important to control their degradation ratio in the human body environment since it influences not only their mechanical integrity along the implantation period but also their biocompatibility. To achieve the ideal degradation rate of Mg alloy devices, it is mandatory to understand their degradation mechanism in biological environment.

Body fluid contains inorganic ions as well as organic compounds such as amino acids and proteins. Since its pH is maintained by the carbonate buffer system, higher concentration of CO₂ in the human body fluid than in air is another important factor influencing biodegradation of Mg alloys inside the human body. We have already reported the accelerating and inhibiting effects of cells, amino acids and serum proteins on pure Mg biodegradation under cell culture condition.^{1,2)} In this study, the effect of carbonate buffer system on the degradation of a Mg alloy is examined under cell culture condition.³⁾

Table 1. Major components and their concentrations in blood plasma and simulated body fluids.

	plasma	Earle(+)	Hanks(+)
Na ⁺ (mol/L)	0.1420	0.1435	0.1418
K ⁺ (mol/L)	0.0050	0.0054	0.0058
Ca ²⁺ (mol/L)	0.0025	0.0018	0.0013
Mg ²⁺ (mol/L)	0.0015	0.0008	0.0008
Cl ⁻ (mol/L)	0.1030	0.1235	0.1423
HCO ₃ ⁻ (mol/L)	0.0270	0.0262	0.0042
HPO ₄ ²⁻ (mol/L)	0.0010	0.0009	0.0008
SO ₄ ²⁻ (mol/L)	0.0005	0.0008	0.0008
amino acids (g/L)	0.25-0.4	-	-
Glucose (g/L)	~1.1	1.0	1.0
proteins (g/L)	63-80	-	-

2. Research Activities

Two types of Mg-2wt%Zn-1wt%Mn(ZM21) samples were prepared; squeeze casted (CAST) and equal channel angular pressed (ECAP). The former has a typical dendritic distribution of second phases whereas no obvious existence of the second phase was observed in the latter. *In vitro* degradation behavior of these samples was investigated in Earle's and Hanks' solutions at 37 °C under 5% CO₂ in humidified air. The chemical components of these solutions are shown in Table 1.

Examples of X-ray CT images After 4 weeks of immersion into these solutions were shown in Fig. 1, indicating extreme localized corrosion on ECAP. Optical microscopic observation (Fig. 2) revealed dendritic patterns of second phase on CAST, suggesting their contribution as a barrier against the progress of corrosion. Weight loss data of these samples (Fig. 3) clearly showed severe degradation on ECAP than CAST. It also indicated that the effect of carbonate

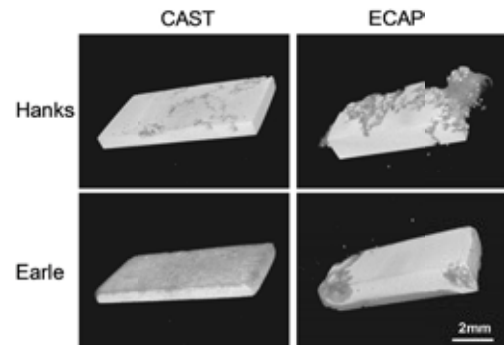


Fig. 1. Examples of X-ray CT images of CAST and ECAP samples after 4w of immersion in Hanks' and Earle's solutions.

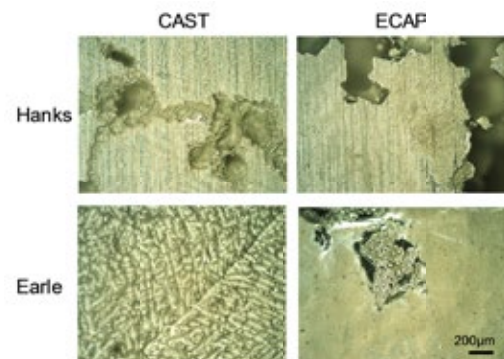


Fig. 2. Examples of optical microscopic images of CAST and ECAP samples after 4w of immersion in Hanks' and Earle's solutions.

buffer system depends on the microstructure of samples. After 24h of immersion, the pH values of Hanks increased around 8.5 for CAST and 8.6 for ECAP, whereas those of Earle were 7.8 for CAST and 8.0 for ECAP. These data proves the importance of carbonate buffer system to maintain the pH of the body fluids. In case of CAST, this lower pH of Earle results in the higher degradation. However, in case of ECAP, higher susceptibility to localized corrosion in higher pH environment results in higher degradation in Hanks.

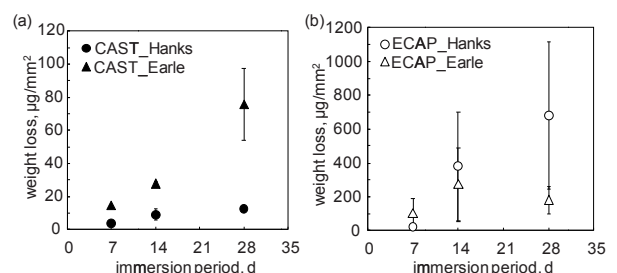


Fig. 3. Weight loss after removal of insoluble salt layer from the immersed samples (mean ± s.d.). (a) CAST and (b) ECAP samples.

References

- 1) A. Yamamoto, S. Hiromoto, *Mater. Sci. Eng. C* **29**, 1559 (2009).
- 2) M.B. Kannan, A. Yamamoto, H. Khakbaz, *Colloids Surf. B* **126**, 603 (2015).
- 3) A. Witecka et al., *Mater. Sci. Eng. C*, submitted.

Laser-Based Inelastic Photoemission Spectroscopy

MANA Independent Scientist **Ryuichi ARAFUNE**



1. Outline of Research

My main objective is to explore and elucidate some aspects of the interaction between light and matter that take place uniquely at solid surfaces and two-dimensional systems. Currently, we concentrate on developing laser photoemission spectroscopy (PES) into a novel technique to probe surface dynamics. Vibrational dynamics of adsorbate modes of adsorbed atoms and molecules can yield direct information on the nature of the bonding with the surface and on the energy exchange between the adsorbate and the substrate. Such modes appear at low-energy region (<100 meV). Unfortunately, no time-resolved surface vibrational technique that is applicable to low-energy vibrational modes has been developed thus far. Thus, a novel technique that can access such low energy vibrational modes is highly demanded.

We found that the photoemission spectra excited by the low energy laser light contain the vibrationally induced inelastic components. This result indicates that the laser excited and low-energy photoelectron strongly interacts with vibrational elementary excitations. We believe that this inelastic interaction brings us a novel way to investigate dynamics arising from the electron-phonon couplings. Thus one of the aims of this research project is developing the laser-PES as a reliable tool for measuring electron-phonon coupling.

Another important subject of this research project is searching for a new two-dimensional material in which novel quantum characters explicitly appears. I believe that such material is a good sample for the laser-based PES technique.

2. Research Activities

(1) *High energy-resolved two-photon photoemission study of elastic scattering in image potential state of Cu(001).*

High energy-resolved two-photon photoemission study of elastic scatterings in image potential state of Cu(001) Electron dynamics in the excited states are governed by inelastic and quasielastic scattering processes. It is required to determine both scattering rates for complete understanding of the electron dynamics. Although time-resolved two-photon photoemission (2PPE) spectroscopy is a unique and powerful tool to measure the scattering rates directly, it is not easy to evaluate the quasielastic scattering rate. Precise measurement of spectral linewidth with high-energy resolution is an alternative way to determine the elastic scattering rate. However, the high energy-resolution 2PPE measurement hasn't been well developed because of the tradeoff between the time and the energy resolutions. In this study, we have succeeded in improving the energy resolution of 2PPE by using narrow band laser pulses. We have measured the 2PPE spectra of image potential states (IPs) of Cu(001), and determined the quasielastic scattering rate for $n = 1$ IPS as well as the binding energies and band dispersions of the higher IPs.

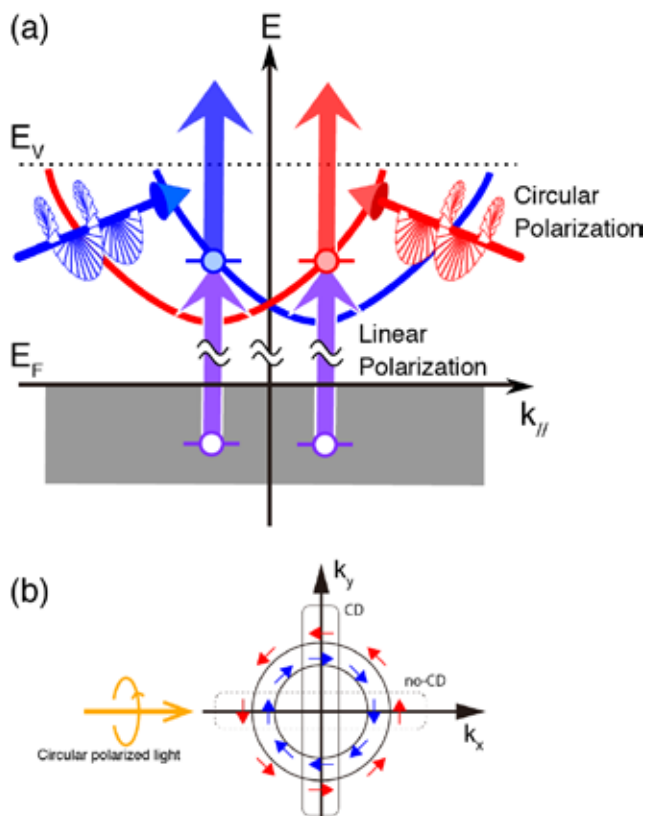


Fig. 1. Schematic energy diagram for (a) CD-2PPE and (b) the Rashba-type spin texture.

(2) *Rashba Splitting in Image Potential State Investigated using Circular Dichroism Two-Photon Photoemission Spectroscopy.*

Control of the electron spin in nonmagnetic materials is a key technology for future device applications. Optical manipulation through spin-orbit interactions (SOIs) is a promising route to achieve this. Although the spin-dependent electronic band structure above the Fermi level caused by the SOI is required, our understanding of SOIs is incomplete because the required experimental methods have not yet established. Here, we use angle-resolved 2PPE-spectroscopy in combination with circular dichroism (CD) to explore the band splitting and the spin-texture of the image potential state on Au(001) derived from the Rashba-type SOI (Fig. 1). The measured CD characteristics are consistent with the spin-splitting energies calculated from the embedded Green's function technique for semi-infinite crystals. The present results demonstrate the powerfulness of CD-2PPE spectroscopy and open a solid pathway to map the spin-dependent unoccupied band structures originating from SOIs in various classes of condensed matters.

Search for New Ferroelectric, Magnetic, and Multiferroic Materials Using High-Pressure Technique

MANA Independent Scientist Alexei A. BELIK



1. Outline of Research

In multiferroic systems, two or all three of (anti) ferroelectricity, (anti)ferromagnetism, and ferroelasticity are observed in the same phase. These systems may have wide technological applications because they allow control of electric properties by magnetic field and control of magnetic properties by electric field (Fig. 1). The application would include, for example, multiple-state memory elements. Multiferroic materials have been studied in the past, but those studies did not attract wide attention most probably due to the lack of materials with strong magnetoelectric coupling and high ordering temperatures. In the field of multiferroic materials, two major problems still remain: (1) preparation of materials with multiferroic properties at and above room temperature (RT) and (2) preparation of materials with strong coupling between different order parameters. The coupling is usually strong in the so-called spin-induced multiferroics where polar structures emerge as results of specific magnetic ordering; however, transition temperatures are quite low in spin-induced multiferroics. The search for new multiferroic materials and understanding their mechanisms are important topics for the development of the field. In our work, the advanced high-pressure synthetic method is used which allows the preparation of many new materials.

2. Research Activities

(1) Magnetic Properties of Multiferroic Solid Solutions Between BiMIO_3 and BiM_2O_5 .¹⁾

Bi-containing perovskites have received a lot of attention as multiferroic materials and lead-free ferroelectrics. The stereochemically active $6s^2$ lone pair of a Bi^{3+} ion plays an important role in producing polar distortions in Bi-containing perovskites. They form a basis for materials with super-tetragonality and a huge spontaneous polarization. We investigate detailed magnetic properties of $\text{BiCr}_{1-x}\text{Ga}_x\text{O}_3$ solid solutions and construct a magnetic phase diagram. Antiferromagnetic order with weak ferromagnetism is observed below $T_N = 54, 36$ and 18 K in the samples with $x = 0.4, 0.5$ and 0.6 , respectively, having a polar $R3c$ structure. Therefore, they can be considered as multiferroic materials.

(2) Multiferroic and Magnetodielectric Properties of R_2NiMnO_6 Perovskites.^{2,3)}

We find a ferroelectric polarization in $\text{In}_2\text{NiMnO}_6$ at $T_N = 26$ K, which is induced by a combination of spin helicity with B-site chemical ordering and octahedral tilting resulting in a “ferriaxial” mechanism unique for the ordered double perovskites (Fig. 1). Two-dimensional magnetic propagation vector found in $\text{In}_2\text{NiMnO}_6$ is quite rare in perovskites. We

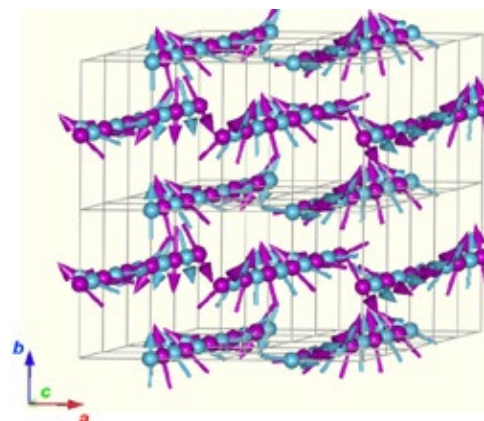


Fig. 1. Non-collinear incommensurate magnetic structure of $\text{In}_2\text{NiMnO}_6$ – the origin of the appearance of an electric polarization below T_N . Mn is purple, Ni is blue.

also find unique properties in $\text{Sc}_2\text{NiMnO}_6$, where Ni^{2+} and Mn^{4+} cations order independently at different temperatures of 17 and 35 K, implying that nearest neighbor superexchange between Ni and Mn is heavily suppressed compared to the next-nearest-neighbor Ni–Ni and Mn–Mn extended superexchanges. A magnetodielectric anomaly arises from an antiferroelectric ordering that results from the exchange striction between the two magnetic sublattices.

(3) Multiferroic Properties of $\text{AMn}_7\text{O}_{12}$ ($A = \text{Cd}, \text{Ca}, \text{Sr},$ and Pb) Perovskites.⁴⁾

$(\text{AA}')_3\text{B}_4\text{O}_{12}$ perovskite-structure materials have received a lot of attention because many members of this family show interesting physical and chemical properties, for example, intersite charge transfer and disproportionation, metal–insulator transitions, giant dielectric constant, good catalytic activities, and multiferroic properties. $\text{CaMn}_7\text{O}_{12}$ was considered to be a multiferroic material with the largest spin-induced polarization below T_{N1} . We clarify multiferroic properties of $\text{AMn}_7\text{O}_{12}$ and find that they have quite small spin-induced polarization below T_{N2} . However, they still have interesting properties because of lattice, spin, and orbital degrees of freedom including incommensurate structural modulations and lock-in transitions.

References

- 1) A.A. Belik, *Sci. Technol. Adv. Mater.* **16**, 026003 (2015).
- 2) N. Terada, D.D. Khalyavin, P. Manuel, W. Yi, H.S. Suzuki, N. Tsujii, Y. Imanaka, A.A. Belik, *Phys. Rev. B* **91**, 104413 (2015).
- 3) W. Yi, A. J. Princep, Y. Guo, R.D. Johnson, D. Khalyavin, P. Manuel, A. Senyshyn, I.A. Presniakov, A.V. Sobolev, Y. Matsushita, M. Tanaka, A.A. Belik, A. T. Boothroyd, *Inorg. Chem.* **54**, 8012 (2015).
- 4) Y.S. Glazkova, N. Terada, Y. Matsushita, Y. Katsuya, M. Tanaka, A.V. Sobolev, I.A. Presniakov, A.A. Belik, *Inorg. Chem.* **54**, 9081 (2015).

Towards Development of Vertical Quantum Field Effect Transistors with Attractive Molecular Dots

MANA Independent Scientist Ryoma HAYAKAWA



1. Outline of Research

The evolution of complementary metal-oxide-semiconductor (CMOS) devices is now reaching a major turning point owing to the critical limit imposed by increasing large-scale integration and growing power consumption. Molecular devices, which are controlled at single molecule level, are promising candidates for exploiting “beyond CMOS” devices. However, the development of such molecular devices is still at the basic research stage and practical application remains a long way off. The main obstacle is the lack of effective device structures for molecular devices.

We are proposing the adoption of functional organic molecules as quantum dots in a metal-oxide-insulator (MOS) structure which offers to integrate attractive molecular functions into current Si devices.¹⁾ We have achieved unique functions brought by attractive molecular dots such as multivalued operation with binary molecules²⁾ and optical manipulation by photochromic molecules,³⁾ which are not obtained in inorganic quantum dots. For further functionalization, we try to develop a vertical resonant tunneling transistor with attractive molecular dots based on a Si-based double tunnel junction (Fig. 1).

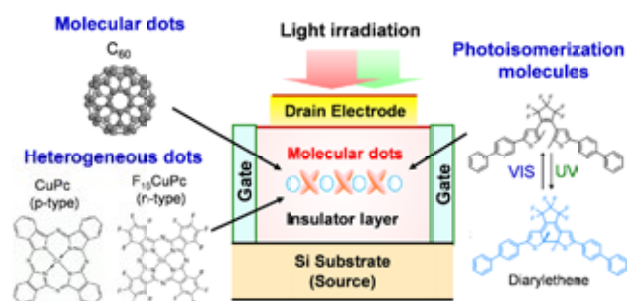


Fig. 1. A schematic illustration of vertical resonant tunneling transistors with functional molecular dots.

2. Research Activities

(1) Formation of one-dimensional mesa structure by electron beam lithography.

We made an effort to form one-dimensional mesa structures, which consist of double tunnel junctions with molecular dots, by a conventional lithography technique. Usually, current lithography techniques are not available for organic based devices because organic resists and solvents cannot be used in the process. Meanwhile, in our devices, individual molecules are embedded in insulating layers which act as protective layers for organic solvents. The feature allows the employment of current lithography techniques and thereby achieves large-scale integration of molecular devices. Fig. 2 shows a typical scanning electron microscopy image of a one-dimensional structure with C_{60} molecules as quantum dots. The width of mesa structure was successfully scaled down to 40 nm, which enables effective application of voltage with side gates.

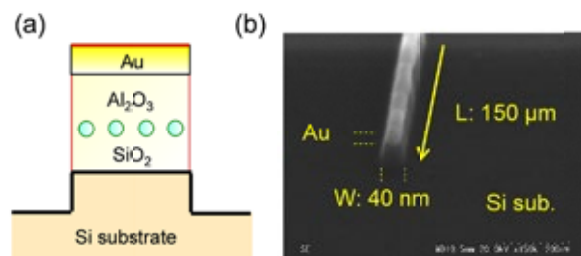


Fig. 2. (a) A schematic illustration and (b) a scanning electron microscopy image of a one-dimensional mesa structure.

(2) Resonant tunneling via molecular dots in the one-dimensional mesa structure.

Current (I)-voltage (V) measurements were performed at 20 K to confirm whether the molecules embedded in insulating layers still survive after the nanofabrication with a standard electron beam lithography. We observed clear staircases in the I - V curve (Fig. 3a). The multiple peaks in the dI/dV coincide with those of HOMO and LUMO levels in C_{60} molecules (Fig. 3b), indicating that resonant tunneling via molecular orbitals appeared. In addition, the probability to observe staircases was considerably improved and the value was achieved to 80 %. Our attempt, therefore, would offer a promising approach to realize practical molecular devices.

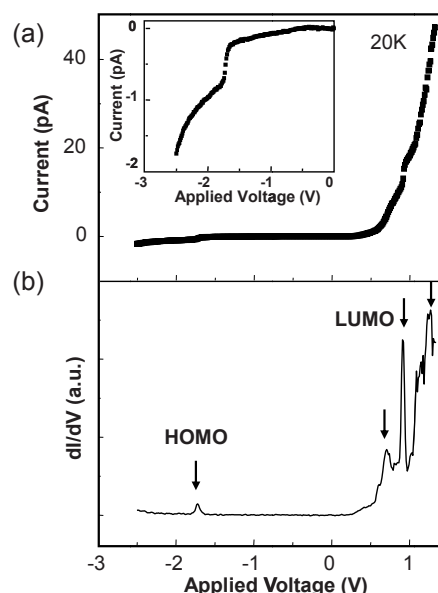


Fig. 3. (a) I - V and (b) differential conductance (dI/dV) curves in a one-dimensional mesa structure at temperature of 20 K.

References

- 1) R. Hayakawa, N. Hiroshiba, T. Chikyow, Y. Wakayama, *Adv. Funct. Mater.* **21**, 2933 (2011).
- 2) H.S. Seo, R. Hayakawa, T. Chikyow, Y. Wakayama, *J. Phys. Chem. C* **118**, 6467 (2014).
- 3) R. Hayakawa, K. Higashiguchi, K. Matsuda, T. Chikyow, Y. Wakayama, *ACS Appl. Mater. Interfaces* **5**, 11371 (2013).

Bifunctional Oxygen Electrocatalysis with Phase-Pure α - Mn_2O_3 Prisms

MANA Independent Scientist Joel HENZIE



1. Outline of Research

Controlling the nanoscale shape and size of colloids is of practical importance in fields including catalysis, energy storage and optics. Yet the chemical methods used to make these nanoparticles is still not well understood, even for simple unary materials such as noble metals. We are developing experimental and theoretical tools to understand the mechanism of shaped nanocrystal growth. Our present focus is on shaped manganese oxides because: (1) the numerous oxidation states of Mn enable the creation multiple different materials with exotic electronic and magnetic properties, and (2) Mn-oxides are important materials in conventional lithium ion batteries and regenerative fuel cell technologies. The practical goal is to use these colloids as building blocks for the assembly of advanced functional composite 3-dimensional (3D) materials for energy generation and energy storage.

2. Research Activities

Oxygen electrochemistry is central to the function of fuel cells, and there is great demand for materials that can drive oxygen evolution (OER) and oxygen reduction (ORR) reactions. Most research is focused on one-way reactions, but there is significant interest in catalysts that can fulfill a dual role—a so-called bifunctional catalyst that can drive both oxygen reduction and water oxidation reactions reversibly—for high energy storage at minimal weight in regenerative fuel cell configurations. Additionally, since most efficient catalysts for oxygen electrochemistry rely on scarce elements including Pt, Pd, Ir and Ru, developing a strategy to utilize Earth-abundant elements is critical for the scalability of these technologies as sustainable energy sources.

Mn-oxides are interesting materials for oxygen electrocatalysts because CaMn_4O_5 clusters are used as oxygen evolving complexes in photosynthesis. Taking this inspiration from nature, researchers have created solid-state equivalents based on Mn-oxide polymorphs to test how catalysis is affected by changes in structure. We developed a simple method to synthesize a phase pure form of α - Mn_2O_3 (bixbyite). Previous reports have suggested that α - Mn_2O_3 is a good catalyst because its electronically degenerate Mn(III) has longer Mn-O bonds, which contribute to structural flexibility at the active site.

Fig. 1A shows an SEM and TEM micrograph of α - Mn_2O_3 prisms bound by $\{100\}$ facets. We used advanced structural analysis to prove this material is a pure orthorhombic phase, and that no other amorphous or nanocrystalline phases exist in the material. This was important because minor phases often dominate the activities of catalysts. After heat treatment, the prisms transform from orthorhombic to cubic phase (Fig. 1B).

We compared the catalytic activity of both cubic and orthorhombic phases of α - Mn_2O_3 for oxygen evolution

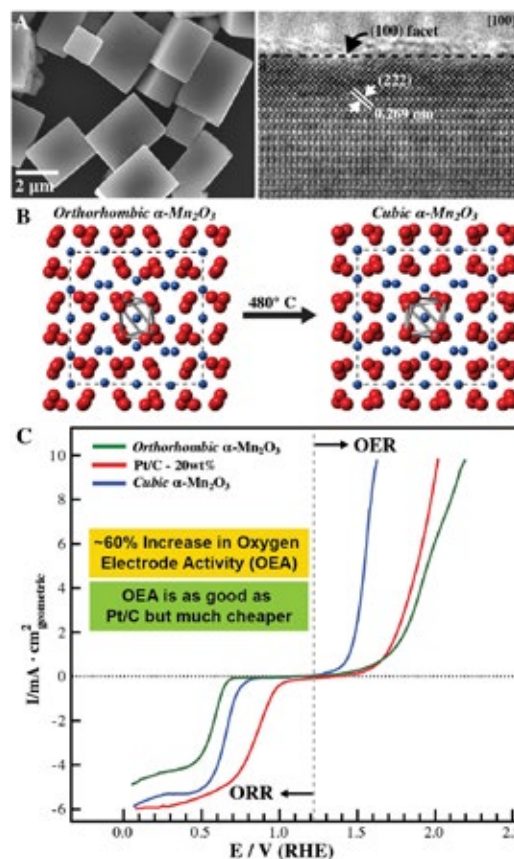


Fig. 1. (A) SEM and TEM micrographs of α - Mn_2O_3 prisms. Crystal structure analysis shows the α - Mn_2O_3 transforms from orthorhombic to cubic phase when heated (B). ORR and OER activities of orthorhombic and cubic phase α - Mn_2O_3 compared to Pt/C (C). The cubic phase has 60% better OEA and is equivalent in activity to Pt/C.

(OER) and oxygen reduction (ORR) reactions and found that the cubic phase exhibited a combined oxygen electrode activity (OEA) of 1.01V, which was a 60% improvement over the orthorhombic phase (Fig. 1C). Surprisingly, the cubic phase α - Mn_2O_3 prisms performed equivalent to or better than platinum on carbon (Pt/C) as a bifunctional OER/ORR catalyst. This very subtle change in topology from the orthorhombic to cubic phase likely enables a more favorable electronic configuration for oxygen electrochemistry.¹⁾

By combining shape-controlled colloidal synthesis with careful structural analysis and the assistance of theoretical modeling, we hope to elaborate more on the details of electronic structure in Mn-oxides, and its role in determining their catalytic activity. We also are working on inexpensive methods to make shape-controlled Mn-oxides and mixed Mn-oxides (LaMnO_x , CoMnO etc.) at a fraction of the cost of current methods.

Reference

- 1) M. Jahan, S. Tominaka, J. Henzie, submitted for publication.

Ultra-High-Resolution Patterning of Functional Inks for Fully-Printed Electronic Devices

MANA Independent Scientist Takeo MINARI



1. Outline of Research

The current production processes for semiconductor electronic devices require huge conveyor lines and large-scale equipment operating under clean conditions, and these top-down technologies result in a substantial waste of materials. These factors also increase production costs and investment in facilities. On the other hand, solution-based patterning of functional materials into microstructures received increasing interests as a facile and low-cost fabrication method of devices in optical, electronic, biological and sensory applications. Recent electronic applications such as high-definition displays require homogeneous device formation in large area with shrinking of device dimensions to a few-micron scale. Thus, fabrication of electronic devices using spontaneous solution patterning with a few-micron resolution is critical for use of such solution-based fabrication techniques in semiconductor manufacturing processes.

2. Research Activities

(1) High-resolution patterning of metal nanoparticles.

Solution-processed patterning of electrode lines can be carried out by selective deposition of metal nanoparticle inks using surface wetting/dewetting phenomena.^{1,2)} Here we use photo-induced hydrophilicity on a hydrophobic polymer surface using area-selective irradiation of vacuum ultra violet light ($\lambda < 200$ nm) to form the wettability contrast on surface. After application of the metal nanoparticle ink by a simple coating method, the different wettabilities effectively guide the solution to be deposited onto the wettable regions only, thus precise electrode patterns can be obtained by a facile solution-based method. Fig. 1 shows the results of the spontaneous patterning of Au nanoparticles. We used room-temperature-processable Au ink as the electrode material, thus all the patterning processes can be carried out under ambient atmosphere at room temperature.²⁾ This technique permits us to selectively deposit the functional inks with a 1- μm feature size, allowing fabrication of high-resolution organic thin-film transistor (OTFT) arrays even with 1- μm channel length.

(2) Patterning short-channel OTFT arrays.

The spontaneous patterning method is useful for printing of short-channel OTFT devices because of the ultra-high resolution down to 1- μm feature size. We also achieved room-temperature fabrication process without use of

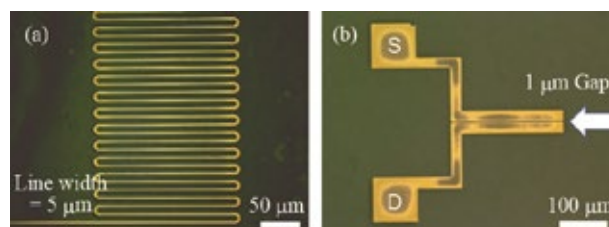


Fig. 1. Optical microscope images showing feasibility of spontaneous solution patterning. (a) Complex electrode lines with the line and space widths of 5 μm . (b) Source/drain electrodes with the gap width of 1 μm .

annealing, which prevents undesired deformation of flexible substrates during the fabrication process and thus enables the high-resolution layer-by-layer printing of OTFT devices. The short-channel OTFT fabricated by the spontaneous solution patterning is shown in Fig. 2. We employed the bottom-contact/top-gate device structure, and the organic semiconductor layer was also patterned to avoid a cross-talk effect among the neighboring devices. The precise patterning method allowed accurate tuning of the gate overlap lengths, which was devoted to improving significantly the device performance, especially enhancing charge injection. The field-effect mobility values of 0.3 and 1.5 $\text{cm}^2\text{V}^{-1}\text{s}^{-1}$ were obtained for 1- and 5- μm devices, respectively, which are comparable with those achieved by vacuum thermal evaporation.³⁾

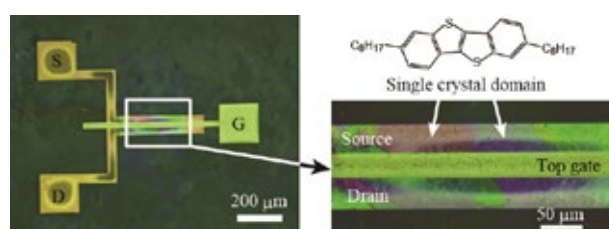


Fig. 2. Optical microscope images of a short-channel OTFT printed on plastic. Photograph of printed bottom-contact/top-gate OTFT (left), and photograph of channel region (right). The 1- μm gap lies beneath the top gate electrode.

References

- 1) T. Minari, C. Liu, M. Kano, K. Tsukagoshi, *Adv. Mater.* **24**, 299 (2012).
- 2) T. Minari, Y. Kanehara, C. Liu, A. Yaguchi, K. Sakamoto, T. Yasuda, S. Tsukada, K. Kashizaki, M. Kanehara, *Adv. Funct. Mater.* **24**, 4869 (2014).
- 3) X. Liu, M. Kanehara, C. Liu, K. Sakamoto, T. Yasuda, J. Takeya, T. Minari, submitted for publication.

Quantum Devices in Nanomaterials

MANA Independent Scientist Satoshi MORIYAMA



1. Outline of Research

A quantum dot is a small metallic island with a single electron charging effect and zero-dimensional confined states, which resembles to the natural atom. For this reason, the quantum dot is often called an artificial atom. Although the atom-like physics is studied their interaction with light, artificial atoms can measure electron transport properties in solid state systems. Therefore, quantum dots are expected for future electric devices that can control the single-electron charge and spin states. Unique features of the quantum dot are the single electron charging effect and the quantized energy levels, and the characteristic energy for the former is the charging energy for a single electron ($E_c = e^2/C_\Sigma$; C_Σ is the self-capacitance of the dot) and is the mean zero-dimensional level spacing (ΔE) for the latter. The single electron devices only need the small dot size for the higher temperature application. The quantum computing devices which may use both the single electron effect and the quantized level need quantum coherence as well. Based on the above background, we explore novel quantum-dot devices that have different functions with conventional transistor. Our research results in this year are the demonstration of single-electron devices in silicon-based tunnel field-effect transistors (TFETs), and the experimental realization of quantum transport in graphene-based superlattices.

2. Research Activities

(1) Single-electron transport via deep levels in Silicon-based tunnel field-effect transistors.

The TFETs are attractive for quantum tunneling devices, as well as a promising candidate to realize much steeper switching with a sub-threshold swing than that of the conventional metal-oxide-semiconductor field-effect transistors (MOSFETs). Recently, we demonstrate a novel single-electron devices that is based on a short channel

silicon-based TFET with deep level defects or impurities in the transport channel.¹⁾ A single- and multi-quantum-dot like transport is observed in the mid-gap region of the short channel TFET that a single- or few deep level defect/impurities can act as quantum dots. A large single-electron charging energy up to 0.3 eV is observed in the Coulomb diamond characteristic and a current peak due to the Coulomb oscillation is visible at the room temperature.¹⁾

(2) Quantum transport in hexagonal boron nitride (hBN)/Graphene/hBN superlattices.

Graphene, a single atomic layer of graphite are one of the attractive two-dimensional (2-D) conducting materials for a new stage of low dimensional physics. Electronic properties are expected to differ from the well-studied case of the 2-D electron gas in semiconductor hetero-structure. These differences are due to the unique band structure of graphene, so-called 'Dirac Cone', which exhibits electron-hole degeneracy and vanishing carrier mass near the point of charge neutrality. From the application point of view, the ballistic transport and high mobility in graphene make them possible candidates for future electronic quantum devices. Recently, heterostructures of 2-D materials have attracted great interests because they form superlattices which allow band engineering as well as use of multiple degenerate degrees of freedom. We have measured the quantum transport properties of encapsulated hBN/graphene/hBN heterostructures with one-dimensional edge contacts as well as a Hall bar geometry, prepared by a dry transfer method. Back-gate voltage dependence of the resistivity and conductivity near the Dirac point are shown in Fig. 1. We obtained a high mobility $\sim 150,000 \text{ cm}^2/\text{Vs}$ near the Dirac point ($V_g \sim 0.3 \text{ V}$) at 5 K. The secondary peak at $V_g \sim -21 \text{ V}$ corresponds to a cloned Dirac point come from moiré pattern due to the 1.8 % lattice mismatch between graphene and hBN. From this voltage, we can estimate the alignment angle between graphene and hBN, $\theta = 0.7\text{-}0.8^\circ$ and the moiré superlattice size $\sim 11 \text{ nm}$.²⁾ These experimental results indicate the high quality of the sample with ballistic transport. We will proceed to fabricate the Graphene QD devices in hBN/graphene/hBN heterostructures, because the performance of such nanostructured devices is expected to depend strongly on the sample quality.

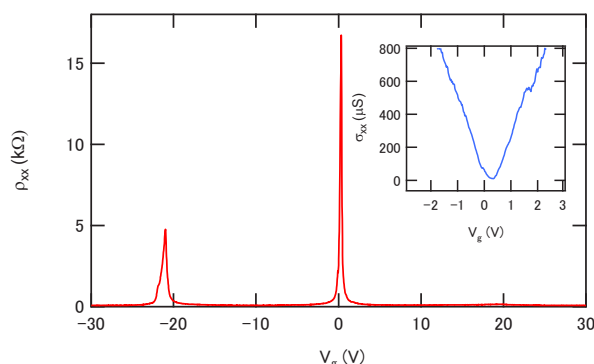


Fig. 1. Back-gate voltage (V_g) dependence of resistivity (ρ_{xx}) at 6 K and $B = 0 \text{ T}$. Inset shows the conductivity (σ_{xx}) near the Dirac point.

References

- 1) K. Ono, T. Mori, S. Moriyama, *Room-temperature single-electron transistor based on tunnel field-effect transistor (TFET) and deep level*, Silicon Quantum Electronics Workshop (2015).
- 2) K. Komatsu, E. Watanabe, D. Tsuya, K. Watanabe, T. Taniguchi, S. Moriyama, *Quantum transport in hBN/graphene/hBN heterostructures with one-dimensional edge contacts*, ISANN2015, International Symposium on Advanced Nanodevices and Nanotechnology (2015).

Development of Photoresponsive Biointerfaces

MANA Independent Scientist Jun NAKANISHI



1. Outline of Research

Biointerface is an interface between biomolecules and materials. It plays a pivotal role in biomedical devices such as materials for drug delivery, tissue engineering, and bioanalysis. The major purpose of the present study is to develop chemically functionalized biointerfaces with photochemically active compounds and apply them for analyzing and engineering cellular functions (Fig. 1).¹⁾

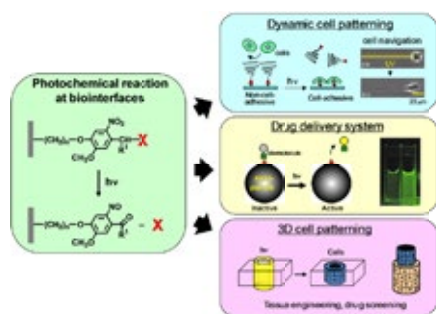


Fig. 1. Photoresponsive biointerfaces developing in this study.

2. Research Activities

(1) *Reduced adhesive ligand density induces an epithelial-mesenchymal-like transition in Madin-Darby canine kidney cells.*²⁾

A synergistic effect of biochemical and mechanical cues in extracellular matrix (ECM) on malignant induction in epithelial cells has been recently observed. However, the effect of quantitative change in the biochemical stimulus at a fixed ECM rigidity and compositions on cell phenotype remains unknown. To test this, we grew epithelial Madin-Darby canine kidney (MDCK) cells on gold surfaces immobilized with varying densities of cRGD (Fig. 2) and analyzed the morphology, migration, cytoskeleton organization and protein expression. Cells displayed an epithelial morphology and growth in clusters on the surface presenting a higher density of cRGD while cells transformed into an elongated fibroblast-like form with extensive scattering on the diluted cRGD surface. Time-lapse imaging of cell clusters grown on the concentrated cRGD surface revealed a collective migration with the intact cell-cell contacts accompanied by the development of the cortical actin. In contrast, cells migrated individually along with the formation of stress fibers on the substrate with sparse cRGD. These data suggest a transdifferentiation of epithelial cells to mesenchymal-like cells when plating on the diluted cRGD surface. Supporting this, immunofluorescence microscopy and western blot analysis revealed increased membrane localization and a total expression of N-cadherin in the cells undergoing mesenchymal-like transition. Taken together, these results suggest a possible role of a decrease in biochemical stimulus from ECM in epithelial phenotype switching. More systematic studies on cell migration behavior

based on photoactivatable surfaces are now underway.

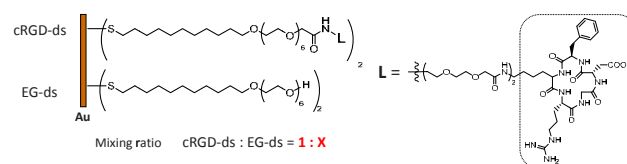


Fig. 2. Mixed self-assembled monolayers with varied cRGD surface density.

(2) *Development and characterization of protein-gold-nanoparticle conjugates bearing photocleavable polymers.*³⁾

Conjugation of diffusible biosignal molecules to solid substrates or soluble nanoparticles (NPs) adds new modalities of biological activities to original ligands due to the changes in diffusivity and intracellular trafficking. For example, Reinhard and coworkers reported that epidermal growth factor (EGF) showed enhanced apoptosis-inducing activity to cancer cells upon conjugating to gold nanoparticles (GNPs). Therefore, such bioconjugates serve as promising tools not only for fundamental biological studies but also for biomedical applications. However, in most studies, their detailed mechanisms of their actions have not been clarified. To tackle this issue, we have developed photoactivatable EGF-GNP conjugates by co-immobilizing photocleavable PEG and EGF on the surface of gold nanoparticles (Fig. 3). The DLS study demonstrated the release of the grafted PEG as the decrease in the particle size. This reaction is expected to decrease the molecular crowding surrounding the immobilized EGF at the nanoparticle surface. The increase in the biological activity of the conjugates in response to near-UV irradiation was demonstrated in HeLa cells by monitoring the phosphorylation level of ERK by cell ELISA. These results represent usefulness of the present strategy for caging/uncaging EGF-GNP conjugates and their potential applications to spatiotemporally resolved mechanism study of such bioconjugates.

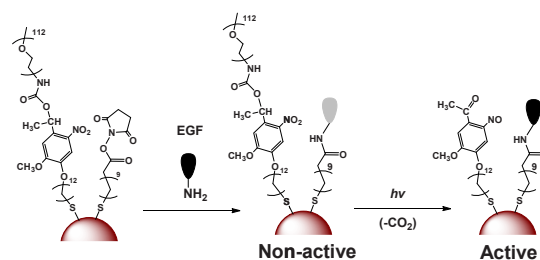


Fig. 3. Photoactivatable EGF-GNP conjugates.

References

- 1) M. Kamimura, O. Scheideler, Y. Shimizu, S. Yamamoto, K. Yamaguchi, J. Nakanishi, *Phys. Chem. Chem. Phys.* **17**, 14159 (2015).
- 2) S. Marlar, S. Abdelaleem, J. Nakanishi, submitted for publication.
- 3) S. Yamamoto, J. Nakanishi, K. Yamaguchi, *J. Photopolym. Sci. Technol.* **28**, 269 (2015).

Photo-energy Converting Alkylated-C₆₀/Graphene Hybrid using Alkyl Chains as Glue between Nanocarbons

MANA Independent Scientist Takashi NAKANISHI



1. Outline of Research

Applying our own development of “alkyl- π engineering” concept,¹⁾ an alkylated-C₆₀ fullerene molecule can be used an excellent exfoliation agent of graphene in organic solvent system through noncovalent attractive interactions. For the as-obtained alkylated-C₆₀/graphene assembly, graphene boots nearly 270-fold higher photocurrent than the alkylated-C₆₀ itself on an electrode.²⁾ Here I would like to emphasize that the attached alkyl chains can act as kind of “glue” between nanocarbons (C₆₀ and graphene).

2. Research Activities

Alkylated- π molecules are getting much attention very recently due to their great controllability in self-assembly of π -systems which is in most of case strongly aggregated in random structures. We have realized the alkylated- π molecules can behave as like surfactants, but full of hydrophobic nature.³⁾ Taking into account a balance between π - π interactions among π -units and van der Waals interactions on alkyl chains, various morphology, physical states including solids, liquid crystals, and isotropic liquids, are available to be produced from the alkylated- π molecules. This unique assembly system has been proposed as “alkyl- π engineering” concept.¹⁾

One important achievement in the alkylated- π molecular systems is epitaxial crystallization of attached alkyl chains could allow and support the functional π -units to align and organize onto graphite, in other words, on carbon lattice of a graphene surface.⁴⁾ Previously we have developed alkylated-C₆₀ molecules can form 1D nanowire structure on graphite surface. Applying this knowledge, alkylated-C₆₀/SWCNT hybrids were also prepared and tested for photo-thermal converting materials⁵⁾ as well as photo-electric converting electrode devices.⁶⁾ The carbon skeleton in SWCNT is essentially same with the one seen in graphene, except curved geometry to fold up as its tubular structure. Therefore, here we have simply taken the technique for graphene to develop C₆₀/graphene hybrid materials with help of alkyl chains as like glue function.

Interestingly, our alkylated-C₆₀ molecule can directly exfoliate few layers of graphene from graphite flakes by applying facile ultra-sonic treatment in organic solvents. This technique allowed to produce graphene of high quantity without much defects. Since it is no needed through oxidation and reduction processes on graphene, also no additional

reagents are required to create hybrid material with additional functions. The exfoliation agent is here the alkylated-C₆₀ molecule as well as the molecule can form C₆₀/graphene hybrid straightforward. The obtained alkylated-C₆₀/graphene assembly (Fig. 1) showed excellent photocurrent generation which is much higher, around 270-fold greater, than that of the alkylated-C₆₀ itself on FTO electrode under photo irradiation.²⁾ Surprisingly, the open-circuit voltage was enhanced from 0.2 mV of alkylated-C₆₀ on FTO to 264 mV of alkylated-C₆₀/graphene on FTO, indicating improvement of about three orders of magnitude. These results clearly indicate that the alkylated-C₆₀/graphene assembly is an excellent electron accepting/charge transporting composite material toward constructing efficient photovoltaic devices as well as optoelectronic switching systems.

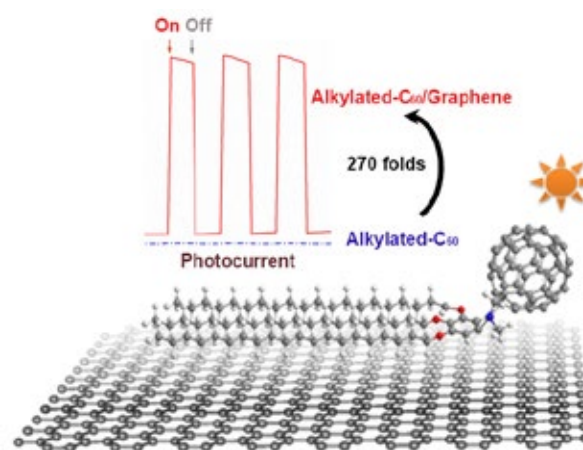


Fig. 1. Schematic illustration of the alkylated-C₆₀/graphene hybrid that can largely enhance the photocurrent of the photovoltaic device as around 270-fold compare to the alkylated-C₆₀ itself.

References

- 1) F. Lu, T. Nakanishi, *Sci. Technol. Adv. Mater.* **16**, 014805 (2015).
- 2) Y. Shen, A. Saeki, S. Seki, J.O. Lee, J. Aimi, T. Nakanishi, *Adv. Optical Mater.* **3**, 925 (2015).
- 3) M.J. Hollamby, M. Karny, P.H.H. Bomans, N.A.J.M. Sommerdijk, A. Saeki, S. Seki, H. Minamikawa, I. Grillo, B.R. Pauw, P. Brown, J. Eastoe, H. Möhwald, T. Nakanishi, *Nature Chem.* **6**, 690 (2014).
- 4) T. Nakanishi, N. Miyashita, T. Michinobu, Y. Wakayama, T. Tsuruoka, K. Ariga, D.G. Kurth, *J. Am. Chem. Soc.* **128**, 6328 (2006).
- 5) Y.F. Shen, A.G. Skirtach, T. Seki, S. Yagai, H.G. Li, H. Möhwald, T. Nakanishi, *J. Am. Chem. Soc.* **132**, 8566 (2010).
- 6) Y.F. Shen, J.S. Reparaz, M.R. Wagner, A. Hoffmann, C. Thomson, J.O. Lee, S. Heeg, B. Hatting, S. Reich, A. Saeki, S. Seki, K. Yoshida, S.S. Babu, H. Möhwald, T. Nakanishi, *Chem. Sci.* **2**, 2243 (2011).

Novel Solar Cell Concept with a Super-wide Response Spectrum Based on III-V Nitride Semiconductors

MANA Independent Scientist Liwen SANG



1. Outline of Research

The photoelectric conversion efficiencies for the current existing photonic and electronic devices are far from their ideality. For example, in the PV field, the current solar cells using Si, CuInGaSe, or GaAs-based materials are all concentrated on the long-wavelength absorption ($< 2\text{eV}$). To achieve the maximum conversion efficiency, full solar spectrum absorption using one material system is necessary. In the solid state lighting field, three-primary color (RGB) mixing is considered to be the most efficient method for generating white light compared to blue/ultraviolet LEDs with phosphors. However, RGB can not be realized by using one material system, which greatly increases the cost and lead to unnecessary efficiency loss during integration.

Superior to Si, Ge or GaAs-based semiconductors, the third-generation III-Nitride semiconductor, including GaN, InN, and AlN, is the only material system with the bandgap energy that can cover all the solar spectrum from deep ultraviolet to infrared region. This unique property provides them the promising application in the full-spectrum solar cells and LEDs. The invention of blue LEDs by using GaN materials won the Noble Prize in Physics in 2014. However, the long-wavelength LEDs ($>500\text{ nm}$) are still difficult to realize by using nitrides due to the difficulty in synthesizing the high-quality InGaN and *p*-InGaN. Similarly, the long-wavelength absorption for the solar cells has not been achieved.

2. Research Activities

The objective of this research is to solve the challenging problem in III-Nitride field of *p*-type doping in InGaN, then develop full-spectrum photoelectric energy conversion devices. To overcome high *n*-type background conductivity and surface electron accumulation for *p*-InGaN, we propose to deposit In-rich InGaN at high pressures with a unique-designed MOCVD and propose a novel physical strategy of polarization-induced doping method for *p*-type doping.¹⁾

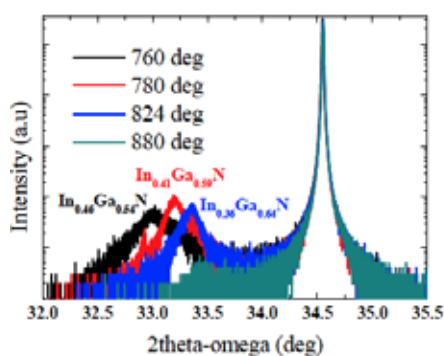


Fig. 1. XRD of In-rich InGaN films grown by HPMOCVD.

(1) In-rich InGaN films by HPMOCVD.

To avoid the incorporation of impurities and reduce the *n*-type background, high temperature growth for InGaN is necessary. However, due to the weak bond of In-N, the InGaN will be decomposed easily with elevated temperature. According to the phase balance theory, the high pressure during growth is required to hinder the decomposition at high temperatures. Based on the growth dynamics of InGaN and the flow pattern optimization at high pressures, we have designed and established a vertical type MOCVD system which can operate at the pressures up to 4 atms. InGaN films with In compositions more than 40% is successfully obtained (Fig. 1).

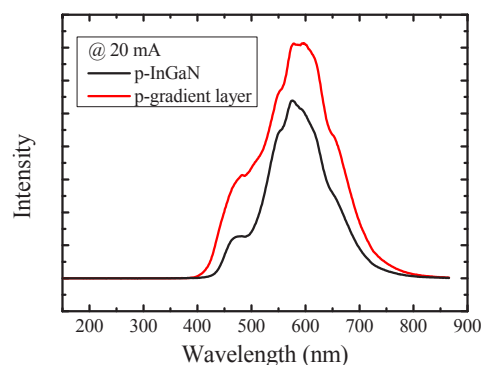


Fig. 2. Comparison of LEDs with and without InGaN gradient *p*-layer.

(2) Long-wavelength LEDs ($\sim 600\text{ nm}$) by using polarization-induced doping method for *p*-InGaN.

Although blue LEDs by using InGaN quantum wells have been well developed, achieving efficient operation of green light at longer wavelength ($>500\text{ nm}$) is challenging as In-rich InGaN quantum structures is difficult to fabricate with good interface. On the other hand, the large polarization field resulted from the great difference of In composition between active region and *p*-type region reduce the radiative recombination rates. To improve the luminescence efficiency of long-wavelength LEDs, it is necessary to increase the In composition of *p*-InGaN/*p*-GaN region. However, due to the bottleneck of high *n*-type background and electron accumulation for InGaN, *p*-InGaN is still difficult to achieve and far from for device utilization. To improve the hole concentration and mobility of *p*-InGaN, the In compositional gradient InGaN layers were utilized for the *p*-type region in the LED structure. The interface property was greatly improved compared to the *p*-InGaN/*p*-GaN structure. The LED showed a much stronger luminescence with a lower turned on voltage and leakage current (Fig. 2).

Reference

- 1) L.W. Sang, M.Y. Liao, Y. Koide, M. Sumiya, *J. Appl. Phys.* **117**, 105706 (2015).

Green Nanochemistry: Bandgap Engineering for Group IV Nanostructures

MANA Independent Scientist Naoto SHIRAHATA



1. Outline of Research

A prospective research scenario of optics and optoelectronics including development of light emitting diodes, solar cells, and lasers utilizes self-standing nanocrystals of semiconductors to attain improved performance of devices and combined technology with printing techniques for advanced wearable devices.

Findings of strong luminescence from nanostructures of group IV semiconductors and their compounds, i.e., Si, Ge, $\text{Si}_x\text{Ge}_{1-x}$, and silicide, have generated a great deal of excitement because their light emitters have a potential to open a new door to silicon photonics. Furthermore, the industrial use of those light-emitters possibly overcomes the unstable supply issue of rare-earth elements which raises a threat to the present industry of light emitters including LED and laser devices, and would give the significant contribution to realize a lightning industry for green & sustainable future.

2. Research Activities

(1) Synthesis of Silicon Nanocrystals with high PL QYs and Tuned PL Spectra in the NIR Range.¹⁾

Functional near-IR (NIR) emitting silicon nanocrystals (ncSi) adapted for two-photon excitation processes were synthesized by thermal disproportionation of amorphous silsesquioxanes prepared from the controlled hydrolysis of triethoxysilane, and subsequent size separation via the column chromatography processes. Octadecyl-terminated ncSi (ncSi-OD) exhibit the size-dependent PL properties in the NIR range (Fig. 1). All of the tuned spectra have linewidths narrower than 300 meV and no long emission tails. The estimated absolute PL quantum yields are 30-48%, and are dependent of ncSi size. Interestingly, the emission peak maxima are tuned by size over the range from 700 nm to 1000 nm, while excitation maxima seen at around 390 nm are insensitive to the difference in size of ncSi. This unique optical property featured to indirect

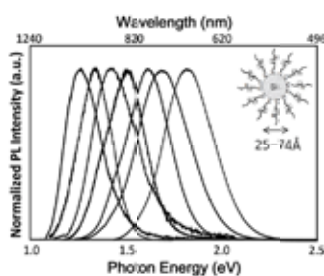


Fig. 1. Octadecyl-terminated Silicon Nanocrystals: Tuned PL spectra in the near-IR range.

bandgap structure implies that all of ncSi-OD samples with different PL maxima can be excited most efficiently at a single wavelength of 780nm via two-photon excitation. The ncSi films self-assembled on a glass substrate showed NIR emission spectra when irradiated with was irradiated with Ti:Sapphire femtosecond pulsed laser. Colloidal solutions of the NIR-emitting silicon nanocrystals will work as the fluorescence labels because of their nontoxic property and transparent feature in the first biological window.

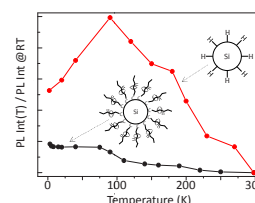


Fig. 2. Plots of PL intensities of ncSi samples with different terminal ligands with respect to PL intensities at room temperature.

(2) Photophysical Study for Determination of Silicon Nanostructures for High PL Quantum Yields.²⁾

Here we report for the first time the notable difference in temperature dependent photoluminescence (PL) properties with relaxation dynamics between free-standing silicon nanocrystals (ncSi) before and after hydrosilylation of 1-alkene in the ranging from 4 to 300K. For this comparison, the nanocrystals were prepared from a same parent sample. The estimated PL quantum yield (QY) increases twentyfold by hydrosilylation. The evolution of PL peak energy with temperature follows the modified Varshni's law in the range from 20-300K, but we see a strong discrepancy to this law below 20K. The PL intensity of hydrogen-terminated ncSi is dependent of temperature, and presented a maximum at 90K whereas the alkane-terminated ncSi exhibited a monotonic increase of PL intensity all over the temperature range (Fig. 2). From the PL decay dynamics study, we conclude that the non-radiative process, which limits the quantum efficiency of hydrogen-terminated ncSi at RT, is thermally activated exciton trapping centers at surface states. The non-radiative relaxation pathways is suppressed by long alkyl-ligand to give high PL QYs. We made an attempt to reveal a role of the surface monolayers for improved PL QY by revising a long-accepted PL spectral trend as a function of temperature.

References

- 1) C. Surov, B. Ghosh, G. Beaune, U. Nagarajan, T. Yasui, T. Shimada, Y. Baba, J. Nakamura, N. Shirahata, F. Winnik, submitted for publication.
- 2) B. Ghosh, N. Shirahata, submitted for publication.

Proton/electron Transports in Dense Metal Organic Frameworks

MANA Independent Scientist Satoshi TOMINAKA



1. Outline of Research

Nanoporous metal-organic frameworks (MOFs), composed of metal cations and anionic organic linkers, exhibit an unusual range of phase transitions under relatively mild conditions because of their flexible and responsive structures. In contrast to the porous structures, dense ones are more similar to classical inorganic materials and are attracting attention on account of their exciting properties. Here I summarize recent our achievements related to proton conduction or electron conduction in new dense MOFs.

2. Research Activities

(1) *First discovery of “insulator-to-proton conductor transition” in a dense MOF.¹⁾*

Phase transitions in solid-state materials lead to nonlinear changes in properties that can play key roles in the development of innovative, functional materials. MOFs exhibit an unusual range of phase transitions under relatively mild conditions because of their flexible and responsive structures.

In this light, we found a new phenomenon occurring in a dense MOF, insulator-to-proton conductor transition upon exposure to humidity. During characterizations of new dense MOFs, we found $((\text{CH}_3)_2\text{NH}_2)_2[\text{Li}_2\text{Zr}(\text{C}_2\text{O}_4)_4]$ exhibits an abrupt increase in proton conductivity from $<10^{-9}$ to 3.9×10^{-5} S/cm at 17 °C (activation energy, 0.64 eV) upon exposure to humidity (Fig. 1a). The conductivities were determined using single crystals,^{2,3)} and the structures were analyzed by X-ray diffraction (Fig. 1b) and X-ray pair distribution function analysis. The initial anhydrous structure transforms to another dense structure via topotactic hydration ($\text{H}_2\text{O}/\text{Zr} = 0.5$), wherein one-fourth of the Li ions are irreversibly rearranged and coordinated by water molecules.

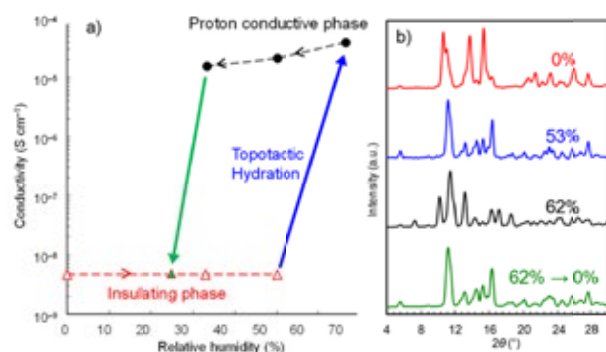


Fig. 1. (a) Humidity dependence of proton conductivity data obtained by single-crystal impedance measurements at 17 °C. The arrows show the direction of RH change from 0% to 67%, and then to 25%. Triangles indicate data below the detection limit (100 GΩ). (b) Powder X-ray diffraction patterns collected under humidity control. The samples were sealed in glass capillaries in dry air (RH = 0%) and in humidified nitrogen at RH = 53%, 62%, and 0% after holding at 62%.

This structure further transforms into a third crystalline structure by water uptake ($\text{H}_2\text{O}/\text{Zr} = 4.0$). The abrupt increase in conductivity is reversible and is associated with the latter reversible structure transformation. The H_2O molecules coordinated to Li ions, which are formed in the first step of the transformation, are considered to be the proton source, and the absorbed water molecules, which are formed in the second step, are considered to be proton carriers.

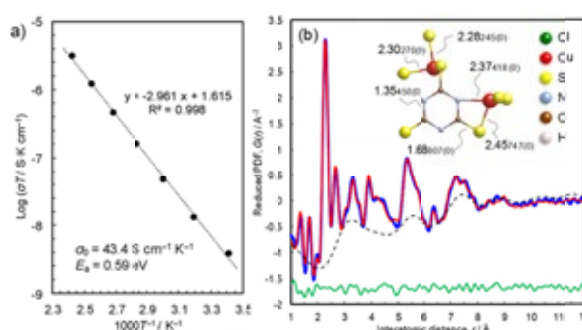


Fig. 2. (a) Arrhenius plot of the electronic conductivity in the amorphous, semiconductive phase. (b) X-ray pair distribution function analysis of the amorphous phase. Inset shows a representative local structure and bond lengths determined by the PDF refinement.

(2) *Topochemical conversion of an insulating dense MOF into an amorphous conductive MOF.⁴⁾*

Treatment of single crystals of $\text{Cu}^{\text{I}}\text{Cl}(\text{ttcH}_3)$ ($\text{ttcH}_3 =$ trithiocyanuric acid) in aqueous ammonia solution yields monoliths of amorphous $\text{Cu}_{1.8}(\text{ttc})_{0.6}(\text{ttcH}_3)_{0.4}$. The treatment changes the transparent orange crystals into shiny black monoliths of the latter compounds with retention of morphology, and moreover increases the electrical conductivity from insulating to semiconducting (7.6×10^{-9} S/cm at 140°C, activation energy = 0.59 eV, Fig. 2a). The structure and properties of the amorphous conductor are fully characterized by AC impedance spectroscopy, X-ray photoelectron spectroscopy, X-ray pair distribution function (PDF) analysis, infrared spectroscopy, diffuse reflectance spectroscopy, electron spin resonance spectroscopy, elemental analysis, thermogravimetric analysis, and theoretical calculations. The PDF analysis (Fig. 2b) revealed that the amorphous structure is composed of networks of Cu-S coordination spheres, which is probably the most important feature to increase the conductivity.

References

- 1) S. Tominaka, F.X. Coudert, T.D. Dao, T. Nagao, A.K. Cheetham, *J. Am. Chem. Soc.* **137**, 6428 (2015).
- 2) S. Tominaka, A.K. Cheetham, *RSC Adv.* **4**, 54382 (2014).
- 3) S. Tominaka, S.; Henke, A.K. Cheetham, *Crystengcomm* **15**, 9400 (2013).
- 4) S. Tominaka, H. Hamoudi, T. Suga, T.D. Bennett, A.B. Cairns, A.K. Cheetham, *Chem. Sci.* **6**, 1465 (2015).

Tailored Synthesis of Nanoporous Pt with Various Architectures

MANA Independent Scientist Yusuke YAMAUCHI



1. Outline of Research

Recently, mesoporous materials with ultra-large mesopores have become a subject of extensive research, because they can facilitate a fast and efficient transport of reactants or effectively adsorb large molecules. Mesoporous silica nanoparticles with pore sizes larger than big biomacromolecules (*e.g.*, protein, DNA) are showcased as an excellent drug delivery system. Up to now, most of the studies on mesoporous materials with ultra-large mesopores have been limited to traditional compositions (*e.g.*, silica, carbon, and metal oxides). The synthesis of metallic mesoporous materials with ultra-large mesopores is still a challenge to overcome.

Soft-templating is a very popular approach to prepare mesoporous metals. Low-molecular-weight amphiphilic molecules (*e.g.*, Brij 58, P123 and F127) have been mostly utilized as pore directing agents, where the hydrophilic PEO units accommodate the metal sources. Electrochemical or chemical reduction of the metal precursors is generally involved in the preparation of mesoporous metals to achieve various morphologies (*e.g.*, films or powders). However, the use of such low-molecular-weight surfactants can only produce small mesopores (less than 10 nm) which ultimately limit the mobility of guest molecules, and further devalue the electrocatalytic performance. Therefore, the use of high-molecular-weight block copolymers is critical to overcome this issue.

2. Research Activities

From typical scanning electron microscopy (SEM) and transmission electron microscopy (TEM) images, the average diameter of the obtained mesoporous Pt nanospheres was measured to be *ca.* 150 nm, and uniformly large-sized mesopores (*ca.* 14 nm) are distributed over the entire surface of the Pt nanospheres (Fig. 1).¹⁾ On the low-angle X-ray diffraction (XRD) profile, the broad peak at 0.38° (marked by the first arrow) corresponds to a pore-to-pore distance of *ca.* 23 nm and highlight that the mesoporous structure is uniform. The obtained N_2 adsorption-desorption isotherm can be categorized as a type IV isotherm with a hysteresis loop at a relative pressure between 0.4 and 0.9. The surface area is measured to be $30.0 \text{ m}^2 \cdot \text{g}^{-1}$. From the BJH pore size distribution curve, it is found that two types of pores exist; mesopores and micropores with a random distribution from 1 to 4 nm. The micropores are originated from the nanovoids (*i.e.*, micropores) between adjacent Pt nanoparticles. From the high-resolution TEM images centered on the edges of a particle, the spacing between fringes (0.23 nm) and the dihedral angle ($\sim 70^\circ$) can be assigned to the (111) plane of a *fcc* crystal. The multiple spots visible on the selected-area electron diffraction (ED) pattern highlight the polycrystalline nature of the structure. The wide-angle XRD profile confirms a *fcc* crystal structure by assigning the (111), (200),



Fig. 1. Synthesis of mesoporous Pt nanospheres with tunable pore sizes prepared from polymeric micelle assembly.

(220) and (311) diffraction peaks.

The creation of mesoporous structure enables to develop high surface area and easy accessibility of interior regions taking part in electrochemical reaction. Using cyclic voltammetry (CV), the electrochemically active surface area (ECSA) was calculated from the charge passed during hydrogen desorption in the potential range from -0.2 V to 0.2 V in 0.5 M H_2SO_4 . Three samples were investigated: mesoporous Pt nanospheres (14 nm pore size), nonporous Pt nanospheres and commercial Pt black (abbreviated as Meso Pt NSs, Pt NSs and Pt black, respectively). The Pt nanospheres with attractive mesoporous architectures have an increased specific ECSA of $16.34 \text{ m}^2 \cdot \text{g}^{-1}$ compared with $8.8 \text{ m}^2 \cdot \text{g}^{-1}$ (Pt NSs) and $8.67 \text{ m}^2 \cdot \text{g}^{-1}$ (Pt black), respectively, due to the presence of a multitude of accessible active sites, especially in the inner regions. In addition, the structural stability was carried out after 900 repetitive cycles at the potential between -0.2 and 1.5 V. Meso Pt NSs exhibit high structural stability with a small loss of ECSAs compared to commercial Pt black. In the methanol oxidation reaction (MOR) activity investigation, two typical anodic peaks can be observed during the forward and backward sweeps, where the Meso Pt NSs exhibit the best catalytic performance. The mass specific current densities in forward sweep are 203.6, 98.7 and $48.7 \text{ mA} \cdot \text{mg}^{-1}$ for the Meso Pt NSs, Pt NSs and Pt black, respectively. Even normalized by ECSA, the specific current density of the Meso Pt NSs ($1.24 \text{ mA} \cdot \text{cm}^{-2}$) is still higher. Such advanced catalytic activity can be ascribed to highly crystallized mesoporous structures and easily accessible active sites. Furthermore, the remarkable negative shift of the peak potential and the onset potential from line-sweep voltammograms indicate an enhanced methanol oxidation for the Meso Pt NSs compared to the other two samples. Chronoamperometric measurements performed at 0.6 V revealed that the current density of the Meso Pt NSs remains higher over a whole cycle of 2,000 s, due to the uniformly distributed mesoporous structure enhancing the accessibility of methanol to catalytically active sites.

Reference

- 1) Y.Q. Li, B.P. Bastakoti, V. Malgras, C.L. Li, J. Tang, J.H. Kim, Y. Yamauchi, *Angew. Chem. Int. Ed.* **54**, 11073 (2015).

Nanomechanical Sensors towards Mobile Olfaction

MANA Independent Scientist Genki YOSHIKAWA



1. Outline of Research

Demands for new sensors to detect or identify target molecules are rapidly growing in various fields; medicine, food, cosmetics, security, environment, *etc.* Nanomechanical sensors have potential to contribute to these global demands owing to their intrinsic versatility. Based on the newly developed platform “Membrane-type Surface stress Sensor (MSS)”,¹⁻³⁾ we are now trying to realize useful nanomechanical sensor systems which can fulfill the practical requirements, such as portability, low-cost, ease of use, in addition to the basic specifications, *e.g.*, high sensitivity and selectivity that will be practically determined with the performance of receptor layers coated on the sensor surfaces.

2. Research Activities

(1) *Development of receptor materials/layers with high performance.*

Nanomechanical sensors detect the mechanical stress induced by the adsorption of gaseous molecules on a receptor layer. The amount of induced stress is determined by various factors, such as chemical affinity between receptor materials and target gases as well as physical parameters including thickness, Young’s modulus, and Poisson’s ratio.^{4,5)} Thus, the nanoarchitectonic development of materials/layers is critically important to achieve effective receptor layers for nanomechanical sensors. In addition to these scientific consideration, most practical applications require additional properties, such as robustness, especially for daily repeated use. Polymers are usually used as receptor materials of nanomechanical sensors for the measurements of gaseous samples, while some polymers are instable under practical conditions. Thus, we have been trying to develop new receptor materials designed for nanomechanical sensing. So far, several types of materials have been confirmed to fulfill the above mentioned requirements. Strategic modification of these materials provides a wide variety of chemical selectivity which covers various gas species. We have also optimized the procedure to coat these materials on the surface of sensing membrane of MSS. Pattern recognition with these receptor layers effectively works for various gases including complex smell with higher sensitivity, chemical resolution, and reproducibility.

(2) *Demonstration of high reproducibility of MSS.*⁶⁾

It is technically not so simple to form a homogeneous layer on small sensing elements of nanomechanical sensors due to various effects, such as the so-called coffee-ring effect. Through experiments and finite element analyses, the MSS structure was found to be much more robust against inhomogeneous functionalization compared to similarly

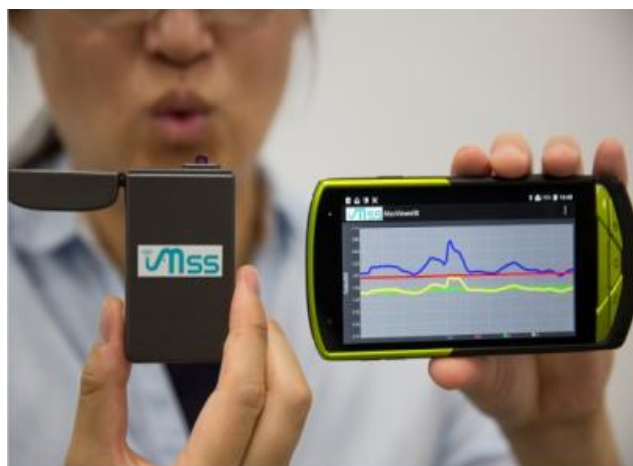


Fig. 1. A prototype of a mobile sensing device based on the MSS technology.

coated piezoresistive cantilevers.

(3) *Demonstration of real-time measurements of gaseous samples on a mobile phone using a compact module connected via wireless communication.*

Since the MSS platform measures the changes in electrical resistance, a very simple setup is required for basic measurements. To explicitly demonstrate this feature, a simple wireless read-out module was developed. Fig. 1 shows an example of the real-time measurements using an MSS chip mounted on this module which communicates with a mobile phone via Bluetooth. As demonstrated so far,^{7,8)} various applications are envisioned. To establish a *de facto* standard for odor analysis and sensor systems employing the MSS technology, the “MSS Alliance” was launched jointly with companies and a university.⁹⁾

References

- 1) G. Yoshikawa, T. Akiyama, S. Gautsch, P. Vettiger, H. Rohrer, *Nano Lett.* **11**, 1044 (2011).
- 2) G. Yoshikawa, T. Akiyama, F. Loizeau, K. Shiba, S. Gautsch, T. Nakayama, P. Vettiger, N.F. de Rooij, M. Aono, *Sensors* **12**, 15873 (2012).
- 3) G. Yoshikawa, F. Loizeau, C.J.Y. Lee, T. Akiyama, K. Shiba, S. Gautsch, T. Nakayama, P. Vettiger, N.F. de Rooij, M. Aono, *Langmuir* **29**, 7551 (2013).
- 4) G. Yoshikawa, *Appl. Phys. Lett.* **98**, 173502 (2011).
- 5) G. Yoshikawa, C.J.Y. Lee, K. Shiba, *J. Nanosci. Nanotechnol.* **14**, 2908 (2014).
- 6) F. Loizeau, T. Akiyama, S. Gautsch, P. Vettiger, G. Yoshikawa, N.F. de Rooij, *Sensors and Actuators A* **228**, 9 (2015).
- 7) F. Loizeau, H.P. Lang, T. Akiyama, S. Gautsch, P. Vettiger, A. Tonin, G. Yoshikawa, C. Gerber, N. de Rooij, *IEEE MEMS* **26**, 621 (2013).
- 8) R.J.S. Guerrero, F. Nguyen, G. Yoshikawa, *EPJ Techniques and Instrumentation* **1**, 9 (2014).
- 9) NIMS Press Release on September 29, 2015 <http://www.nims.go.jp/eng/news/press/2015/10/201510130.html>

Diamond Power Devices – Defects Control by Multilayer Formation

ICYS-MANA Researcher **Alexandre FIORI**



1. Outline of Research

Diamond is the ultimate semiconductor for high power device, and high frequency electronics. However, even if important developments concern large surface substrate fabrication, epitaxial growth by plasma-assisted CVD, and doping techniques, the success of low loss switches is struggling. Main problems are coming from the large ionization energies of its dopants, and from its contact interfaces with metals.

As example, the ionization energy of boron dopant (0.38 eV) results in a very low equilibrium carriers concentration, and thus in a large intrinsic resistivity. However, boron-doped diamond shows contrasting properties: from insulator to superconductor.¹⁾ In our studies, electronic properties and crystal defects are tuned by alternating different dopant concentrations in multilayers (Fig. 1). Those multilayers are composed of an alternate of heavily ($p^+ > 10^{20} \text{ at}\cdot\text{cm}^{-3}$) and lightly boron-doped diamond films ($p^- < 10^{16} \text{ at}\cdot\text{cm}^{-3}$).

Metallic contacts on diamond are reacting with carbon at elevated temperature or under high current flow. That produces metal carbides, which degrades the electrical properties of Schottky barriers, and increases electrical power losses.²⁾ At the moment, the formation of oxide interlayer is experimented in order to obtain thermally stable and ideal Schottky interface with diamond.

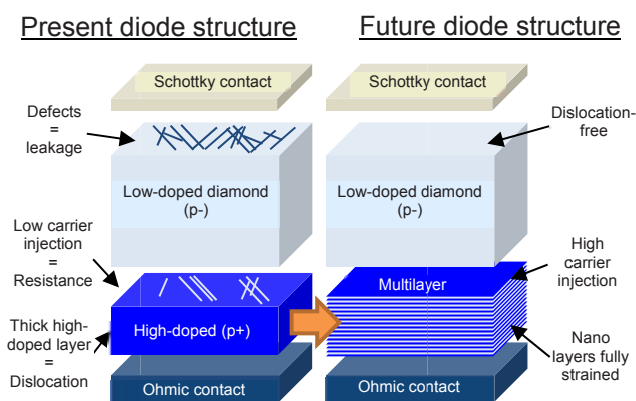


Fig. 1. Schematic of diamond Schottky diodes developed in this study.

2. Research Activities

(1) Nano-scale multilayer.

The strategy to control precisely nanometer range thickness and boron doping close to 1% in epitaxial layers is based on the slow diamond growth. This is achieved by the reduction of the carbon partial pressure in the reactive plasma. Under such conditions, the equilibrium between growth and etching is unstable and careful precautions (pressure, temperature, energy) are required. New doping conditions are currently in development. Plasma diagnostic and gas monitoring are performed in order to follow in-situ

the equilibrium between growth and etching of diamond.

(2) High carrier injection.

Nano-scale multilayers are expected to facilitate the injection of carriers in semi-insulating diamond, by mean of band-bending and/or tunneling transport. In our study, such multilayers are employed as conductive layer, which once capped by a drift layer (low boron doped) completed a “push-trough” Schottky diode (Fig. 1). The deep etching of drift diamond layer over several micron is required in order to contact electrically the multilayer of such diode device. In collaboration with the NIMS nanofabrication platform, we actively optimize the etching process of diamond in order to measure the gain in carrier injection.

(3) Dislocation-free substrate.

The diamond lattice constant is distorted by heavily doping with boron atoms. More precisely, the cubic lattice is deformed into a tetragonal lattice until a critical thickness that causes its relaxation. This critical thickness depends essentially from the dopant concentration.³⁾ In collaboration with CNRS/Inst. Neel in France, and the university of Cadiz in Spain, we started the stratigraphic observation on cross-sections of diamond multilayers (Fig. 2), and we studied dislocation mechanisms.⁴⁾ The understanding of generation and propagation of those dislocations will help us to obtain dislocation-free diamond substrates grown on doping multilayer buffers.

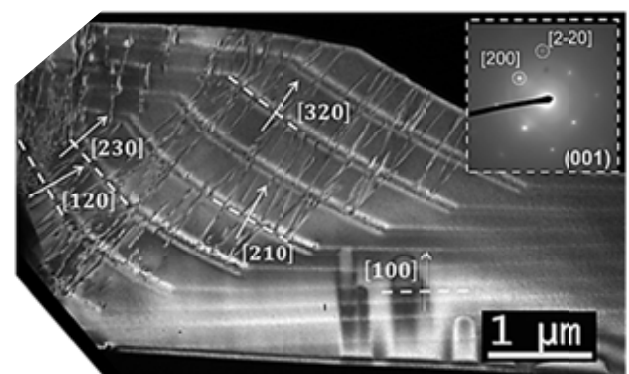


Fig. 2. Large field TEM micrograph of a cross-section made along the [010] direction observed at (001) pole. White dashed lines and arrows indicate the position of p⁻ layers and growth directions, respectively.

References

- 1) A. Fiori, F. Jomard, T. Teraji, G. Chicot, E. Bustarret, *Thin Solid Films* **557**, 222 (2014).
- 2) A. Fiori, T. Teraji, Y. Koide, *Appl. Phys. Lett.* **105**, 133515 (2014).
- 3) M.P. Alegre, D. Araújo, A. Fiori, J.C. Piñero, F. Lloret, M.P. Villar, P. Achatz, G. Chicot, E. Bustarret, F. Jomard, *Appl. Phys. Lett.* **105**, 173103 (2014).
- 4) F. Lloret, A. Fiori, D. Araujo, D. Eon, M.P. Villar, E. Bustarret, *Appl. Phys. Lett.*, accepted for publication.

New Polymeric Nano-System for Diagnosis and Therapy

ICYS-MANA Researcher

Yohei KOTSUCHIBASHI



1. Outline of Research

It is of great interesting that polymeric materials show different physicochemical properties by their structures. Over the last decade, the design of these polymeric materials has become simple with development of synthetic techniques such as controlled/living radical polymerizations (CLRPs) and click chemistry. Using the combination of these techniques, new polymeric nanomaterials and systems are created for diagnosis and therapy.

2. Research Activities

(1) Nanoparticle-kit for everyone.

Recently, several types of nanoparticles have been used in a wide range of fields as biomaterials. The nanoparticles are required to adjust their physicochemical properties according to the use via a simple method. To achieve the request, a nanoparticle-kit that is composed of several kinds of block copolymers was developed. The block copolymers have a common temperature responsive segment and the nanoparticles are easily prepared via increasing solution temperature. Their physicochemical properties are designed by the mixed block copolymers. The customized nanoparticles are applied in not only *in vitro/in vivo* tests but also basic polymer chemistry. We discovered that temperature responsive copolymers could recognize their optimum copolymers when they form mixed nanoparticles.¹⁾ The rapid preparation (less than 1 min) is one of the advantages of the nanoparticle-kit. The customized nanoparticles having fluorescent agents were injected via heart injection and the tumor tissue was successfully labeled after 36 h (Fig. 1).

The temperature responsive copolymers were also applied in anti-bacterial surfaces.²⁾ The precise design is necessary to these self-assemble materials. These unique materials are collected as book chapter in the Biomaterials Nanoarchitectonics.^{3,4)} Moreover, I reported a review of dual (multi) temperature responsive copolymers.⁵⁾ It will be the third review on the copolymers in the world.

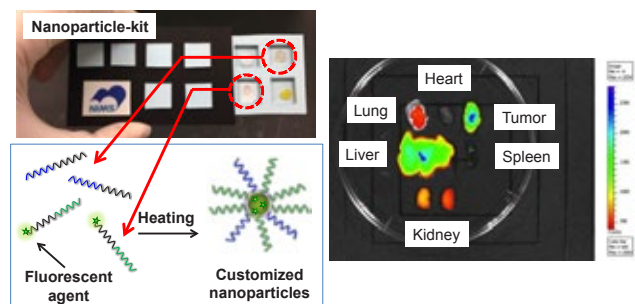


Fig. 1. Nanoparticle-kit: the customized fluorescent nanoparticles were injected to tumor-bearing CB/17/SCID mice via heart-injection. The fluorescent intensity was detected after 36 h using IVIS.

(2) Facile functionalization of electrospun EVOH nanofibers via the benzoxaborole-diol interaction.

Poly(ethylene-co-vinyl alcohol) (EVOH) has been one of the best known flexible thermoplastic materials and used in medical applications for the high biocompatibility. The modification of EVOH, however, is limited due to a need of multi-steps of reaction processes. Therefore, it remains a big challenge to propose a simple EVOH modification system. To achieve this system, EVOH was mixed with the water-soluble benzoxaborole-based copolymers (BOPs) in organic solvent and was found to show a gelation via a benzoxaborole-diol interaction. Using the mixture solution, EVOH nanofiber meshes with BOP were prepared by electro-spinning (Fig. 2). The nanofiber meshes had a stable cross-linked structure in aqueous solution due to the reversible covalent bonding (over 97 % of nanofiber remained without changing their morphology). Using this simple method, the EVOH nanofibers were successfully functionalized with stimuli-responsive copolymers.⁶⁾ The functionalized EVOH nanofibers will be applied in a new diagnosis system. The BOPs were also applied in a flocculation of impurity materials in water.⁷⁾ Moreover, the nanofiber techniques were used in a controlled drug release for treatment of basal cell carcinoma.⁸⁾

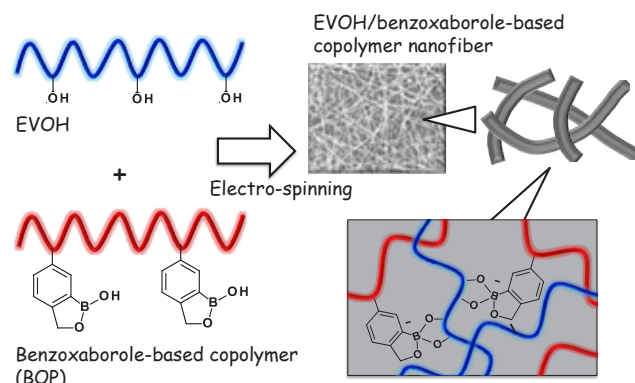


Fig. 2. Schematic representation of EVOH/benzoxaborole-based copolymer nanofiber.

References

- 1) Y. Kotsuchibashi, M. Ebara, A.S. Hoffman, R. Narain, T. Aoyagi, *Polym. Chem.* **6**, 1693 (2015).
- 2) Y. Wang, Y. Kotsuchibashi, Y. Liu, R. Narain, *ACS Appl. Mater. Interfaces* **7**, 1652 (2015).
- 3) Y. Kotsuchibashi, R. Narain, Book: *Biomaterials Nanoarchitectonics*, Chapter 2.4, Elsevier, Netherlands, in press.
- 4) Y. Kotsuchibashi, Y. Nakagawa, M. Ebara, Book: *Biomaterials Nanoarchitectonics*, Chapter 2.1, Elsevier, Netherlands, in press.
- 5) Y. Kotsuchibashi, M. Ebara, T. Aoyagi, R. Narain, *Polym. Chem.*, submitted.
- 6) Y. Kotsuchibashi, M. Ebara, *Polymers*, submitted.
- 7) H. Lu, Y. Wang, L. Li, Y. Kotsuchibashi, R. Narain, H. Zeng, *ACS Appl. Mater. Interfaces* **7**, 27176 (2015).
- 8) R. Garrett, E. Niyama, Y. Kotsuchibashi, M. Ebara, *Fibers* **3**, 478 (2015).

Directional Control of Energy and Electron Transfer by Metal Ion Choices in Porphyrinoids

ICYS-MANA Researcher Huynh Thien NGO



1. Outline of Research

Due to its intrinsic properties, porphyrinoids have been of great interest in a wide range of research area, *e.g.*, catalysis, photodynamic therapy, and molecular electronics, depending on the substitution patterns on the periphery or core of these tetrapyrrolic macrocycles. Recently we focus on the fabrication of supermolecular porphyrinoid conjugates linked by rotaxane architecture. The ability to interchange the metal centers in the tetrapyrrolic systems allows us to control the direction of the energy/electron transfer.

2. Research Activities

Our recent synthetic efforts have led to high yielding metal corrole-porphyrinoid hybrids (Fig. 1). Electrochemical and computational studies revealed the electron-deficient nature of the copper(III) corrole in the conjugates in terms of facile reduction and the locations of the LUMO orbitals. The oxidized and reduced products of the conjugates were characterized spectroelectrochemically and used in the interpretation of transient spectral data from femtosecond transient measurements. The energy level diagram, established by using the spectroscopic, electrochemical, and computational data, predicts the occurrence of charge separation from 1ZnP^* , and indicates that the charge-separated state relaxes directly to the ground state during the

charge-recombination process. Proof for charge separation was obtained from femtosecond transient spectroscopic studies as it was possible to spectrally characterize the existence of ZnP^{C^+} and CuIIC species. The k_{CS} determined for the conjugates were of the order of 10^{10} s^{-1} , revealing ultrafast charge separation. These studies illustrate the importance of copper(III) corrole as a potent electron acceptor for the construction of energy-harvesting model compounds, and constitute the first definitive proof of charge separation in ZnP-CuIIC systems. These observations lead to a hot paper¹⁾ in *Chemistry – A European Journal* with the back cover page shown in Fig. 2.

To reduce the flexibility of the linker, mono-, di- and tetra-rotaxane linkers were introduced as linker between different porphyrinoids to gain more rigidity and control over the energy transfer. Both conjugate derivatives containing with and without rotaxane linker are under comparative investigation of photophysical properties (Fig. 3). We strongly believe that the rotaxane moieties induce extra rigidity in the linker leading to a more efficient energy transfer from the outer corroles to the core porphyrin. First obtained data showed a faster charge separation with rotaxane moieties confirming our hypothesis. By small change of metal centers we are able to alter the direction of the energy transfer from corrole to porphyrin and *vice versa*.



Fig. 2. Our Back Cover page in issue 4 of *Chemistry – A European Journal*.

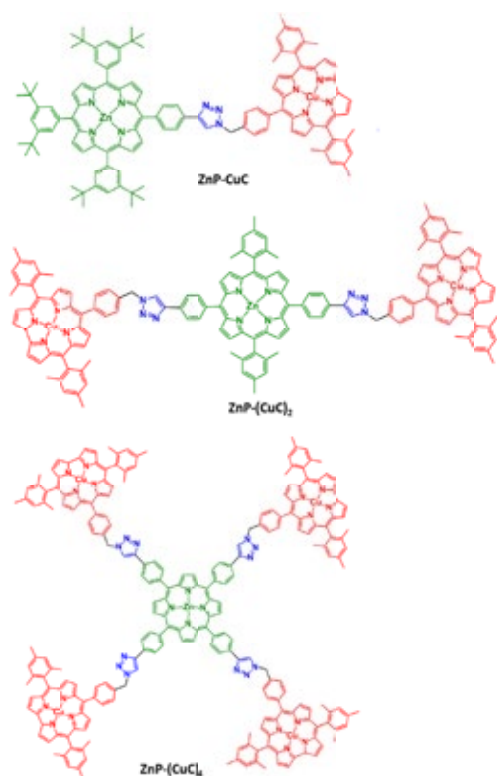


Fig. 1. Copper corrole zinc porphyrin hybrids.



Fig. 3. Rotaxane corrole porphyrin conjugate.

Reference

- 1) T.H. Ngo, D. Zieba, W.A. Webre, G.N. Lim, P.A. Karr, S. Kord, S.B. Jin, K. Ariga, M. Galli, S. Goldup, J.P. Hill, F. D'Souza, *Chem. Eur. J.* **22**, 1301 (2016).

Theoretical Design of Nanocarbon Materials for Device Applications

ICYS-MANA Researcher

Thanh Cuong NGUYEN



1. Outline of Research

Atomic-layer nanomaterials such as graphene, boron-nitride or transitional-metal dichalcogenide are of great interest owing to their unique physical/chemical properties. For practical application of these materials for electronic devices, it is necessary and important to control the physical and chemical properties of atomic-layer materials under realistic environments such as defects, external electric field, hybrid structure with foreign materials, etc. These environmental factors could suppress or induce the novel functionality of atomic-layer materials. Our research goal is to explore and utilize the novel functional atomic-layer nanomaterials in atomic scale based on the computational materials science. In particular, we focus on the hybrid structure of graphene and copper nanowire that could be used as interconnect in semiconductor chip or transparent conductors. Furthermore, we also design the novel two-dimensional materials from organic molecules.

2. Research Activities

(1) Graphene-Copper hybrid structure.

Copper is the crucial material for interconnects in the silicon complementary metal-oxide semiconductor technology. Therefore, highly conductive copper nanowires are required for designing and fabricating high-performance electronic devices. Recently, by using graphene as coating layer, the electrical conductivity of copper nanowires has been enhanced by 15 percent than that of pristine copper nanowire.¹⁾ However, the origin of this high conductivity of graphene-coated copper nanowires is still unclear. In this work,²⁾ based on the first-principles electronic structure calculations for graphene-copper-graphene hybrid materials (Fig. 1), we unravel the physical origin of the high electrical conduction of graphene-coated copper nanowire.

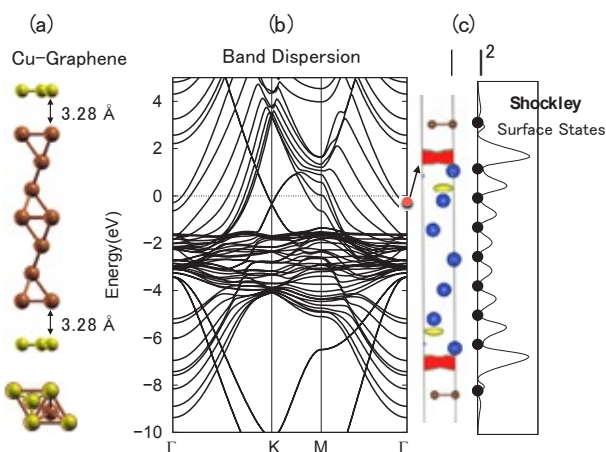


Fig. 1. (a) Atomic structure, (b) electronic band structure of graphene-Cu-graphene hybrid material, and (c) wavefunction distribution of the α -state at the Γ -point.

The graphene coating layer weakly bound on the copper surfaces, as shown in Fig. 1a. Therefore, the intrinsic surface states (Shockley states)³⁾ around the Fermi level of copper nanowire are preserved, as shown in the Figs. 1b and 1c. These Shockley surface states exhibit the 2D nearly-free electron characteristics, leading to the enhanced electrical conductivity of copper nanowire. On the other hand, without graphene protective layer, the Shockley surface states of copper could be destroyed by oxygen adsorption or metal deposition, that lead to the substantial surface scattering decreasing the electrical conductivity.

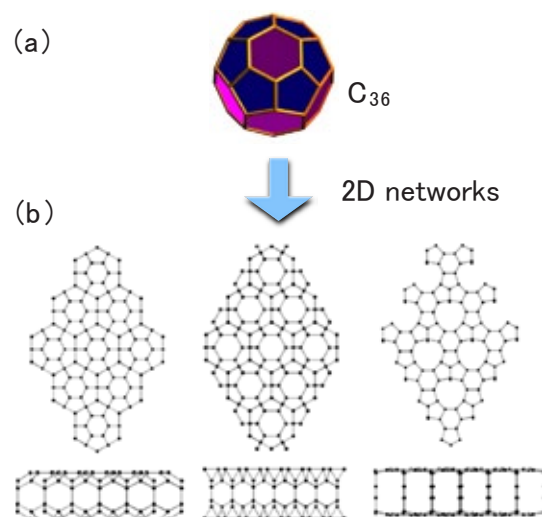


Fig. 2. Geometric Structures of (a) a C_{36} fullerene molecule, (b) 2D carbon networks of fused C_{36} molecules.

(2) Design of novel two-dimensional carbon materials by fusing C_{36} fullerenes.

3D polymerized fullerene (C_n , $n < 60$) polymers exhibit the unique electronic properties depending on their covalent network. Therefore, it is interesting to explore the 2D carbon network materials by assembling fullerenes molecules. In collaboration with Prof. Susumu Okada (Univ. of Tsukuba), the layered network materials of fused C_{36} fullerenes have been theoretically designed. We found three stable network topologies derived from fused C_{36} fullerenes (Fig. 2).⁴⁾ The electronic structures of these materials are semiconducting or metallic depending on their network topologies. Furthermore, by injecting holes into the valence bands under a normal electric field, C_{36} sheets exhibit spin polarization with a magnetic moment of approximately $2\mu_B/\text{nm}^2$.

References

- 1) R. Mehta, S. Chugh, Z. Chen, *Nano Lett.* **15**, 2024 (2015).
- 2) N.T. Cuong, S. Okada, submitted for publication.
- 3) F. Schiller, C. Laubschat, *Phys. Rev. B* **74**, 085109 (2006).
- 4) M. Maruyama, N.T. Cuong, S. Okada, *J. Phys. Soc. Jpn.* **84**, 084706 (2015).

Nanostructured Polymeric Nanomaterials

ICYS-MANA Researcher

Gauthier RYDZEK



1. Outline of Research

Polyaniline is an insoluble conductive semi-rigid rod-like material that presents metallic, crystalline, salt and polymeric characteristics. Polyaniline tends to undergo spontaneous self-organization processes under mild conditions in water and offers a variety of post-assembly modifications. The first year of this ICYS project is devoted to structurally characterize polyaniline (PANI) yolk-shell architectures and demonstrate their potential for catalytic applications. A unique type of nanocatalysts will be designed: metallic NPs hierarchically and selectively distributed within the yolk and the shell parts of these PANI nanocapsules. NPs confined in the core are anticipated to achieve increased catalytic performances by confinement and cooperative effects. By using a sequential approach, the final goal is to obtain specific localization of one type of NP (Cu) in the core of the nanocatalyst and another type (Au) in its shell. In a first study, gas phase catalysis will be performed for CO thermal oxidation.

trapped in the yolk part, with a kinetic control. In a second step, gold nanoparticles were deposited in an auto-catalytic process on the shell part of PANI capsules (Fig. 1). By using a step-by-step approach, the catalytic activity loaded PANI capsules, at every stage of synthesis, has been investigated for CO oxidation at 150 and 300 degrees (Fig. 2). Results exhibited an enhancement of the catalytic activity for copper particles confined in the core part, and a cooperative effect when both gold and copper nanoparticles were present.

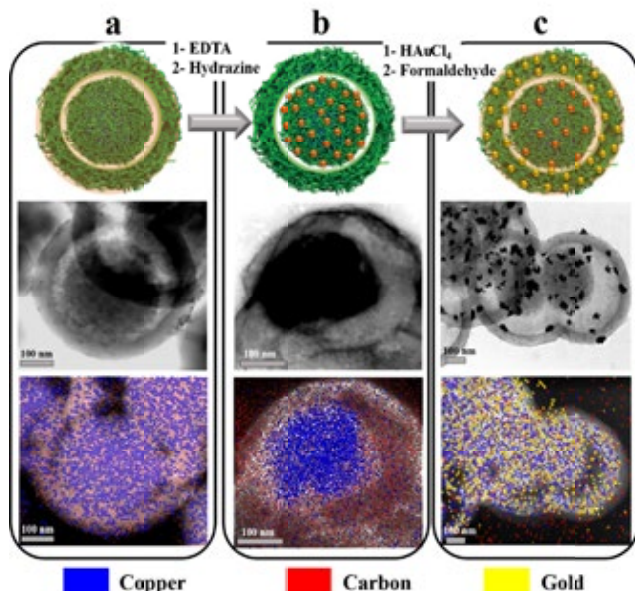


Fig. 1. General schematic structure, TEM and EDX analysis of the intended hierarchically loaded PANI yolk-shell structures.

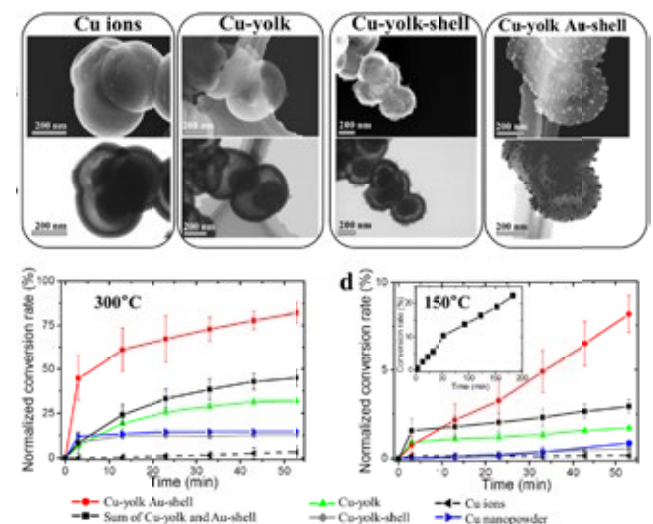


Fig. 2. Structure of some intermediate product during the synthesis process of hierarchically loaded yolk-shell PANI capsules, and corresponding catalytic activities at 150 and 300 degrees. As a control (blue line) a 50 nm Cu nanopowder was used.

(2) Bulk plastics from polyelectrolytes.

Competing with hydrogels, a new research field is emerging with the processing of bulk materials composed of polyelectrolytes complexes plasticized by salts (COPECs). Impact on several fields, including catalysis, energy sparing and biomaterials, is expected. A collaborative project is now beginning to assess how these materials are reacting to changes of their environment (ex: type of salt) and their potential applications (Fig. 3).

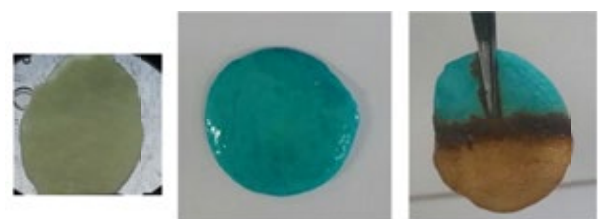


Fig. 3. General view of a COPEC after synthesis with NaCl, after replacing the salt with CuCl₂ and after half-hydrazine treatment.

2. Research Activities

(1) Physico-chemical characterization of PANI yolk-shell nanocapsules and their activity.

Nanostructured yolk-shell capsules of PANI were obtained, in its emeraldine form, with diameters between 380 and 500 nm, containing a 200 nm “yolk” and a shell of thickness 40 nm (Fig. 1). By using the polyelectrolyte properties of PANI, metallic cations have been selectively

Development of Versatile Receptor Layer Materials for Nanomechanical Sensor-based Detection/Discrimination

ICYS-MANA Researcher Kota SHIBA



1. Outline of Research

Nanomechanical sensors, which can detect mechanical deformation induced by analyte adsorption on the surface, are usually coated with various materials depending on target molecules. Polymers are known as one of the common receptor layer materials because of their versatility and commercial availability. Besides the polymers, however, there are a vast number of materials that are potential receptor layers with high sensitivity, specific target selectivity, robustness and so on. According to a previous study,¹⁾ it was pointed out that larger Young's modulus basically results in higher sensitivity, for example. Taking into account that the largest Young's modulus of polymers is approx. 10 GPa, inorganic materials such as various metals, oxides etc. and inorganic-organic hybrid materials are expected to realize higher sensitivity. Furthermore, diversity of these materials would lead to tunable analyte selectivity.

2. Research Activities

(1) Controlled growth of silica-titania hybrid functional nanoparticles through a multistep microfluidic approach.

To realize sensitive and selective sensing, it would be a good way to prepare a receptor layer composed of inorganic or inorganic-organic hybrid nanoparticles. The nanoparticle film seems a better option than a dense, monolithic film because the nanoparticle film possesses larger specific surface area. I have been working on the synthesis of inorganic oxide-based hybrid functional nanomaterials. Recently, a novel approach based on a multistep microfluidic reaction was developed for the synthesis of well-defined functional nanoparticles.²⁾ A concept of this approach is schematically shown in Fig. 1. Important points of the present approach are as follows: separation of nucleation and growth processes, and acceleration of the growth by the nucleation. Taking advantage of this approach, titania and silica-based hybrid nanoparticles with a narrow size distribution and an average size of 30 nm were obtained. These nanoparticles have core-shell structure with multiple cores inside (see TEM in Fig. 1). Judging from the unique

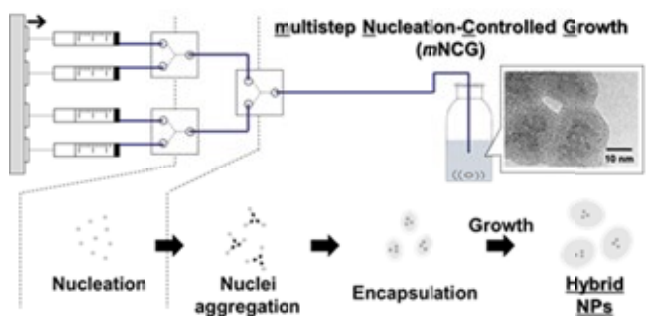


Fig. 1. Illustration of the mNCG method.

structure, pre-formed titania nuclei were encapsulated by silica shell. I also confirmed that the present approach was successfully applied to the preparation of the hybrid nanoparticles with different surface functionalities

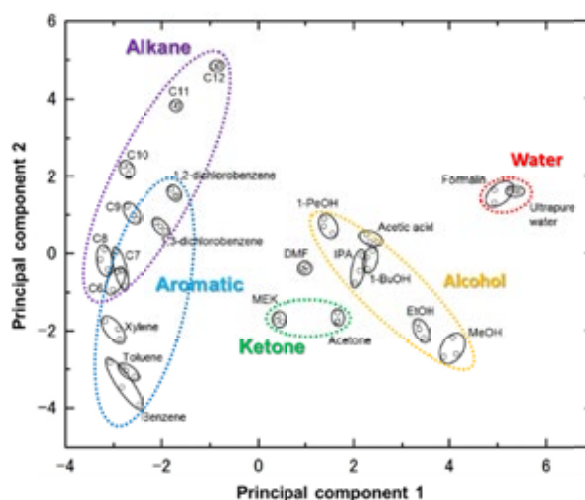


Fig. 2. A PCA result for the discrimination of 23 chemical compounds. These compounds include ultrapure water, formalin, acetic acid, methanol, ethanol, isopropanol, 1-butanol, 1-pentanol, acetone, methylethyl ketone, N,N-dimethylformamide, hexane, heptane, octane, nonane, decane, undecane, dodecane, benzene, toluene, xylene, 1,2-dichlorobenzene and 1,3-dichlorobenzene.

(2) Smell-based discrimination of multiple analytes utilizing a sensor array coated with chemically different receptor layer materials.

As I successfully synthesized nanoparticles with various functionalities, I preliminarily coated them onto the surface of a recently-developed nanomechanical sensor platform, a nanomechanical membrane-type surface stress sensor (MSS) with four independent sensing channels. In this case, nanoparticles with four different surface functionalities were chosen as the receptor layer materials and individually coated them onto each sensing channel. Then, vapor of 23 chemical compounds were measured. Consequently, each channel showed characteristic responses depending on a type of analytes. A principal component analysis was performed to discriminate the compounds. As demonstrated in Fig. 2, the clusters derived from the 23 compounds can be categorized into several groups, which seem to have a quite reasonable trend. I confirmed that sub-ppm level detection was also possible for some compounds. I am planning to apply the present technique for practical applications such as breath analysis.

References

- 1) G. Yoshikawa, *Appl. Phys. Lett.* **98**, 173502 (2011).
- 2) K. Shiba, T. Sugiyama, T. Takei, G. Yoshikawa, *Chem. Commun.* **51**, 15854 (2015).

Advanced Binder-free Anodes for the Energy Storage Application and their Storage Mechanisms at Atomic Scale

ICYS-MANA Researcher

Xi WANG



1. Outline of Research

Lithium-ion batteries (LIBs) have dominated the portable power market in the last several years and are now being extended to large applications such as cordless power tools and electric vehicles (EV). In the general preparation of electrode in a conventional LIB device, conductive additives and binders are necessary, but they are electrochemically inactive and some side effects between electrolytes and these inactive materials may happen. Unlike traditional batteries, binder-free LIBs require the development of binder-free components. Among them, binder-free anodes are usually made from various functional organic and/or inorganic materials built on flexible conductive membrane substrates without conductive additives and binders. Therefore the amount of non-active substances is minimized in the whole cells.

On the other hand, the most commonly used graphite anodes in current LIBs show poor rate capability due to their low Li diffusion coefficient, and poor cycle life. An essential component of the current endeavor in this area is to design advanced candidate anodes for the next generation of LIBs.¹⁻⁶⁾ Among the candidates, spinel $\text{Li}_4\text{Ti}_5\text{O}_{12}$ and N-doped graphene (GN) have attracted enormous attention because of its several inherent advantages. However, there are still challenges on developing some feasible strategies for making binder-free electrodes with ultrafast storage properties for above candidates. In addition, there is no direct experimental evidence and fundamental understanding of the lithium storage mechanisms at the atomic scale. Revealing these for them may shed a light on the reasons of its ultrafast lithium storage feature and high capacity found in the experiments. And there still remain other issues, such as SEI composition, the differences between the material edges and its surface in storing mechanism.

2. Research Activities

(1) Synthesis of binder-free anodes for rechargeable batteries.

We developed some new strategies and fabricated novel binder-free electrodes for fast Li/Na transport including bicontinuous nanoporous $\text{Cu}/\text{Li}_4\text{Ti}_5\text{O}_{12}$ electrode, and N-doped graphene papers. For example, a new route was used to fabricate a bicontinuous $\text{Cu}/\text{Li}_4\text{Ti}_5\text{O}_{12}$ scaffold that consists of $\text{Li}_4\text{Ti}_5\text{O}_{12}$ nanoparticles (LTO NPs) with highly exposed (111) facets and nanoporous Cu scaffolds,²⁾ which enable simultaneous high-capacity and high-rate lithium storage. When tested as the anode in lithium-ion batteries LIBs, Cu/LTO showed superior performance, such as a lifespan greater than 2000 cycles and an ultrafast charging time (<45 s). Notably, the ultrahigh capacity slightly larger than the theoretical value was also observed in Cu/LTO at low current density. Furthermore, a binder-free N-doped graphene paper anode was also prepared via a simple solution method,⁶⁾ which exhibited both high capacity and ultrafast lithium storage properties.

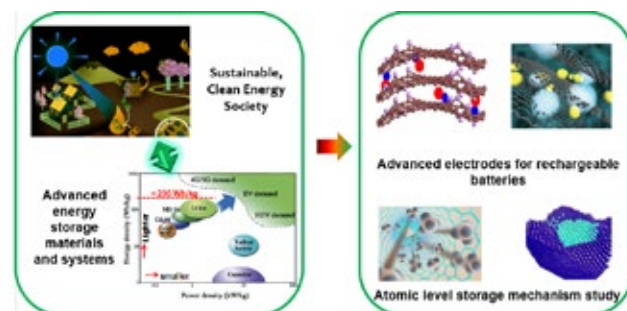


Fig. 1. Design advanced electrode materials combined with their atomic level mechanism study will contribute to the clean energy society.

(2) The atomic-level mechanisms via advanced TEM and DFT calculations.

By using advanced in-TEM, STEM techniques and the theoretical simulations, we systematically studied and understood their storage mechanisms at the atomic scale (Fig. 1), which shed a new light on the reasons of the ultrafast lithium storage property and high capacity for these advanced anodes. To answer some mechanism questions, building a single-particle-based nanobattery are therefore critical. For instance, we constructed a single GN-based nano-LIBs device. Therefore, the atomistic insights of the GN energy storage could be revealed. The lithiation process on edges and basal planes is directly visualized, the pyrrolic N “hole” defect and the perturbed solid-electrolyte-interface configurations are observed, and charge transfer states for three N-existing forms are also investigated. In situ high-resolution TEM experiments together with theoretical calculations provide a solid evidence that enlarged edge {0002} spacings and surface hole defects result in improved surface capacitive effects and thus high rate capability and the high capacity are owing to short-distance orderings at the edges during discharging and numerous surface defects. In addition, density functional theory calculations and detailed characterizations could also utilized to uncover that the highly exposed (111) facets on the edge are the reason for its unique storage mechanism (8a+16c), which is different from the transition between 8a and 16c in bulk LTO.

References

- 1) W. Tian, X. Wang, C. Zhi, T. Zhai, D. Liu, C. Zhang, D. Golberg, Y. Bando, *Nano Energy* **2**, 754 (2013).
- 2) X. Wang, D.Q. Liu, Q.H. Weng, J.W. Liu, Q.F. Liang, C. Zhang, *NPG Asia Mater.* **7**, e171 (2015).
- 3) X. Wang, W. Tian, M.Y. Liao, Y. Bando, D. Golberg, *Chem. Soc. Rev.* **43**, 1400 (2014).
- 4) X. Wang, W. Tian, D. Liu, C. Zhi, Y. Bando, D. Golberg, *Nano Energy* **2**, 257 (2013).
- 5) D. Liu, X. Wang, X. Wang, W. Tian, Y. Bando, D. Golberg, *Sci. Rep.* **3**, 2543 (2013).
- 6) X. Wang, Q.H. Weng, X.Z. Liu, X.B. Wang, D.M. Tang, W. Tian, C. Zhang, W. Yi, D.Q. Liu, Y. Bando, D. Golberg, *Nano Lett.* **14**, 1164 (2014).

Nanosheets of Boron-Carbon-Nitrogen System for Energy and Composite Applications

ICYS-MANA Researcher Xue-Bin WANG



1. Outline of Research

The high-energy high-power electricity storage devices are essential for energy issues. 2D functional nanosheets of light elements in boron-carbon-nitrogen system, *e.g.* representative graphene and boron nitride (BN) nanosheets, are outstanding models of 2D nanosheets offering unique physics and exciting functionalities. Herein my research focuses on the novel syntheses of graphenes and BN nanosheets and on their applications for high-power supercapacitors and thermo-conductive composites.

In order to accomplish this purpose, we set up a full set of state-of-the-art instruments for syntheses and characterizations of nanomaterials, such as induction furnace, electrochemical workshop and transmission electron microscope *etc.* We also conducted analyses of electrochemistry, thermology, dielectrics and mechanics with respect to batteries, supercapacitors and composite materials.

2. Research Activities

(1) Novel Strutted-Graphene: Synthesis and High-Power-Density High-Energy-Density Supercapacitors.^{1,2)}

3D graphene can in principle maintain all the extraordinary nanoscale properties of individual graphenes. Currently interconnected self-supported reproducible 3D graphenes remain unavailable. Here we developed a new general synthesis method, *i.e.* ammonium-assistant chemical blowing, to produce a new-type 3D graphenes (Fig. 1), named by us as strutted-graphene (SG). SG consisted of continuous graphitic membranes which were homogeneously connected and spatially supported by the networks of micrometer-width graphitic struts. Such a topological microconfiguration provided intimate structural interconnectivities, freeway for electron/phonon transports, huge accessible

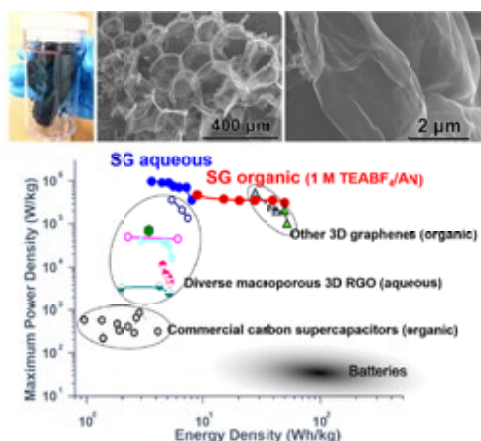


Fig. 1. Top: Photo and 2 SEM images of SG with a huge graphene membrane full of nanosized ripples. Bottom: A survey of maximum power density vs. energy density of EDL-type supercapacitors based on diverse 3D graphenes (RGO = reduced graphene oxide).

surface area, as well as robust mechanical properties.

We further developed the high-energy-density high-power-density supercapacitors based on strutted graphenes. The additive/binder-free strutted graphenes are good electrodes, which achieve the highest maximum-power-density (10^6 W/kg) among 3D-graphene based electron-double-layer-type supercapacitors in aqueous system, and realize high the energy density of 50 Wh/kg at the high maximum-power-density of 340 kW/kg in organic system.

(2) Massive Synthesis of High-Quality Boron Nitride Nanosheets for Advanced Composites.³⁾

BN nanosheets attract intensive interests, however their research is rather limited by the insufficient production. Here we provided a highly effective way to synthesize gram-scale-level BN nanosheets using graphite and boron oxide. Single-crystalline BN sheets have a mean lateral size of several hundred nanometers and a thickness ranging from 5 to 40 nm (Fig. 2).

Utilization of nanosheets for the reinforcement of polymers revealed that the Young's modulus of BN/PMMA composite had increased to 1.9 GPa when the BN fraction was only 5 wt%, thus demonstrating a 44% gain compared to a blank PMMA film. In addition, the nanosheets were further utilized for making thermal conductive and electrically insulating epoxy/BN composites with a 14-fold increase in thermal conductivity. It suggests that the BN nanosheet is an ideal reinforcing filler for polymers.

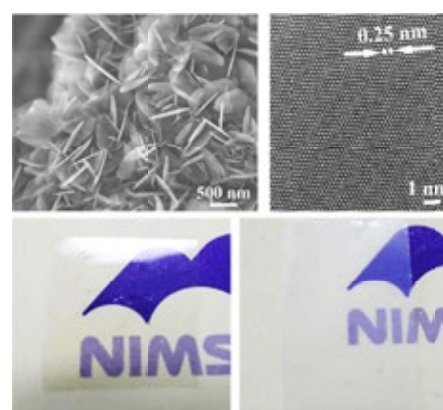


Fig. 2. Top: SEM and HRTEM images of BN nanosheets showing hexagonal phase and well crystalline structure. Bottom: Photographs of the BN/PMMA composite films at 0 and 5 wt% BN respectively.

References

- 1) X.F. Jiang, X.B. Wang, P.C. Dai, X. Li, Q.H. Weng, X. Wang, D.M. Tang, J. Tang, Y. Bando, D. Golberg, *Nano Energy* **16**, 81 (2015).
- 2) X.B. Wang, Y.J. Zhang, C.Y. Zhi, X. Wang, D.M. Tang, Y.B. Xu, Q.H. Weng, X.F. Jiang, M. Mitome, D. Golberg, Y. Bando, *Nature Commun.* **4**, 2905 (2013).
- 3) X.F. Jiang, Q.H. Weng, X.B. Wang, X. Li, J. Zhang, D. Golberg, Y. Bando, *J Mater. Sci. Technol.* **31**, 589 (2015).

Towards Metal-Organic Framework Nanoarchitectonics: Fundamentals of Synthesis and Design

ICYS-MANA Researcher Hamish Hei-Man YEUNG



1. Outline of Research

Metal-Organic Frameworks (MOFs) are a class of material with great potential for tailoring to suit many different applications. Molecular analogues to TinkerToy®, the modular arrangement of different nanoscale building blocks in robust, atomically-precise structures has enabled the discovery of new materials that boast a diverse range of physical properties, including microporosity, magnetism, luminescence and ionic conductivity.¹⁾ The fascinating thing about MOFs, compared with classical materials, is that the synergy between “organic” and “inorganic” components results in new properties and interesting behaviour.²⁾

My research explores various fundamental aspects of MOFs, such as their crystallization energetics and structure-property relationships, which are necessary to determine the extents, and limits, to which these new materials might be designed to suit tomorrow’s nanotechnology.

2. Research Activities

(1) In-situ diffraction of MOF crystallization.

Mild solvothermal synthesis used to make MOFs often allows access to various phases from the same reagents. Using high energy, in-situ synchrotron X-ray powder diffraction we have monitored the crystallization of lithium *meso*-tartrate MOFs, observing the successive crystallization and dissolution of three competing phases in one reaction.³⁾ By determining rate constants and activation energies, we have quantified the reaction energy landscape, which gives predictive power for choice of reaction conditions (Fig. 1). The different reaction rates we observe are explained by the structural relationships between products and the reactants; larger changes in conformation result in higher activation energies.

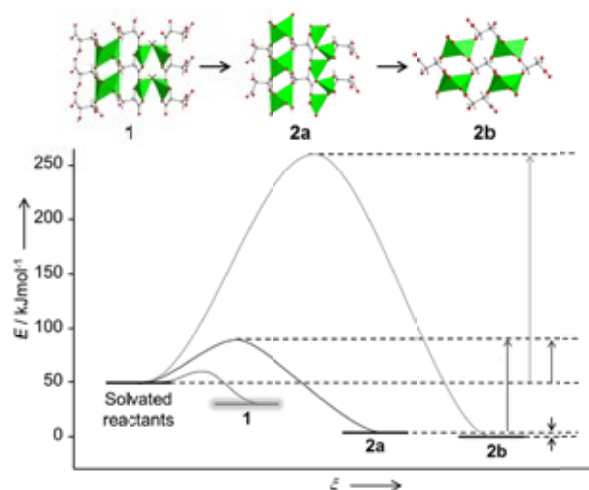


Fig. 1. Reaction energy landscape for successive crystallizations of competing lithium tartrates, quantified using in-situ XRD.

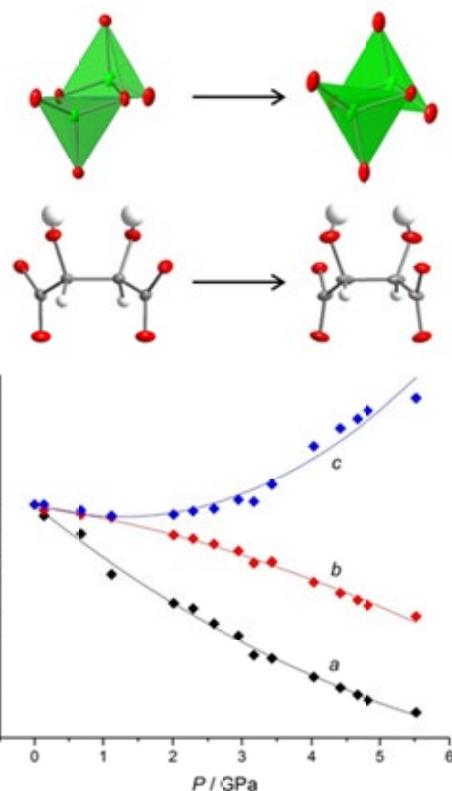


Fig. 2. Distortion of the metal coordination sphere and ligand upon hydrostatic pressure, accompanying NLC in lithium tartrate.

(2) Negative linear compressibility in a dense MOF.

Negative linear compressibility (NLC) is the rare phenomenon by which certain materials under the application of uniform pressure actually expand in one direction, making them highly sought after for several emerging applications that include pressure sensors and artificial muscles.⁴⁾ We have discovered that lithium L-tartrate exhibits a large and increasing coefficient of NLC with median value $K_{\text{NLC}} = -10(2) \text{ TPa}^{-1}$, giving it one of the largest NLC capacities ever reported.⁵⁾ Using synchrotron single crystal X-ray diffraction, we have rationalized the bulk mechanical behavior in terms of the underlying crystal structure, finding that NLC arises from the combination of its topology and the intrinsic flexibility in both the metal node and the ligand components (Fig. 2).

References

- 1) M.D. Allendorf, A. Schwartzberg, V. Stavila, A.A. Talin, *Chem. Eur. J.* **17**, 11372 (2011).
- 2) S. Horike, S. Shimomura, S. Kitagawa, *Nature Chem.* **1**, 695 (2009).
- 3) H.H.M. Yeung, Y. Wu, S. Henke, A.K. Cheetham, D. O’Hare, R. I. Walton, *Angew. Chem. Int. Ed.*, in press.
- 4) A.B. Cairns, A.L. Goodwin, *Phys. Chem. Chem. Phys.* **17**, 20449 (2015).
- 5) H.H.M. Yeung, R. Kilmurray, A.K. Cheetham, S.A. Moggach, manuscript in preparation.

Engineering Topological Superconductivity in Surface Materials

ICYS-MANA Researcher

Shunsuke YOSHIZAWA



1. Outline of Research

Topological superconductor is predicted to possess Majorana quasiparticles (MQPs) as zero-energy edge states. They are the condensed-matter analogue of Majorana fermions in particle physics and are expected to be useful for storing quantum information. In two-dimensional topological superconductor, MQPs are confined in quantum vortices, and manipulation of the vortices allows us to manipulate the MQPs. The most direct technique for observing the MQPs in vortices is low-temperature scanning tunneling microscopy (STM). The technique requires atomically flat and clean surfaces on samples.

So far we have studied superconducting atomic-layer indium on a silicon surface, Si(111)-($\sqrt{7\times\sqrt{3}}$)-In, and have succeeded in vortex imaging by using STM.¹⁻³⁾ With this background, we aim to create topological superconductivity in clean surface materials prepared in an ultra-high vacuum (UHV) condition and to observe MQPs with STM.

2. Research Activities

(1) *Detection of disorder-induced suppression of superconductivity in atomic-layer indium on silicon.*⁴⁾

To achieve high-quality superconducting surfaces, it is important to clarify how crystalline disorder affects the superconducting properties. For this purpose we investigated the influence of disorder on the superconducting characteristics of Si(111)-($\sqrt{7\times\sqrt{3}}$)-In with low-temperature STM. The sample was prepared with a lower annealing temperature than the usual condition. The obtained sample surface is totally covered with the ($\sqrt{7\times\sqrt{3}}$)-In phase, but contains two types of regions with different degrees of disorder (Fig. 1a). In less-disordered regions, tunneling spectra show a superconducting gap at the Fermi energy (E_F) and superconducting vortices are observed in magnetic fields, as shown in Fig. 1b. In contrast, disordered regions contain dense nanometer-sized grains separated by atomic steps. Tunneling spectra show a broad dip structure at E_F

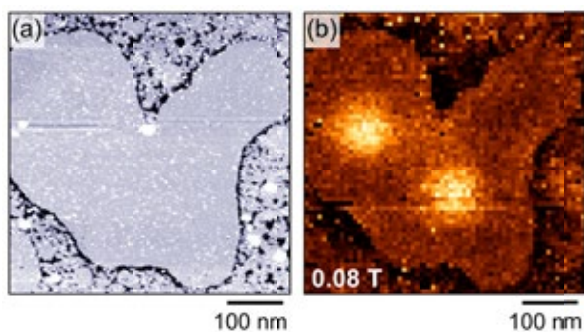


Fig. 1. (a) STM image of an atomically-flat superconducting region surrounded by disordered non-superconducting regions. (b) Zero-bias conductance image obtained at ~ 0.5 K in a magnetic field of 0.08 T. Two vortices are observed in the flat region.

instead of the superconducting gap. The dip structure is attributed to the zero-bias anomaly that is characteristic to two-dimensional disordered metal. Fitting analysis based on existing theoretical formulae allows us to estimate the suppressions of mean free path and superconducting critical temperature in both the flat and rough regions.



Fig. 2. Photo of the UHV-compatible cryostat for transport measurement in magnetic fields.

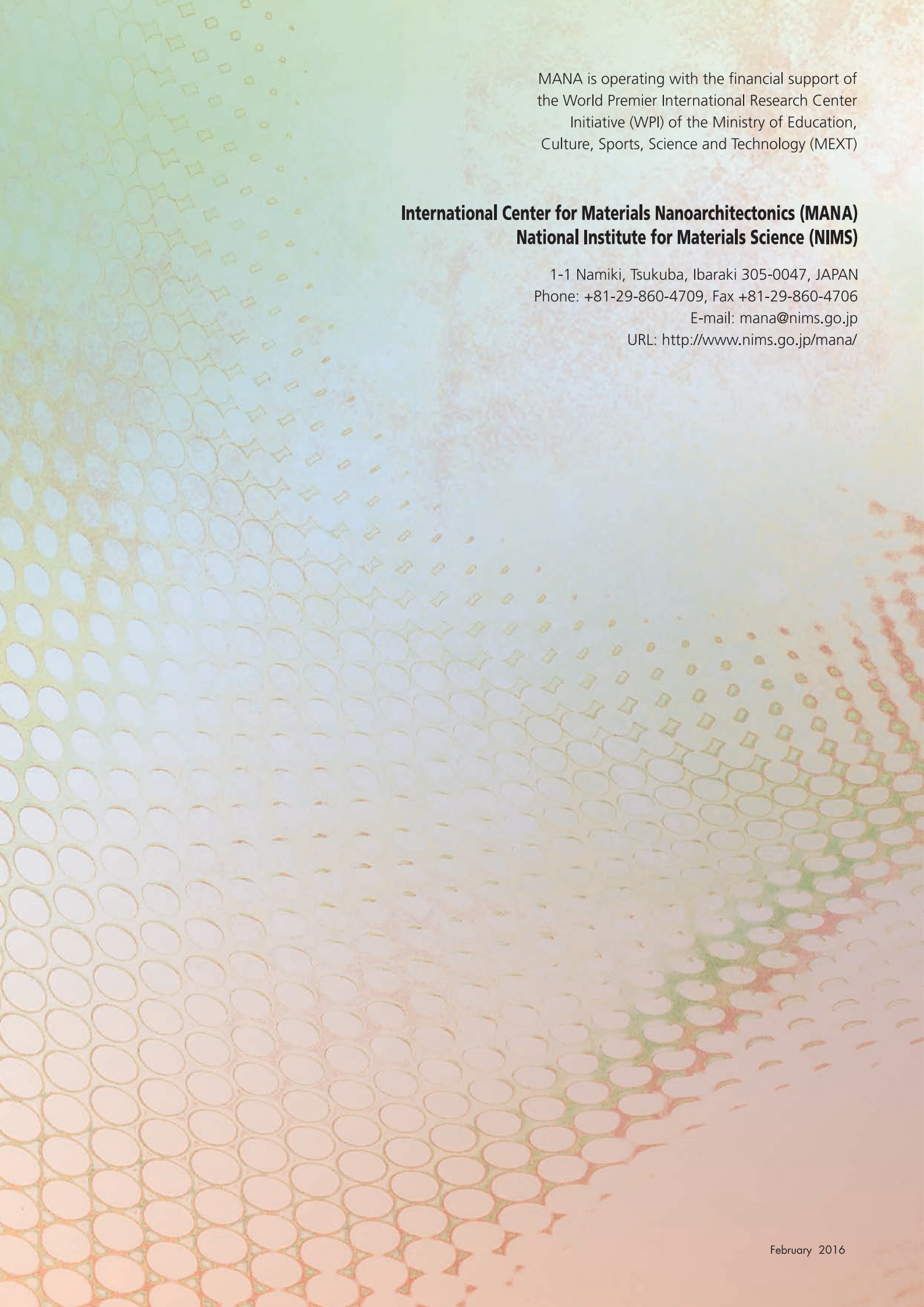
(2) *Development of UHV-compatible cryostat for transport measurement under in-plane magnetic fields.*

Topological superconductivity can be created by combining three ingredients: s-wave superconductor, the spin-orbit interaction, and the Zeeman effect. It is advantageous to start from materials where two of the three are already involved. For example, when surface states with strong spin-orbit interaction exhibit superconductivity, the resulting superconducting state can contain spin-triplet component, which is closely related to topological superconductivity. One of the criteria for such an unusual superconductivity is the enhancement of upper critical field for in-plane magnetic fields. However, conventional low-temperature equipment with a superconducting magnet cannot be used for our purpose, because we should avoid surface contamination resulting from air exposure.

We have developed a UHV-compatible cryostat for electrical transport measurement in magnetic fields (Fig. 2). It allows us to perform sample preparation and measurements in UHV and thus to obtain reliable data. The lowest measurement temperature is below 1 K and magnetic fields up to 5 T can be applied. By rotating the sample stage *in-situ*, the direction of magnetic fields with respect to the sample surface can be varied from the perpendicular to the parallel direction.

References

- 1) S. Yoshizawa, T. Uchihashi, *J. Phys. Soc. Jpn.* **83**, 065001 (2014).
- 2) S. Yoshizawa, H. Kim, T. Kawakami, Y. Nagai, T. Nakayama, X. Hu, Y. Hasegawa, T. Uchihashi, *Phys. Rev. Lett.* **113**, 247004 (2014).
- 3) S. Yoshizawa and T. Uchihashi, *Kotai Butsuri (Solid State Physics)* **50**, 323 (2015).
- 4) S. Yoshizawa, H. Kim, Y. Hasegawa, T. Uchihashi, *Phys. Rev. B* **92**, 041410(R) (2015).



MANA is operating with the financial support of
the World Premier International Research Center
Initiative (WPI) of the Ministry of Education,
Culture, Sports, Science and Technology (MEXT)

**International Center for Materials Nanoarchitectonics (MANA)
National Institute for Materials Science (NIMS)**

1-1 Namiki, Tsukuba, Ibaraki 305-0047, JAPAN
Phone: +81-29-860-4709, Fax +81-29-860-4706
E-mail: mana@nims.go.jp
URL: <http://www.nims.go.jp/mana/>